



Final Report for the Atmospheric CO₂ Observations from Space (ACOS) Task

**David Crisp (JPL/Caltech), ACOS Science Lead
Ralph Basilio (JPL/Caltech), ACOS Task Manager
and the ACOS Team**

September 2012





Objectives of the ACOS Task

The objectives of the Atmospheric CO₂ Observations from Space (ACOS) Task Plan are to:

- Advance carbon cycle science using NASA's investment in OCO-unique calibration, retrieval algorithm, and validation capabilities
- Meet NASA commitments identified in the NASA-JAXA (Japanese Aerospace Exploration Agency) Memorandum of Understanding (MOU) for OCO-GOSAT (Greenhouse gases Observing SATellite) collaboration as far as possible without OCO
- Implement an operational science data processing system that will significantly reduce the latency for data product delivery from any potential OCO re-flight opportunity.



Overview of this Report

- We begin by summarizing the background of the OCO/GOSAT collaboration
- We then summarize the progress made in the calibration, retrieval algorithm development, and validation activities described in the Statement of Work that was included in the ACOS Task Plan
 - Each section
 - Cites the specific tasks being addressed
 - Includes a list of publications from that activity
- We then provide a final report on the budget and schedule



ACOS / GOSAT Background





The Pioneers: GOSAT and OCO



OCO and GOSAT were the first two spacecraft designed to monitor CO₂ with the accuracy needed to identify and quantify surface fluxes. The OCO and GOSAT teams formed a close partnership during the mission implementation phase.

- Formalized through a Memorandum of Understanding between NASA and JAXA

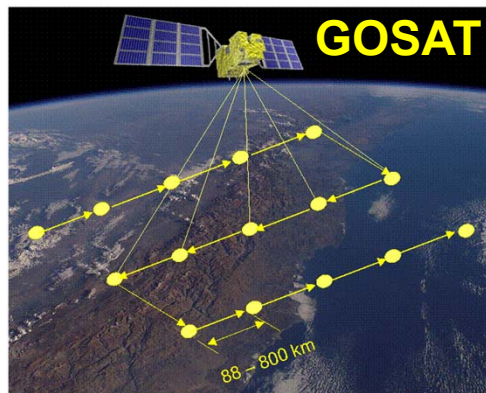


The OCO / GOSAT Collaboration

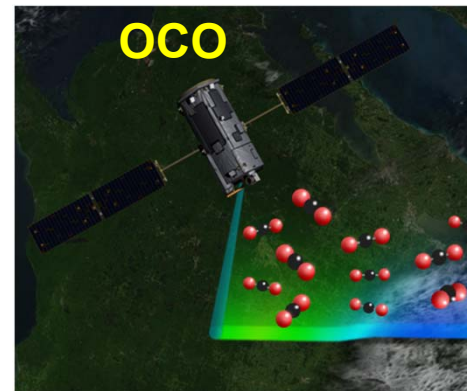
- The objectives of this partnership were to:
 - Accelerate understanding of this new data source
 - Facilitate combining GOSAT and OCO results in flux inversion models
- The approach included two major components:
 - Cross calibrate OCO and GOSAT instrument radiometric standards
 - Cross validate OCO and GOSAT X_{CO_2} retrievals against a common standard: the Total Carbon Column Observing Network (TCCON)



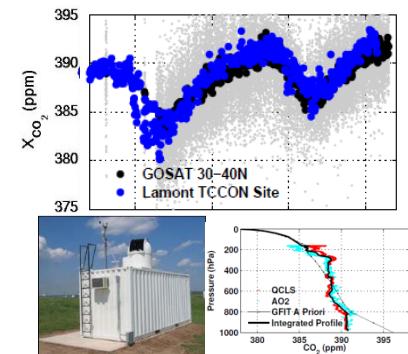
Cross calibration of radiometric standards prior to launch.



Uniform sampling with 3-day repeat cycle



Continuous high resolution measurements along track



Validation against TCCON observations



The Launch of GOSAT and OCO



GOSAT launched successfully
on 23 January 2009



OCO was lost a month later
when its launch system failed



Working with the GOSAT Team

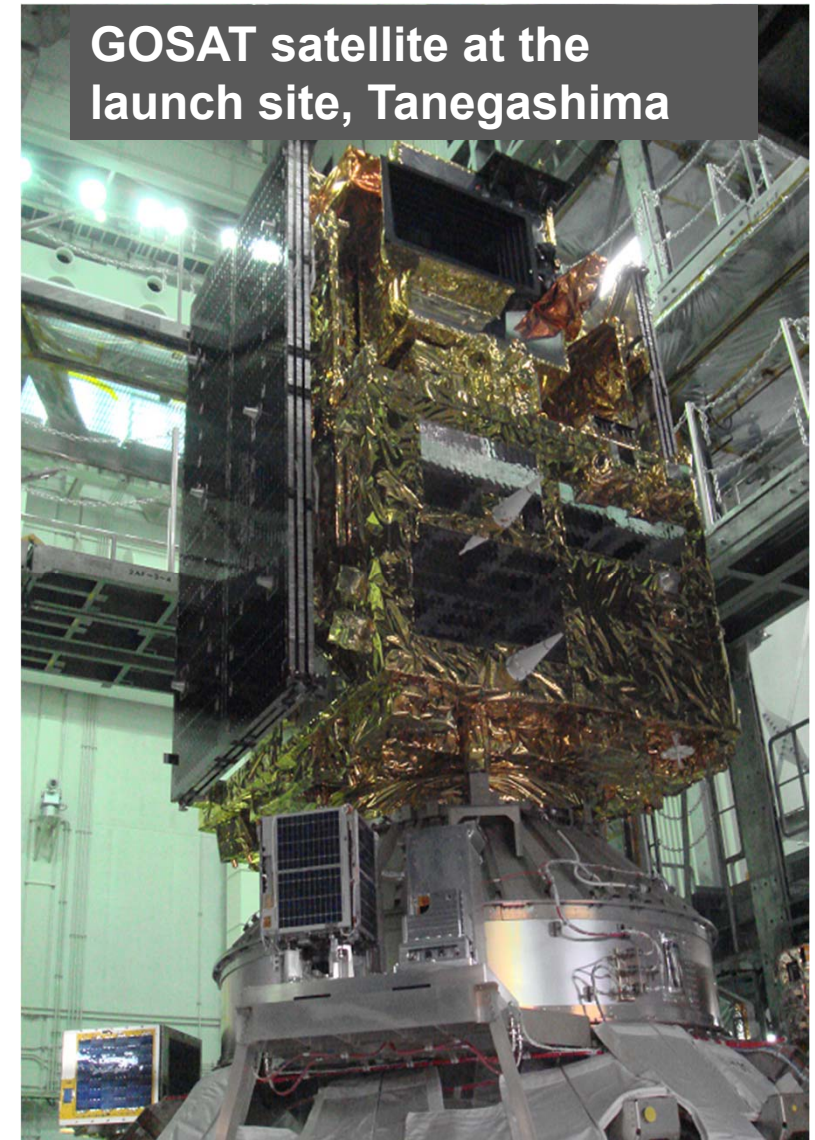
- Immediately after the loss of the OCO Mission, the GOSAT Project manager invited the OCO Team to participate in the GOSAT data analysis
- NASA reformulated the OCO team as the “Atmospheric CO₂ Observations from Space” (ACOS) team
- This collaboration benefits the GOSAT team by:
 - Combining the ground based calibration and validation resources of both teams to maximize the accuracy of the GOSAT data
 - Combining the scientific expertise from both teams to accelerate our understanding of this new, space-based data source
- This collaboration benefits the NASA and the OCO team by
 - Providing direct experience with the analysis of space based CO₂ measurements
 - Accelerating the delivery of precise CO₂ measurements from future NASA carbon dioxide monitoring missions



Introduction to the GOSAT mission

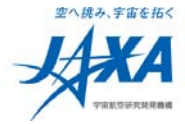


- GOSAT is
 - Greenhouse gases Observing SATellite.
 - Monitoring global distribution of Greenhouse Gases from space
 - Target for Carbon dioxide and Methane
 - at 100-1000km spatial scale
 - with relative accuracy of 1% (4ppm) for CO₂ and 2% (34ppb) for CH₄
- Joint project by
 - JAXA (Japan Aerospace Exploration Agency),
 - NIES (National Institute for Environmental Studies)
 - MOE (Ministry of the Environment)
- Launch: 23 January 2009, H2A launch vehicle from Tanegashima
- Mission lifetime: 5 years

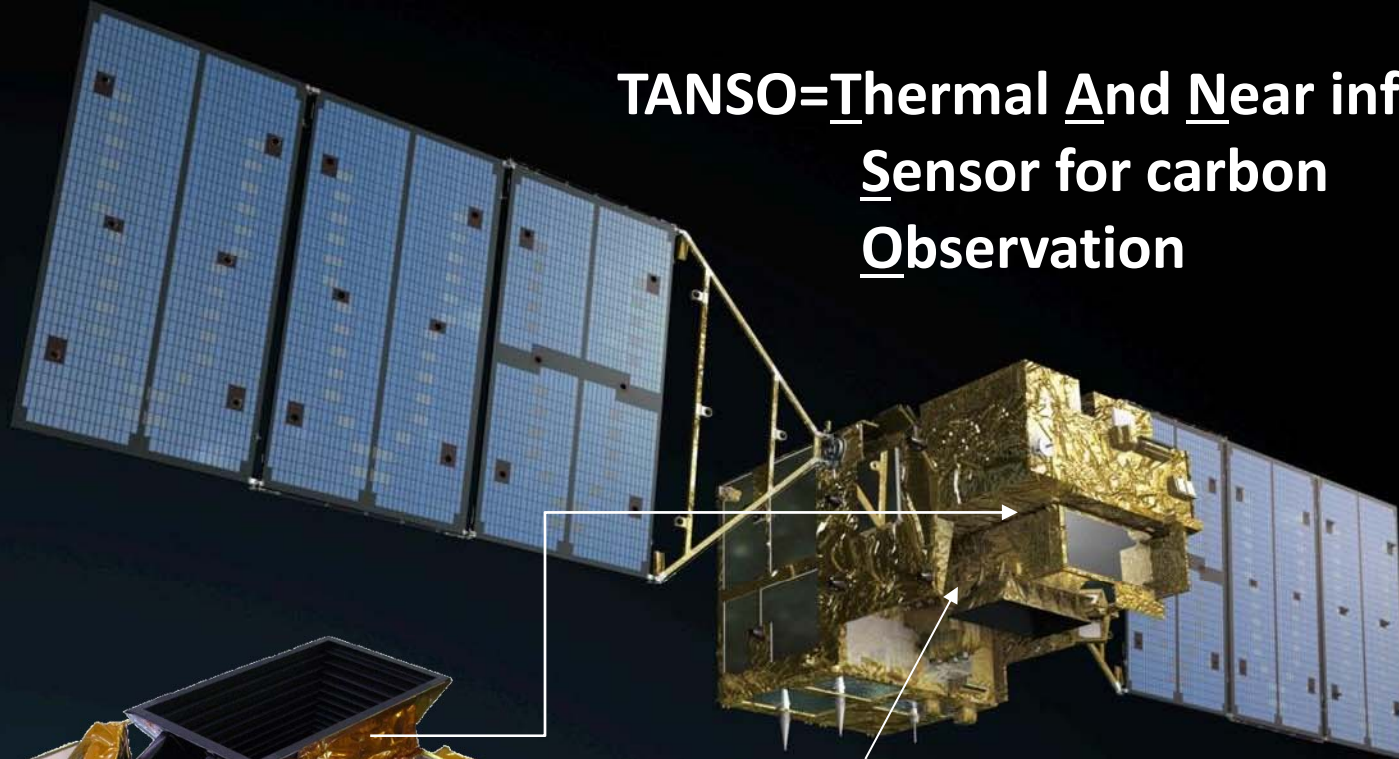




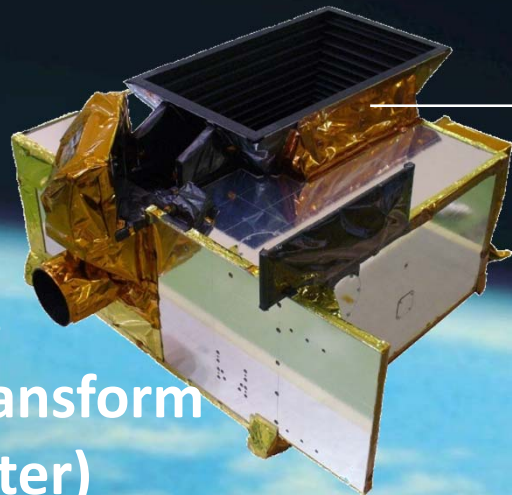
GOSAT Satellite and Sensors



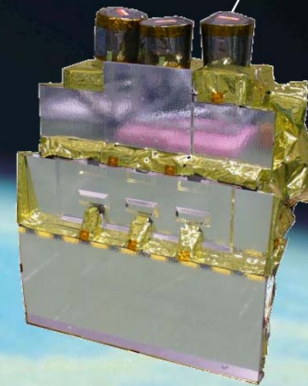
**TANSO=Thermal And Near infrared
Sensor for carbon
Observation**



**TANSO-FTS
(Fourier Transform
Spectrometer)**



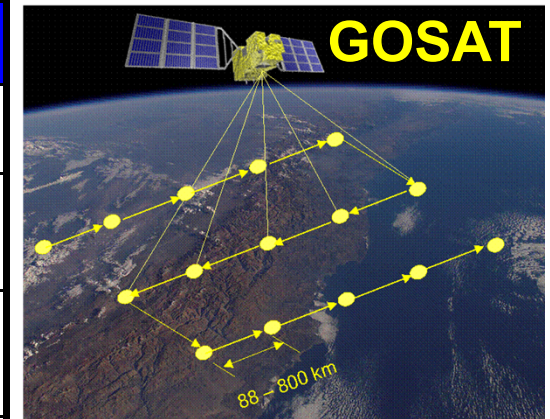
**TANSO-CAI
(Cloud and Aerosol
Imager)**



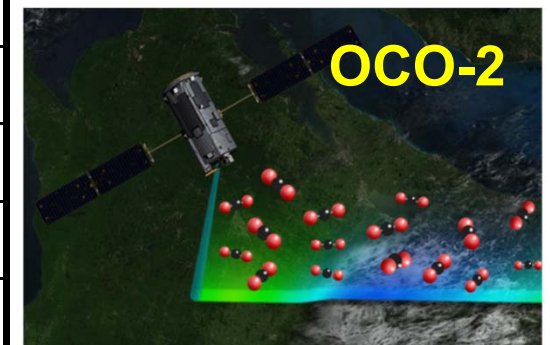


Comparison of OCO-2 and GOSAT

	GOSAT	OCO-2
Gases Measured	CO ₂ , CH ₄ , O ₂ , O ₃ , H ₂ O	CO ₂ , O ₂
Instruments	SWIR/TIR FTS, CAI	Grating Spectrometer
IFOV / Swath (km)	FTS: 10.5 / 80-790 (160) CAI: 0.5 / 1000	1.29 x 2.25 / 5.2-10.4
Spectral Ranges (μm)	0.758-0.775, 1.56-1.72, 1.92-2.08, 5.56-14.3	0.757-0.772, 1.59- 1.62, 2.04-2.08
Soundings/Day	10,000	500,000 to 1,000,000
Sampling Rate	0.25 Hz	12 to 24 Hz
Orbit Altitude	666 km	705 km
Local Time	12:48	13:30
Revisit Time/Orbits	3 Days/72 Orbits	16 Days/233 Orbits
Launch Vehicle	H-IIA	Delta-II
Launch Date	January 2009	July 2014
Nominal Life	5 Years	2 Years



GOSAT was optimized for spectral & spatial coverage

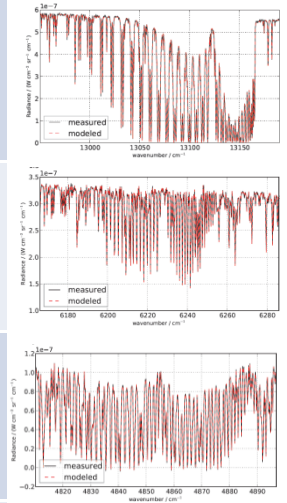


OCO-2 was optimized for sensitivity and resolution



TANSO-FTS and ACOS Spectral Ranges

Band	Target Species	TANSO-FTS Spectral Range	Spectral Resolution	ACOS/OCO-2 Range Used	Band Name
1	O ₂ A-band	12900 to 13200 cm ⁻¹ (0.758 to 0.775 μm)	1P 0.356 cm ⁻¹ 1S 0.367 cm ⁻¹	12950 to 13190 cm ⁻¹ (0.758 to 0.772 μm)	ABO2
2	CO ₂ , CH ₄	5800 to 6400 cm ⁻¹ (1.56 to 1.72 μm)	2P 0.258 cm ⁻¹ 2S 0.257 cm ⁻¹	6166 to 6286 cm ⁻¹ (1.591 to 1.622 μm)	WCO2
3	CO ₂	4800 to 5200 cm ⁻¹ (1.92 to 2.08 μm)	3P 0.262 cm ⁻¹ 3S 0.263 cm ⁻¹	4810 to 4897 cm ⁻¹ (2.042 to 2.079 μm)	SCO2
4	H ₂ O, O ₃ , CO ₂ CH ₄	700 to 1800 cm ⁻¹ (5.56 to 14.3 μm)	0.27 cm ⁻¹	N/A	N/A



GOSAT TANSO-FTS spectral bands and ACOS/OCO-2 spectral ranges. The spectral resolution (full width at half maximum of the instrument line shape function) for the two polarizations, P and S, are specified separately (Kuze et al. 2009a).



TANSO-FTS Calibration Issues

TANSO-FTS has been working well, but a few anomalies have been identified:

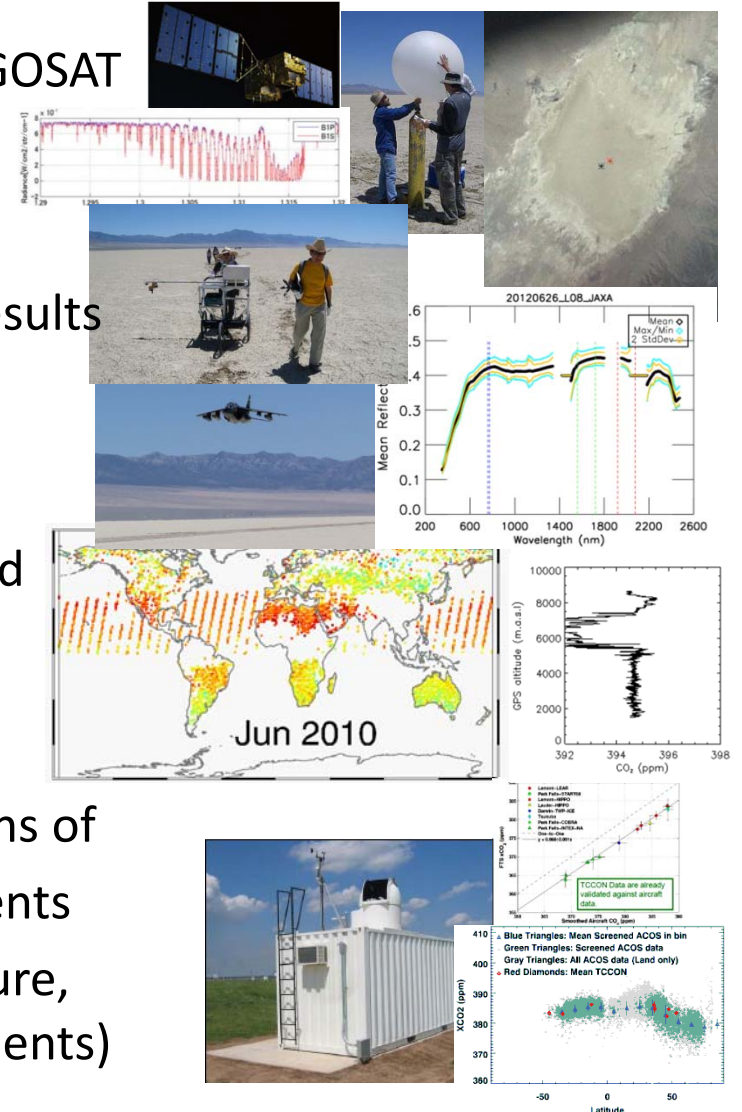
- 10-20 % of recorded interferograms have anomalous fluctuations.
 - Can be distinguished by checking level 1 data quality flag.
- TANSO-FTS Zero Path Difference (ZPD) shift
 - Problem mitigated by resetting FTS once every 2 weeks
- Sampling laser signal level decreases very slowly due to misalignment
 - No impact on performance (small wavelength shift).
- TANSO-FTS onboard camera data detected a variable pointing offset.
- Time-dependent degradation of radiometric response has been observed
 - Correction developed using RRV data and on-board solar diffuser
- TANSO-FTS Band 1 Nonlinearity – Currently under investigation
 - ACOS team supporting analysis and validation

*Strong ACOS role



The OCO/GOSAT Collaboration

- The ACOS team is collaborating closely with the GOSAT teams at JAXA and NIES to:
 - Conduct vicarious calibration campaigns in Railroad Valley, Nevada, U.S.A. and analyze results of those campaigns
 - Retrieve X_{CO_2} from GOSAT spectra
 - Model development, implementation, and testing
 - Data production and delivery
 - Validate GOSAT retrievals through comparisons of
 - GOSAT retrievals with TCCON measurements
 - Other validation standards (surface pressure, aircraft and ground-based CO_2 measurements)



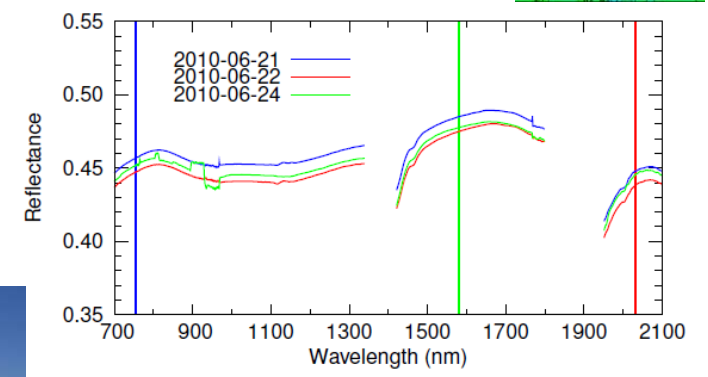
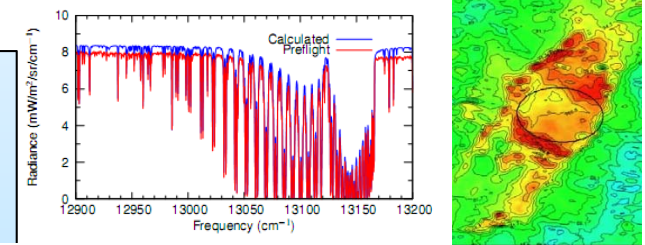
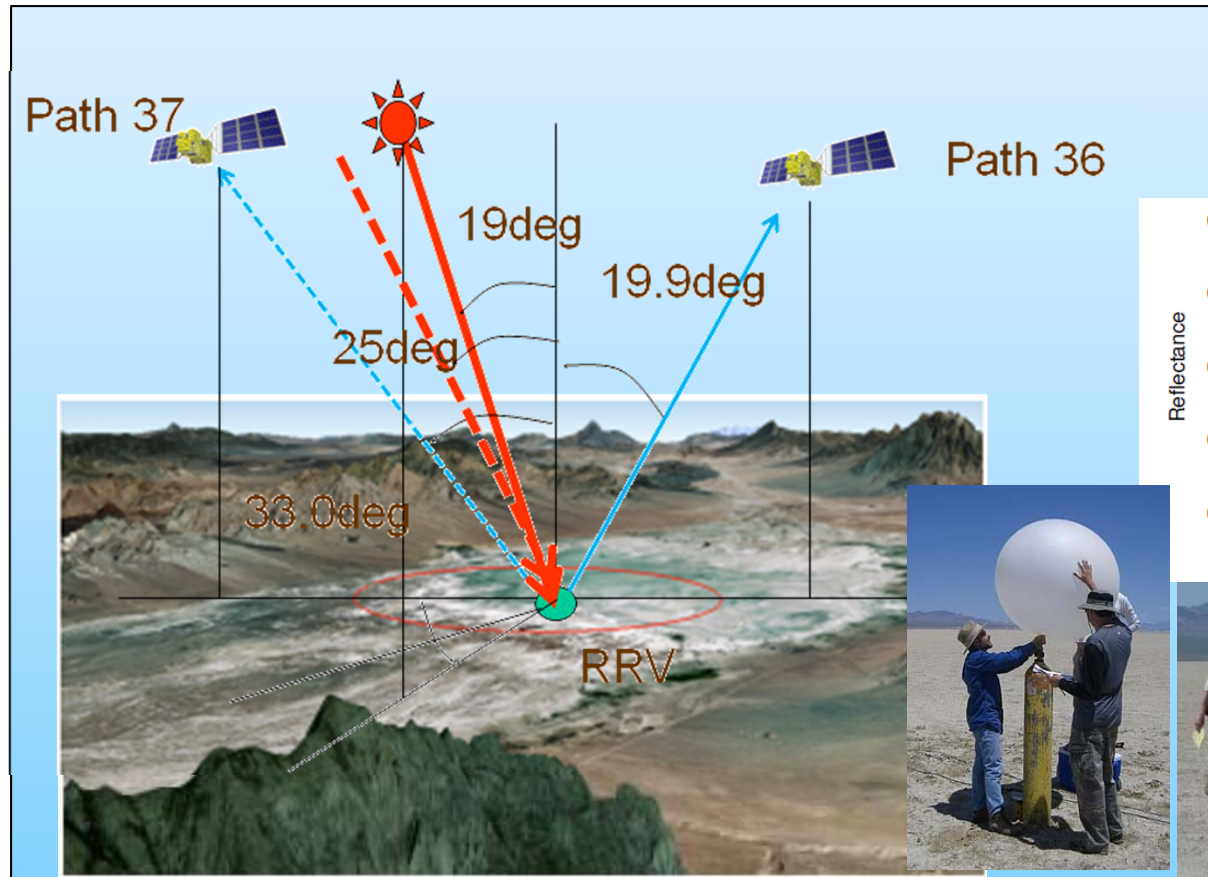


TANSO-FTS Vicarious Calibration in Railroad Valley (RRV), Nevada





Vicarious Calibration in Railroad Valley, NV

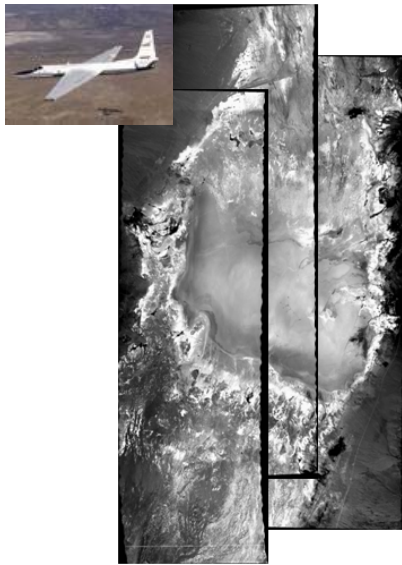


The NASA and GOSAT teams collaborated in four, joint vicarious calibration campaigns, collecting ground based and aircraft measurements over Railroad Valley (RRV), during GOSAT overflights to monitor the calibration of the GOSAT instruments



Characterizing the Surface Reflectance of RRV

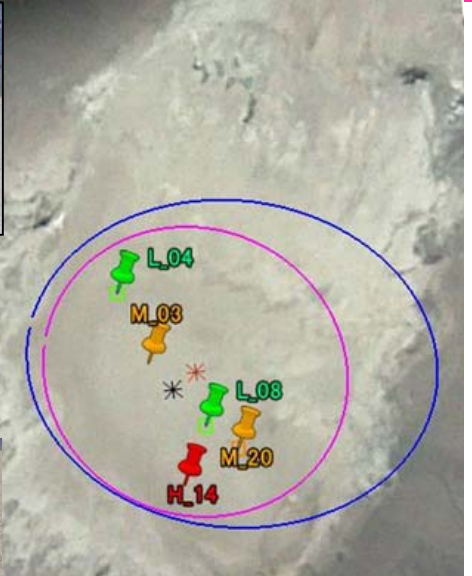
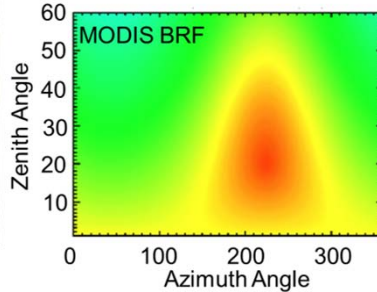
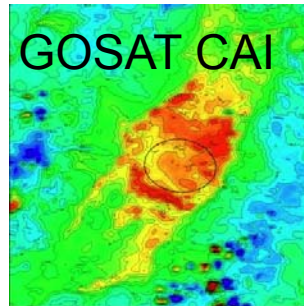
- Because the TANSO-FTS footprint is large compared to the size of Railroad Valley (RRV), spatial variations in surface reflectance were characterized by ground-based measurements collected at several sights across the valley floor.
- Aircraft (ER-2 AVIRIS and MASTER) and spacecraft (ASTER, MODIS, CAI) were used to extrapolate these results to the full valley floor.



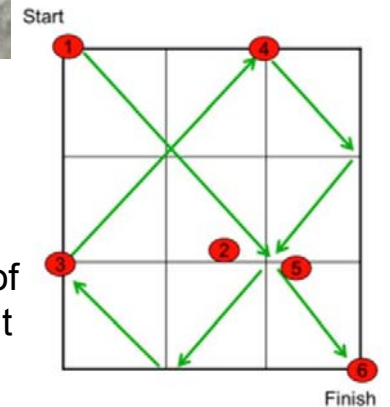
AVIRIS



MASTER



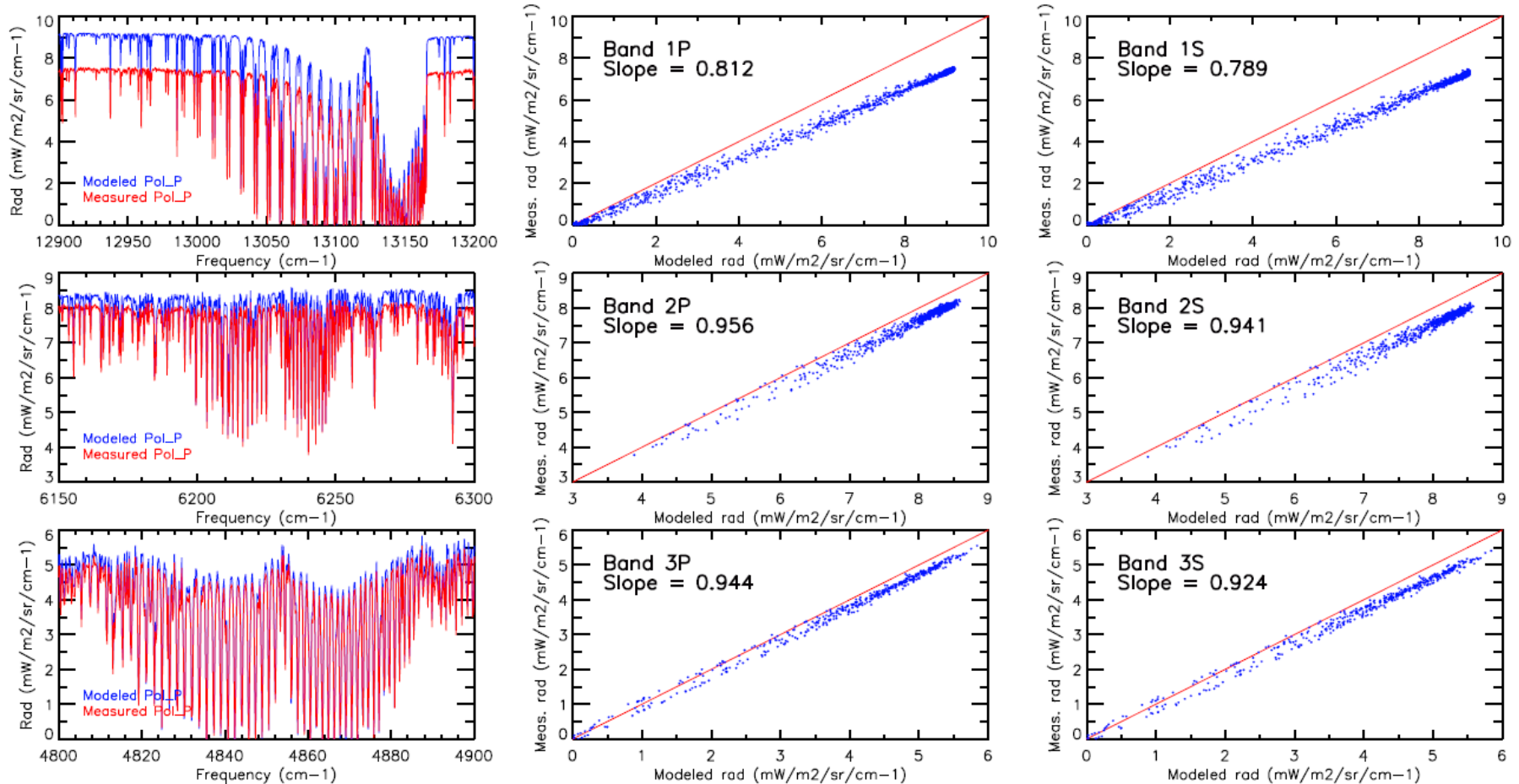
TANSO-FTS CAM image showing footprints for Path 36 (red) and 37 (blue) along with locations of surface measurement grids. Each grid is sampled with a baby buggy-mounted ASD (inset) sampling pattern shown at right.



Red circles show ASD calibration locations. *Kuze et al. (in prep - 2012)*



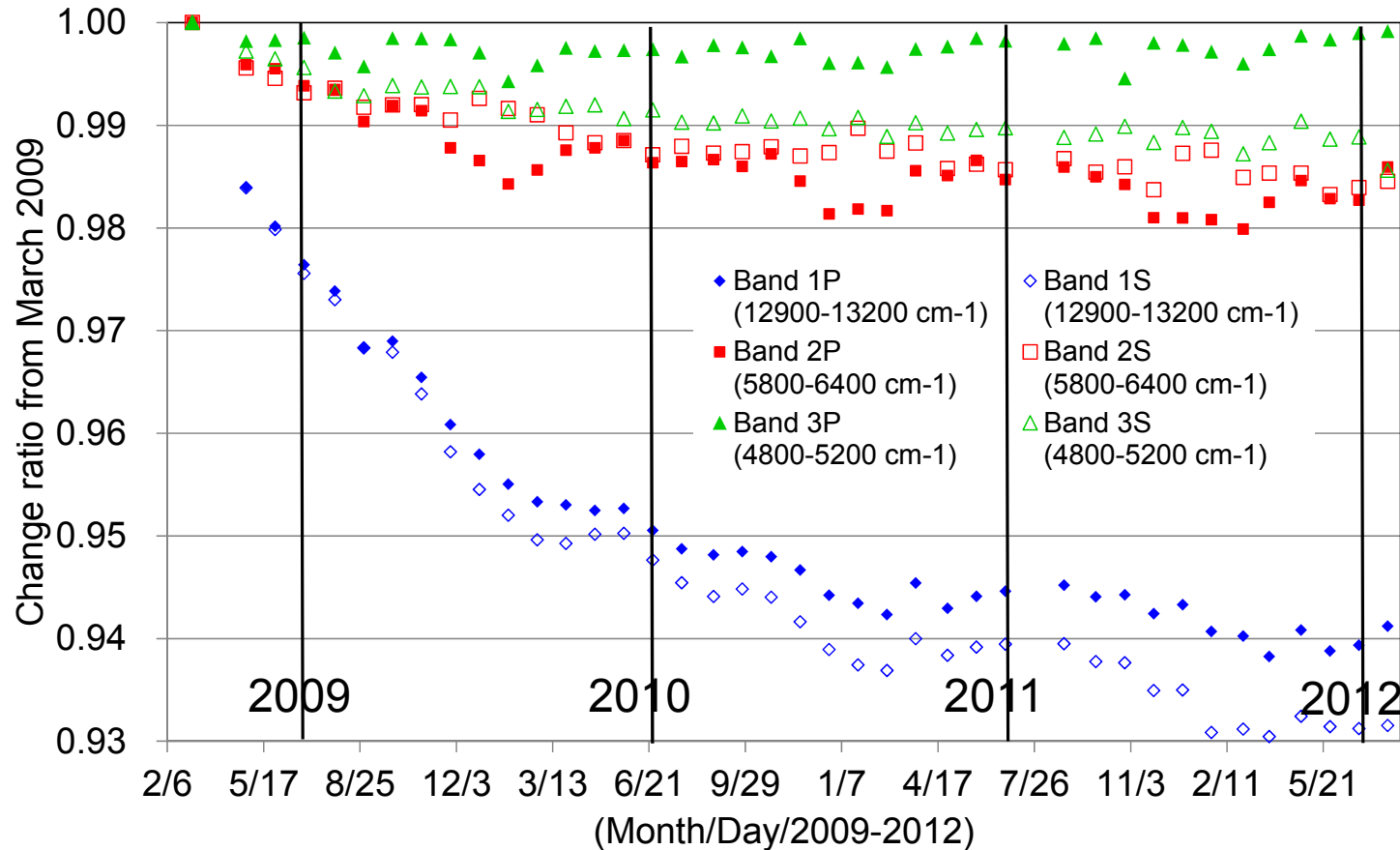
Deriving TANSO-FTS Calibration Coefficients



Spectra of modeled and measured radiances are shown in left panels for P polarization and bands B1, B2, B3 (rows). The measured values are adjusted using the preflight radiance conversion factors. Scatter plots of the measured versus modeled values are shown for P (middle panels) and S (right panels) polarizations. The slope of a linear least square fit line, forced to pass thru the origin, gives the calibration of the measured radiances relative to the modeled values (Kuze et al. in prep. 2012).



Throughput Degradation Rate Decreasing with Time



Results from Railroad Valley and the on-board solar diffuse indicate that the throughput degradation is greatest in Band 1 (O₂ A-Band), but the rate is decreasing in all 3 SWIR bands. The vertical lines indicate the time of the Vicarious Calibration Campaigns in 2009, 2010, 2011, and 2012.



Summary of Radiometric Calibrations for FTS SWIR and CAI

		Days from launch	TANSO-FTS			CAI			
			B1	B2	B3	B1	B2	B3	B4
Vicarious calibration (vs. pre-launch calibration)	June 23-July 4, 2009	160	$-11 \pm 7\%$	$-3 \pm 7\%$	$-4 \pm 7\%$	-17%	+4%	0%	-18%
	June 21-22 2010	520	$-14 \pm 7\%$	$-2 \pm 5\%$	$-6 \pm 5\%$	-21%	-4%	-4%	-20%
Solar diffuser plate (back side) (vs. onboard initial calibration)	June 2009	160	-2.7%	-0.9%	-0.4%	N/A	N/A	N/A	N/A
	June 2010	520	-5.1%	-1.6	-0.5%	N/A	N/A	N/A	N/A
Sahara	2009-2010		-2%	0%	0%	-1.6%	-4.0%	-1.2%	-1.1%
			April-September			June-Sep			

Shiomi et al. IWGGMS8

RRV: Provides the absolute calibration

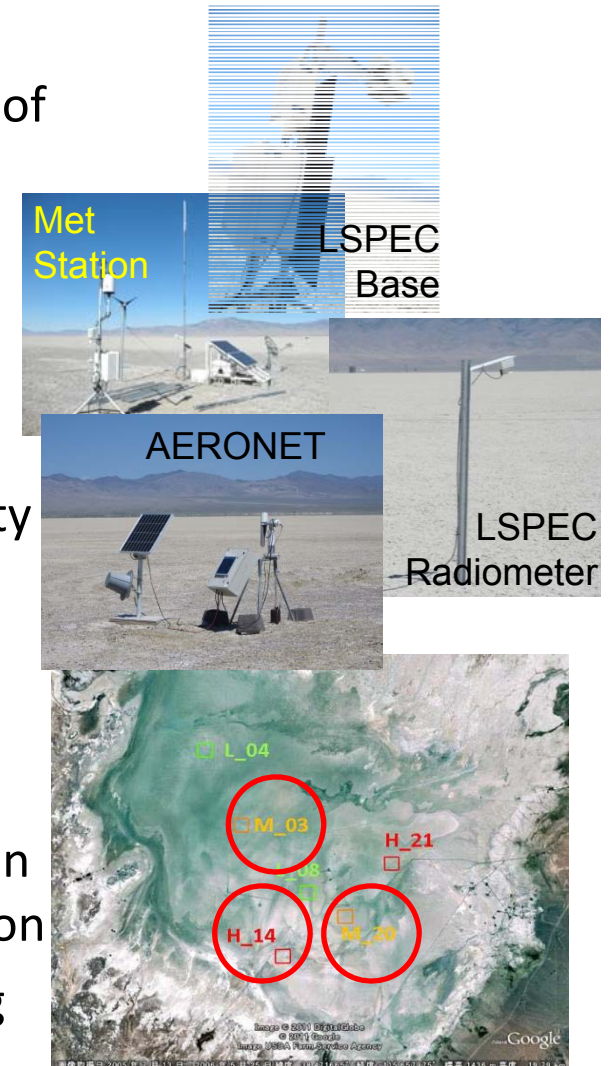
Solar diffuser plate: relative (monitoring change with time)

Sahara Data: relative (monitoring change with time)



Automated Vicarious Calibration at Railroad Valley

- To augment the temporal coverage provided by the annual RRV Vicarious Calibration campaigns, a series of automated spectrometers have been deployed at 3 locations on the RRV playa
- RRV deployment based on heritage from LED Spectrometer (LSPEC) deployment at Frenchman Flat
- Autonomous LSPEC surface measurements are combined with AERONET observations from University of Arizona (UofA) installation at RRV, and surface Meteorological data from the JPL station at RRV.
- Data are uplinked using a PC to satellite modem
- The 2012 RRV campaign was the first opportunity to provide a comprehensive, end-to-end cross calibration of the campaign instruments and the LSPEC installation
- Results from this intercomparison are currently being analyzed



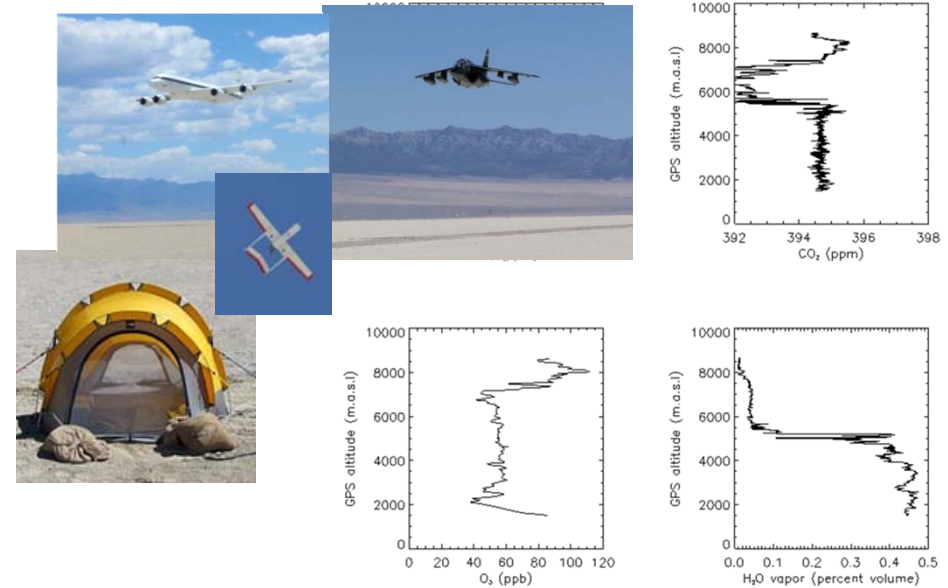
Components and locations of LSPEC installation on RRV





Characterizing the Atmosphere above RRV

- Because GOSAT TANSO-FTS collects data within atmospheric absorption bands, a comprehensive description of the atmosphere is needed to interpret RRV observations.
 - Meteorological observations are collected by a surface weather station and weather balloons
 - CO₂, CH₄, H₂O, and O₃ measurements are collected by Picarro cavity ringdown spectrometers at the surface, and installed in the Alpha Jet and Sierra UAV (NASA Ames)
- Aerosol measurements are collected by the RRV Aeronet station (University of Arizona)



Picarro spectrometers installed in the Alpha Jet, Sierra UAV, and at the surface measure CO₂ and CH₄.



Aerosol Optical Thickness from Aeronet Station

Meteorological data were collected by the surface weather station and by balloons.

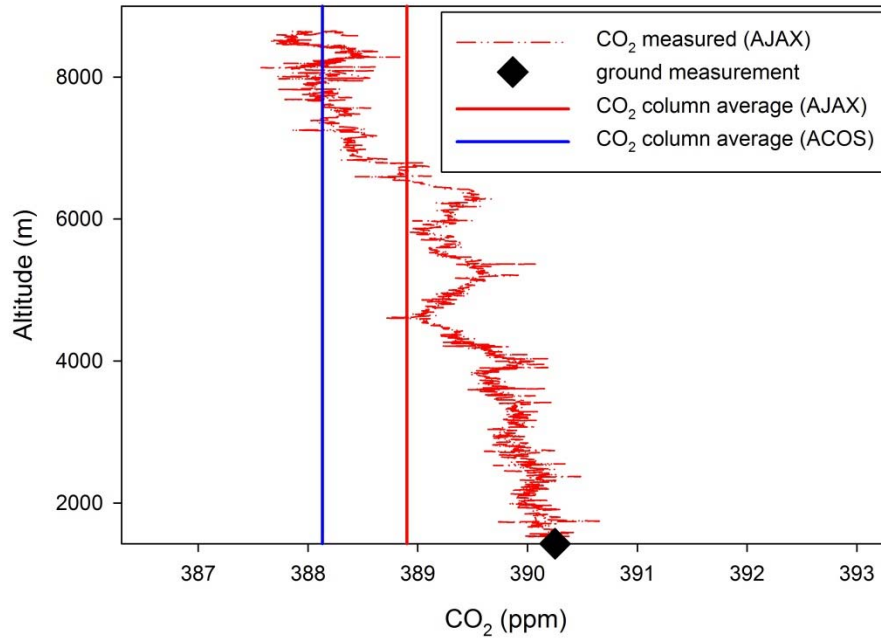


Comparison of Vertical Profiles to Columns

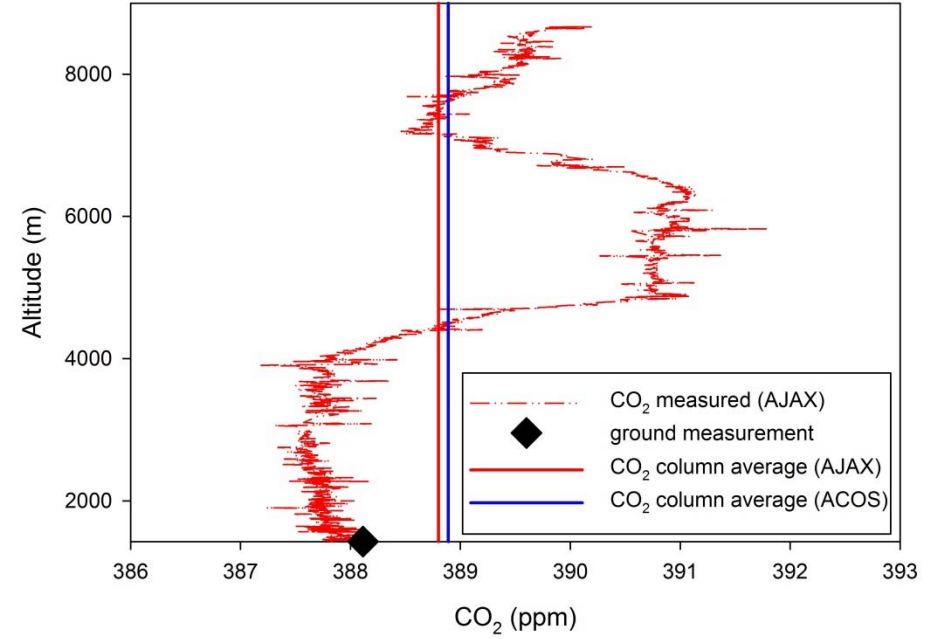


- Pressure-weighted average of in-situ data (NASA Ames), compared to satellite retrievals

CO₂ change with altitude 25.06.2011



CO₂ change with altitude 26.06.2011





The RRV Field Team

2009



2010



2011



2012





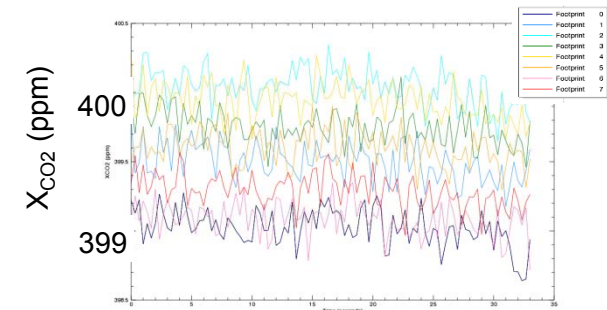
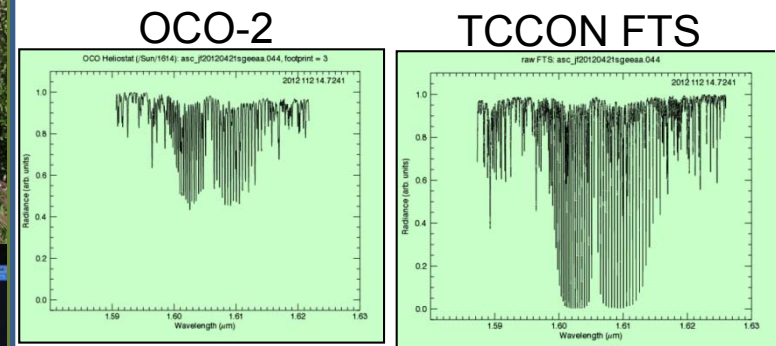
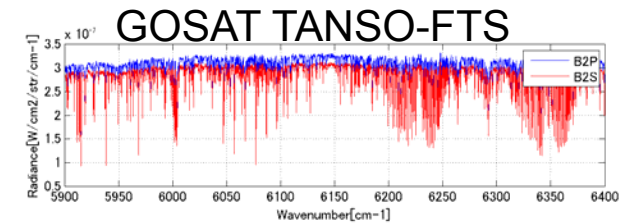
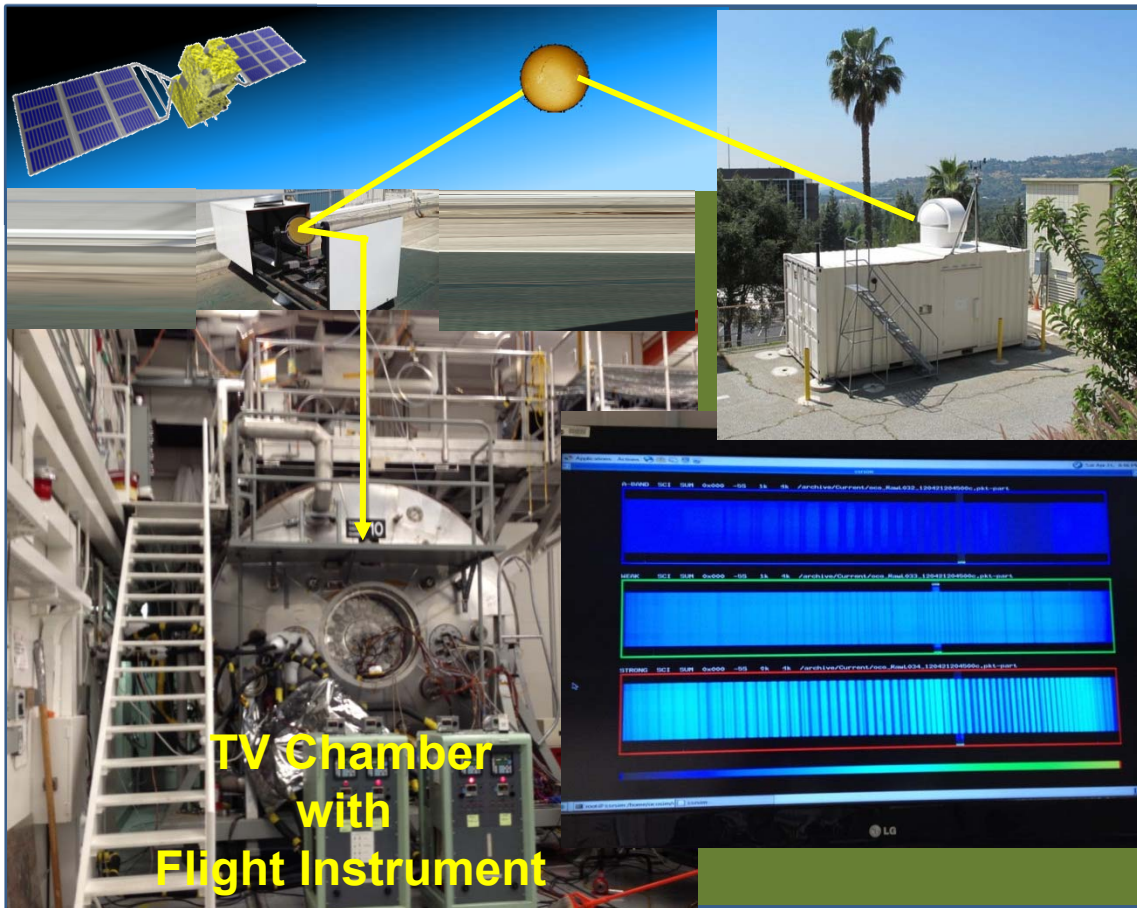
Bonus: Simultaneous TCCON, GOSAT, and OCO-2 Observations over Los Angeles

- The first simultaneous TCCON, GOSAT, and OCO-2 observations were recorded over the Los Angeles Basin on Friday, 20 April and Saturday, 21 April.
- The GOSAT TANSO-FTS collected targeted observations near JPL, Caltech, and downtown Los Angeles as it flew just to the east of LA on orbit path 36 at 1:47 PM Pacific Daylight Time.
- The OCO-2 flight instrument was collecting heliostat observations and the JPL TCCON station was recording near simultaneous up-looking atmospheric measurements to calibrate the OCO-2 instrument line shape.
- Near simultaneous OCO-2 and JPL TCCON observations were also collected Saturday 21 April, as GOSAT targeted the LA basin from the west, on orbit path 37.
- These observations will be analyzed as part of the ACOS GOSAT vicarious calibration program, and used to establish the relative performance of the OCO-2 and GOSAT TANSO-FTS instruments



Pre-Flight Instrument Qualification and Characterization

On April 20, 2012, simultaneous observations over the LA Basin were taken by GOSAT, the JPL TCCON Station, and the OCO-2 flight Instrument.



OCO-2 X_{CO2} Retrievals During Overpass

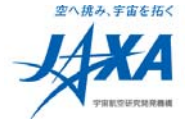


*Other GOSAT TANSO-FTS Calibration
Activities Supported by ACOS*

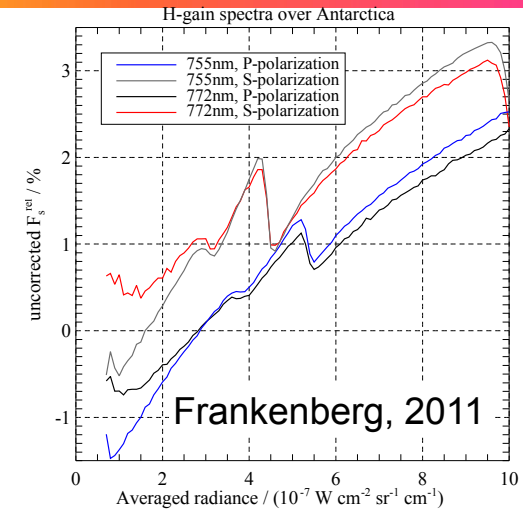




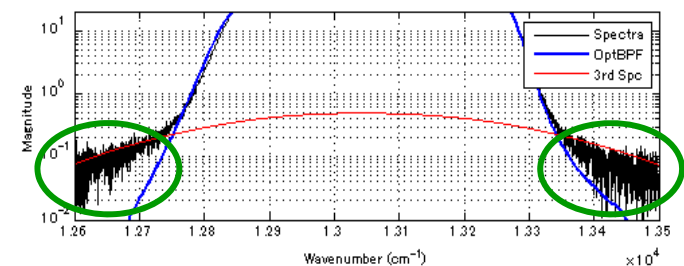
Diagnosing TANSO-FTS Band 1 (O₂ A-band) Nonlinearity



- Studies of solar Fraunhofer lines by ACOS team member, C. Frankenberg, showed that Band 1 has a non-linear response to incident radiation
 - Produces a -1 to +3% zero-level offset in spectra
- The ACOS team has been working closely with GOSAT calibration team members at JAXA to diagnose and correct this problem
 - JAXA engineers used the TANSO-FTS Engineering Model (EM) to characterize the non-linearity and to trace its source of to specific hardware components
 - ACOS team assessed the impact of proposed correction algorithms on surface pressure and X_{CO2} retrievals
- The non-linearity has been largely corrected in the latest version of the L1B products (v150.150)



The Band-1 non-linearity was discovered in studies of chlorophyll fluorescence, which revealed a signal-dependent zero-level offset (Frankenberg et al. 2012).

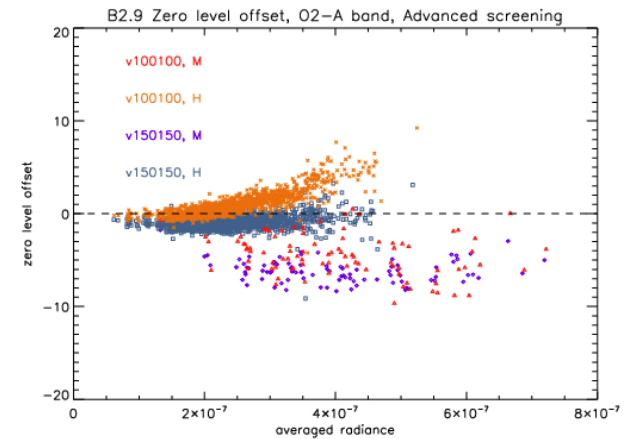


EM studies show that the Band-1 non-linearity also produces spurious out-of-band signals, proportional to intensity.

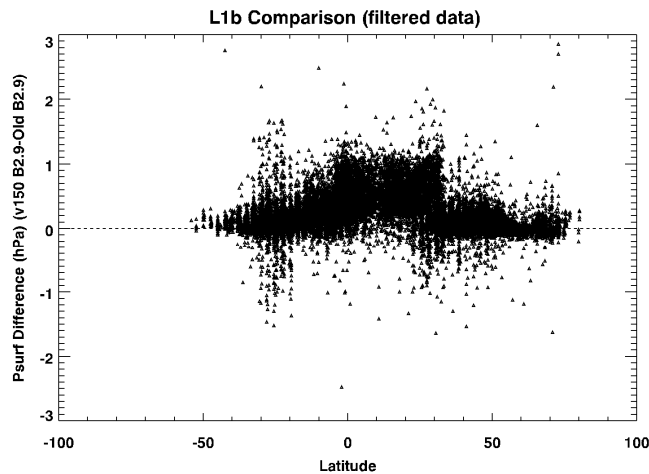


Impact of Band-1 Non-Linearity Correction

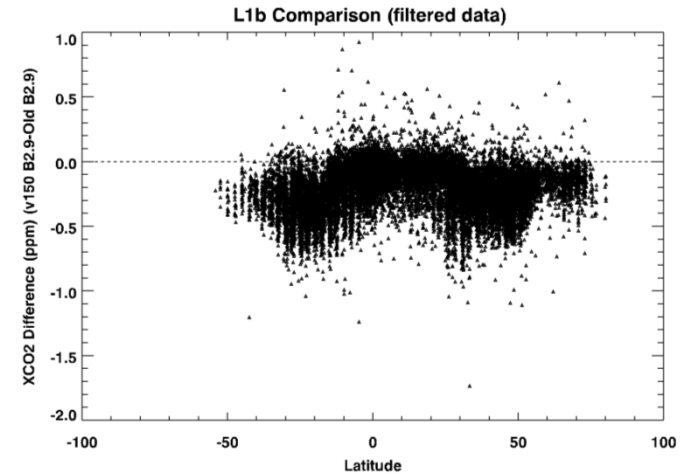
- To accommodate the Band 1 non-linearity, the ACOS team modified the L2 algorithm (B2.9) to retrieve a zero level offset correction for each sounding
- The ACOS team is now evaluating the impact of the Band-1 non-linearity correction in L1B v150.150
 - The retrieved H-gain zero level offsets are substantially reduced
 - Surface pressure retrievals increased by up to 1 hPa
 - X_{CO2} estimates have been reduced by up to 0.5 ppm



Zero level offsets with (v150150) and without (v100100) are compared.

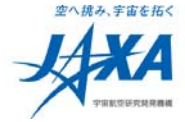


V150150 surface pressures are ~1 hPa higher (left) and XCO2 retrievals are ~0.5 ppm lower (right) than those in v100100

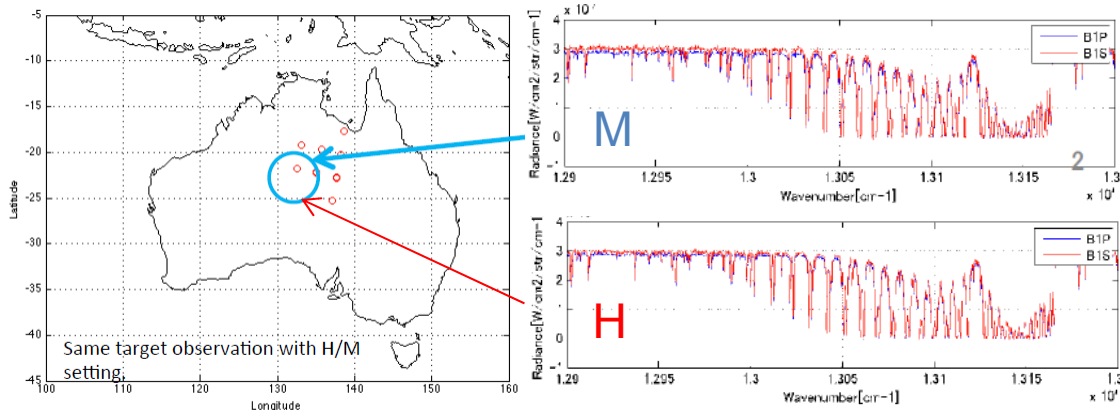
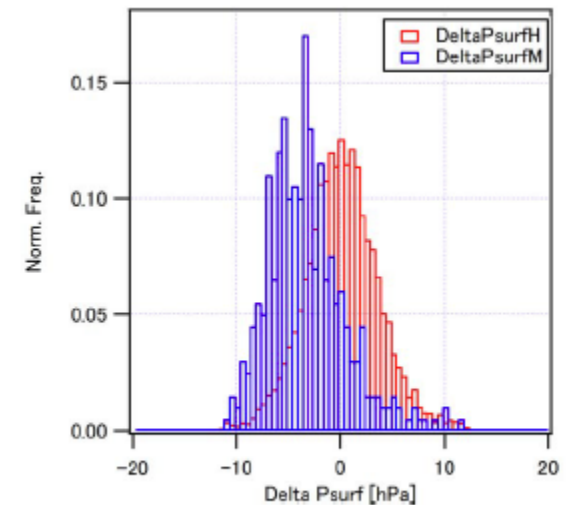
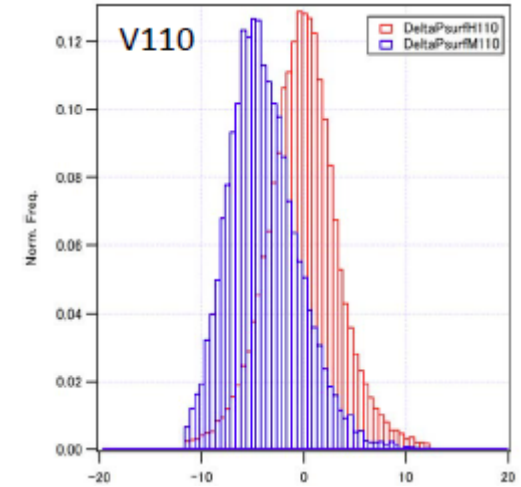




Biases between Gain M and Gain H Observations



- The non-linearity correction included in L1B v150.150
 - improves the zero level offset in the H-gain data
 - still yields a persistent bias between the high gain (gain-H) and medium gain (gain-M) results similar to that seen in earlier L1B products
- To investigate the origin of this bias, observations of central Australia were obtained in gain H and gain M on alternate repeat cycles, and the spectra from coincident footprints were compared.



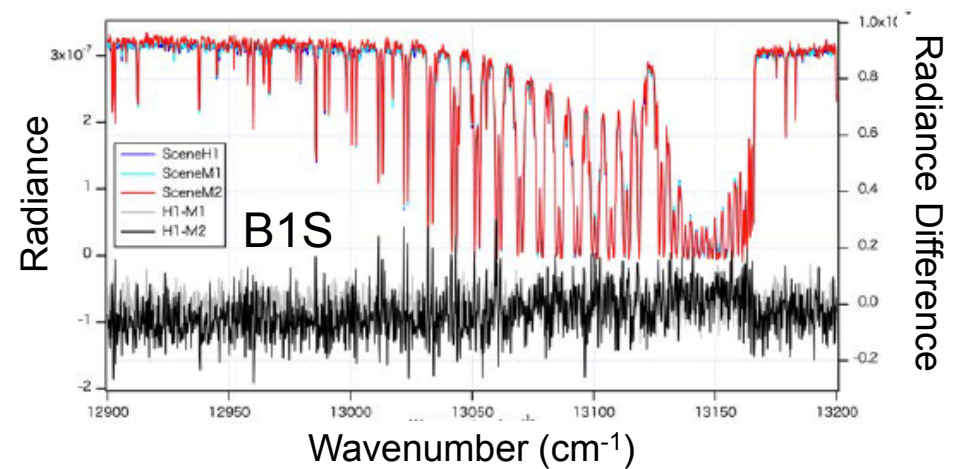
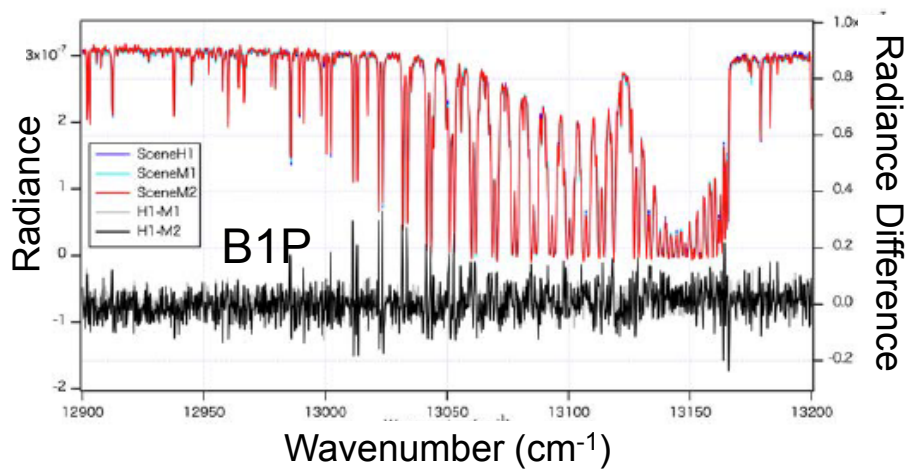
Examples of coincident soundings over Australia collected using Gains H and M on adjacent ground repeat cycles.



Diagnosing the source of Gain H/M Bias



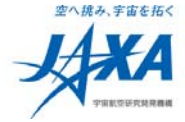
Time	Lat	Lon	XCO ₂	Psurf	ΔPsurf	MQF	Gain	SNR O ₂	Total	Ice	Kahn_2b	Kahn_3b	Water	
2012/05/05 03:02:35	145.78	-23.11	390.09	970.91	2.60	0	H	146.8		0.0805	0.0164	0.0210	0.0249	0.0182
									H	0.0143	0.0052	0.0018	0.0022	0.0052
									M	0.0313	0.0061	0.0084	0.0110	0.0058
									L	0.0348	0.0051	0.0109	0.0117	0.0072
2012/05/05 03:02:39	145.78	-23.10	391.74	969.42	1.05	0	H	138.9		0.0843	0.0170	0.0219	0.0246	0.0208
									H	0.0152	0.0051	0.0017	0.0020	0.0063
									M	0.0330	0.0068	0.0088	0.0107	0.0068
									L	0.0361	0.0051	0.0114	0.0119	0.0077
2012/05/05 03:02:44	145.78	-23.10	394.81	962.62	-5.63	0	M	92.3		0.0610	0.0115	0.0159	0.0167	0.0168
									H	0.0112	0.0036	0.0015	0.0016	0.0044
									M	0.0243	0.0046	0.0067	0.0071	0.0059
									L	0.0255	0.0033	0.0077	0.0081	0.0065



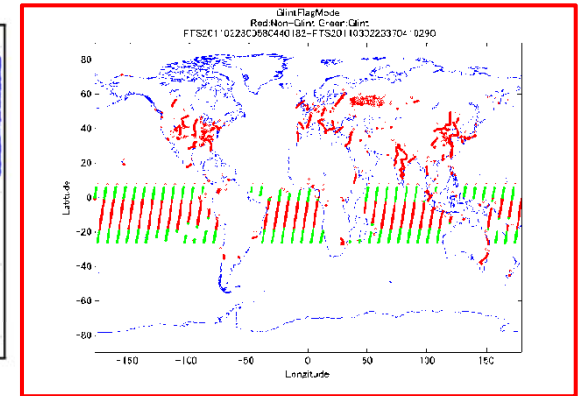
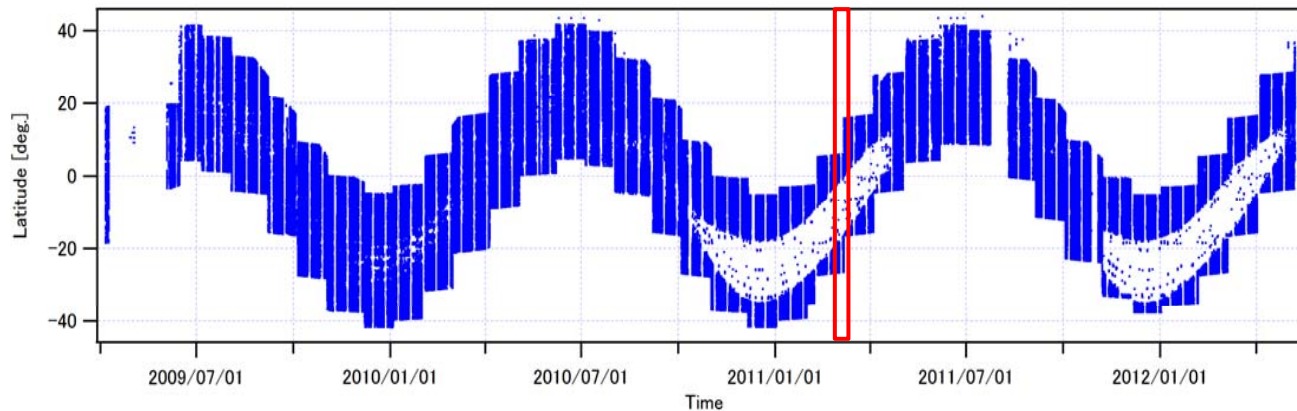
- Observations obtained in Gain M yield lower surface pressures and higher X_{CO₂} estimates
- Differences between Gains H and M are often highly correlated with gas absorption
- The cause of these differences is being tested with the TANSO-FTS Engineering Model



Correcting the Sun Glint Flag



Sun glint flags in V080,100,110,130, 150



- The ACOS team discovered an error in the TANSO-FTS sun glint flag in the L1B data, starting on 8/1/2010
 - This flag was not being set over much of the range of latitudes where sun glint observations were taken
- The ACOS team alerted JAXA to the problem and modified the ACOS L2 production algorithm (b2.9) to identify sun glint soundings.
- The sun glint flag was corrected in L1B v150.151 products

No-sun glint flag
Sun glint flag



Summary of TANSO-FTS L1 Products



Version	Date	Major Updates
V006.006	Jan., 2009	The first version
V007.007	Jul., 2009	Unit correction of spectral radiance Wavenumber correction Apodization of phase correction
V050.050	Oct., 2009	Low frequency and vignetting correction, Quality flag
V080.080	Feb., 2010	Pointing error telemetry correction Quality flag (spike flag) correction
V100.100	Mar., 2010	TIR polarization and radiometric correction
V110.110	Nov., 2010	TANSO-FTS band 4 (TIR) detector non- linearity correction TANSO-FTS band 1 speed instability correction (gain M)
V130.130	Apr., 2011	TANSO-FTS band 1 ADC non-linearity correction TANSO-FTS band 4 deep space view obscuration correction Sun glint flag correction
V150.150	Apr., 2012	<u>Non-linearity correction (B1)</u> Non uniformity correction of laser sampling intervals Band 1 gain M speed instability correction (modified) TIR ZPD detection (modified)
V150.151	Jun., 2012	Sun glint flag correction (corresponding to V130)



ACOS Calibration Publications

- Crisp, D., B. M. Fisher, C. O'Dell, C. Frankenberg, R. Basilio, H. Bösch, L. R. Brown, R. Castano, B. Connor, N. M. Deutscher, A. Eldering, D. Griffith, M. Gunson, A. Kuze, L. Mandrake, J. McDuffie, J. Messerschmidt, C. E. Miller, I. Morino, V. Natraj, J. Notholt, D. M. O'Brien, F. Oyafuso, I. Polonsky, J. Robinson, R. Salawitch, V. Sherlock, M. Smyth, H. Suto, T. E. Taylor, D. R. Thompson, P. O. Wennberg, D. Wunch, and Y. L. Yung: The ACOS CO₂ retrieval algorithm--Part II: Global XCO₂ data characterization, *Atmos. Meas. Tech.*, 5, 687–707, 2012, doi:10.5194/amt-5-687-2012.
- Frankenberg, C., Fisher, J. B., Worden, J., Badgley, G., Saatchi, S.S., Lee, J.-E., Toon, G. C., Butz, A., Jung, M., Kuze, A., and Yokota, T.: New global observations of the terrestrial carbon cycle from GOSAT: Patterns of plant fluorescence with gross primary productivity, *Geophys. Res. Lett.*, 38, L17706, doi:10.1029/2011GL048738, 2011.
- Kuze, A., O'Brien, D. M., Taylor, T. E., Day, J. O., O'Dell, C. W., Kataoka, F., Yoshida, M., Mitomi, Y., Bruegge, C. J., Pollock, H., Basilio, R., Helmlinger, M., Matsunaga, T., Kawakami, S., Shiomi, K., Urabe, T., and Suto, H.: Vicarious calibration of the GOSAT sensors using the Railroad Valley desert playa, *IEEE Trans. Geosci. Remote Sens.* 49, 1781-1795, doi: 10.1109/TGRS.2010.2089527, 2011.
- Sakuma, F., C. J. Bruegge, D. Rider, D. Brown, S. Geier, S. Kawakami, and A. Kuze, OCO/GOSAT preflight cross-calibration experiment, *IEEE Trans. Geosci. Remote Sens.* 48, 2010, doi: 10.1109/TGRS.2009.2026050



ACOS Level 2 (L2) Retrieval Algorithm Development



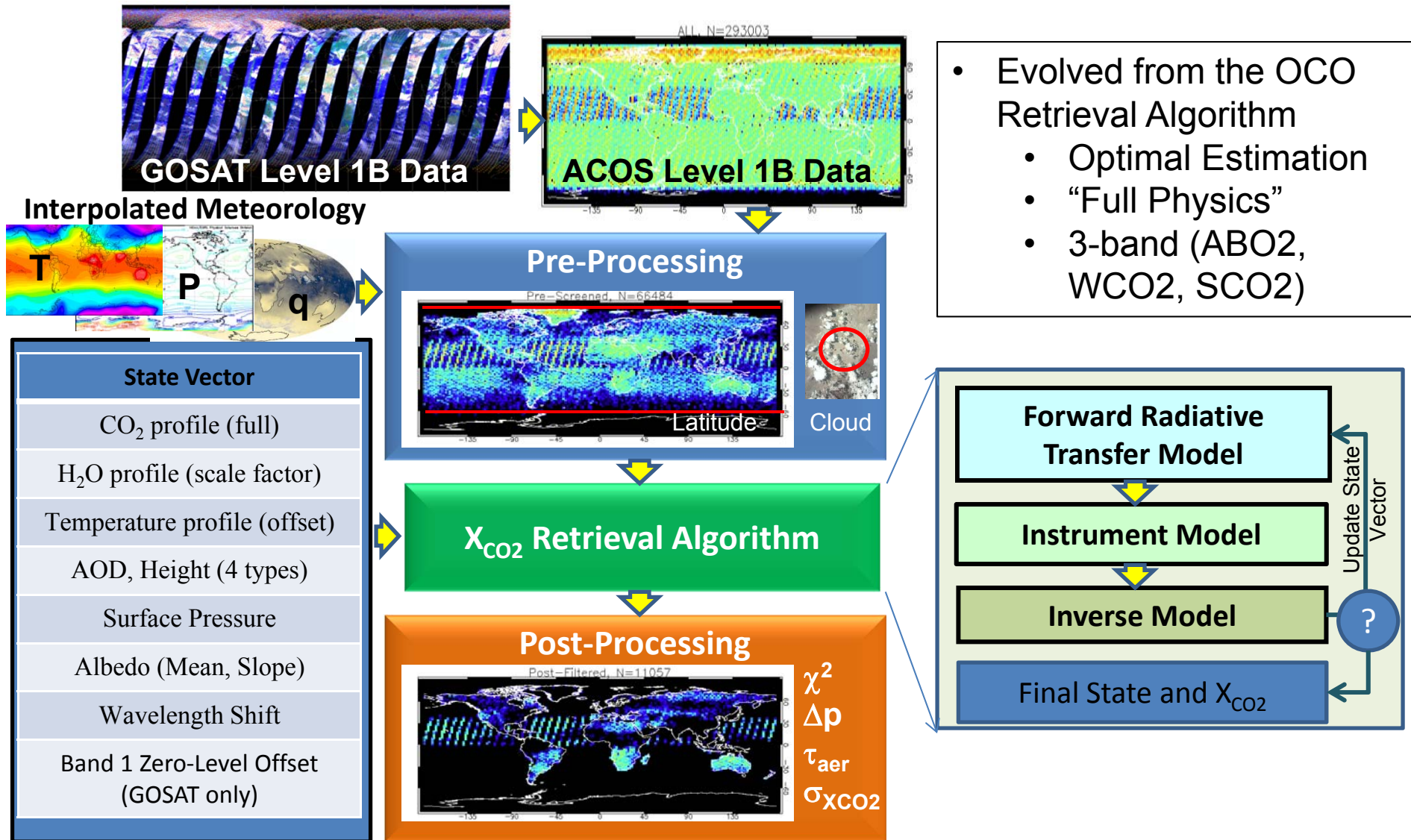


Retrieving X_{CO_2} from GOSAT TANSO-FTS Spectra

- The ACOS GOSAT X_{CO_2} retrieval approach evolved from the OCO retrieval algorithm, which is based on Bayesian optimal estimation (*Rodgers 2000; Bösch et al., 2006; Connor et al., 2008; Bösch et al., 2011; O'Dell et al., 2011*).
- The ACOS/OCO-2 X_{CO_2} retrieval algorithm incorporates the following major components:
 - Pre-processing filter: Identifies cloud-free soundings that are likely to converge and to initialize the surface-atmosphere state,
 - “Forward” radiative transfer model: Generates synthetic spectra,
 - TANSO-FTS instrument model: Simulates the observed spectral resolution and dispersion,
 - Inverse model: Updates the surface-atmosphere state to improve the agreement between the observed and simulated spectra, and
 - Post-processing filter: Identifies and rejects bad retrievals.



Retrieving X_{CO_2} from GOSAT Spectra



- Evolved from the OCO Retrieval Algorithm
 - Optimal Estimation
 - “Full Physics”
 - 3-band (ABO2, WCO2, SCO2)



The Preprocessor Module

- The pre-processing module uses the sounding geometry to determine the location of the footprint on the Earth's surface and interpolate meteorological fields to produce an initial guess for the surface and atmospheric state.
 - Operational forecasts of surface pressure, humidity and temperature profiles from the European Center for Medium Range Weather Forecasts (ECMWF) are used as priors.
 - These values are interpolated to the sounding location and elevation.
- The CO₂ a priori and covariance was originally derived from a multi-year global run of the Laboratoire de Météorologie Dynamique (LMDZ) global atmospheric transport model (Chevallier et al. 2010). This prior was replaced with the TCCON prior for B2.10
- The surface elevation over continents is determined from a digital elevation model (DEM) derived from data returned by the Shuttle Radar Topography Mission (SRTM), supplemented with other data sources at latitudes > 60° to yield 3 arc-second (~90 m x 90 m) resolution over the globe (Zong, 2008).



Objectives of the ACOS Levels 2 Algorithm Effort

The intent of this item was met, but TANSO-CAI data were not used in the ACOS production algorithm.

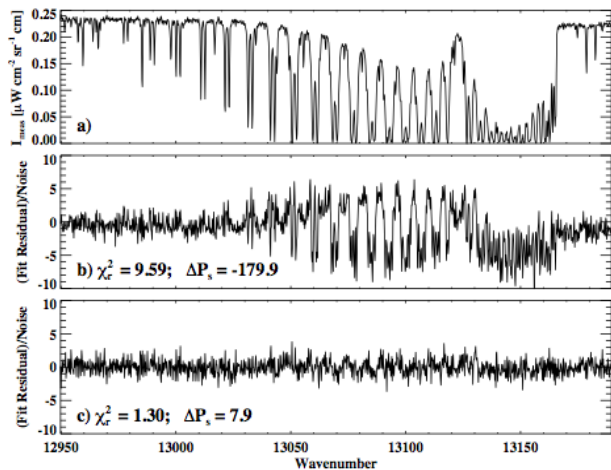
- Taylor et al. (2010) performed detailed comparisons between the results of the ACOS spectroscopic (ABO2) cloud screening method, a cloud screening method based on GOSAT TANSO-CAI observations nearly coincident MODIS data
 - All 3 methods agree > 80% of the time over land and 90% over ocean
 - ABO2 method was more accurate for identifying clear scenes
 - CAI method was more accurate for identifying cloudy scenes
 - Other factors, such as TANSO-FTS pointing errors, and the lack of true bore sighting between TANSO-FTS and CAI for glint reduce value of CAI further
- TANSO-CAI data were therefore not used in the production cloud screening code.

Taylor, T. E., O'Dell, C. W., O'Brien, D. M., Kikuchi, N., Yokota, T., Nakajima, T. Y., Ishida, H., Crisp, D., and Nakajima, T.: Comparison of cloud-screening methods applied to GOSAT near-infrared spectra, *IEEE Trans. Geosci. Remote Sens.*, 50, 295-309, doi: 10.1109/TGRS.2011.2160270, 2012.



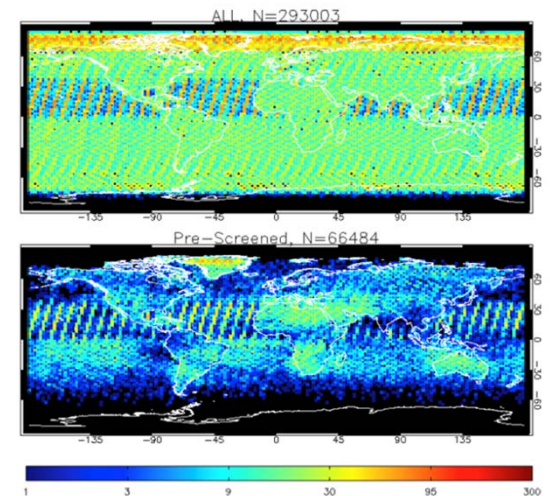
Pre-Processing Filters

- The ACOS GOSAT Pre-Processing Filters screen out the following L1B data:
 - Soundings acquired at solar zenith angles $> 85^\circ$
 - Soundings contaminated by optically-thick clouds
- A Spectroscopic cloud screening algorithm based on the O₂ A-band (ABO2) is currently being used for GOSAT retrievals (Taylor et al. 2011)
 - Fits a clear sky atmosphere to every sounding in the O₂ A band
 - High values of χ^2 and large differences between the retrieved surface pressure and the ECMWF prior indicate the presence of clouds



Example A-Band fit

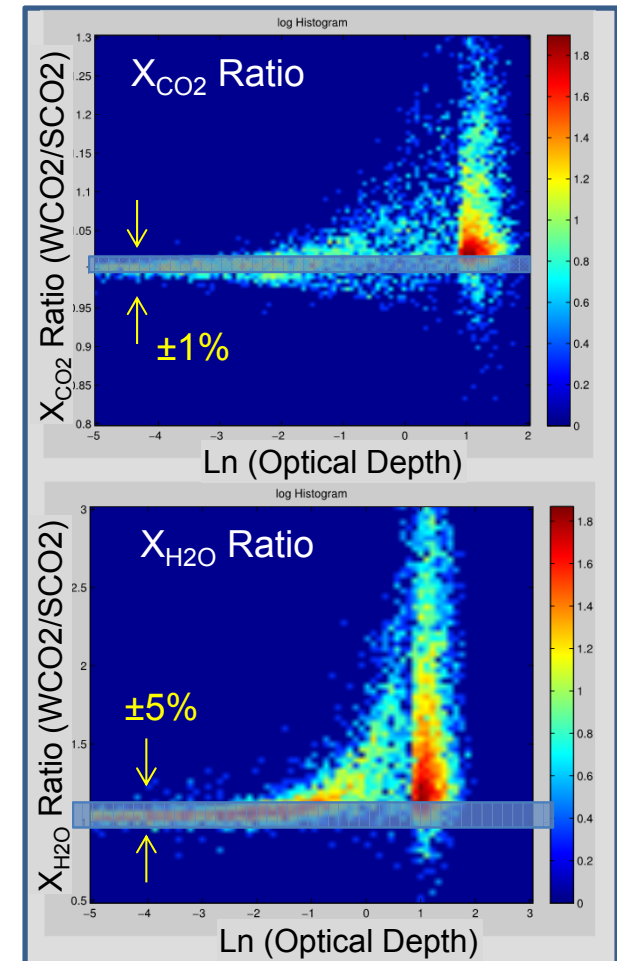
- Poor fit ($\chi^2 = 9.6$) indicates presence of cloud
- Small residuals and good agreement between retrieved and ECMWF surface pressure indicates cloud free sounding





The ACOS Cloud Filter

- The ABO2 cloud screen works well on optically thick altostratus and cirrus clouds, but
 - Simulator experiments and comparisons with MODIS cloud products indicate that it misses 20-30% of low clouds
- A modified cloud filter using a fast, Iterative Maximum A posteriori-Differential Optical Absorption spectroscopy (IMAP-DOAS) method, is currently being tested
 - The new screen combines the A-band cloud screen with IMAP-DOAS screens excluding soundings where:
 $0.99 < X_{CO_2}(1.61 \mu\text{m})/X_{CO_2}(2.06 \mu\text{m}) > 1.01$ or
 $0.95 < X_{H_2O}(1.61 \mu\text{m})/X_{H_2O}(2.06 \mu\text{m}) > 1.05$
 - Comparisons with simulations indicate that this methods eliminates almost all low clouds



Many soundings with large cloud optical depths that are missed by the A-band filter are caught by the X_{CO_2} and X_{H_2O} ratio filters.



Use of Machine Learning for Sounding Selection

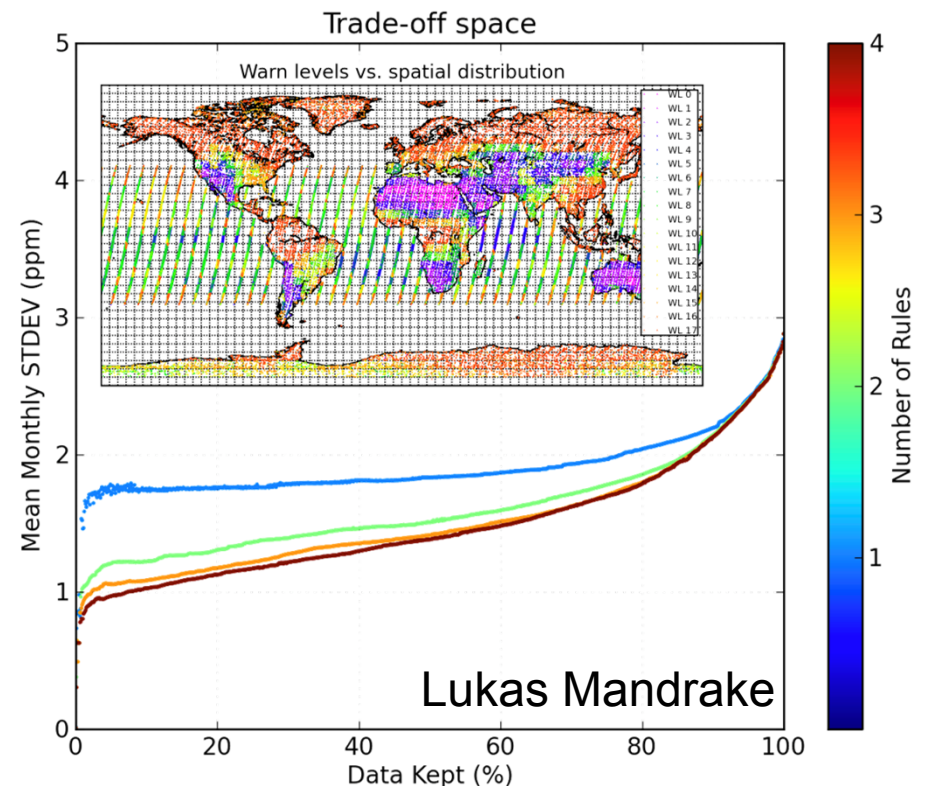
Issue: OCO-2 will gather up to 96 times as much data as GOSAT, but, like GOSAT, up to 80% of the soundings are compromised by clouds, ice, other issues.

Challenge: How do we (rapidly) select the best ~6% to process through Level 2?

Solution: Design a Sounding Selector to find “best” soundings using L1B data alone.

Used Machine Learning to develop a method that autonomously constructs a sounding selector for GOSAT data

- User specifies X% of data to retain, selector returns which soundings to process
- Guarantees uniform spatial and temporal coverage, minimal data distortion, and runs instantly
- Depends on two, well-understood, ACOS OCO-2-derived quantities with easily interpreted rules





Machine Learning as a Tool for Debugging/Research Support

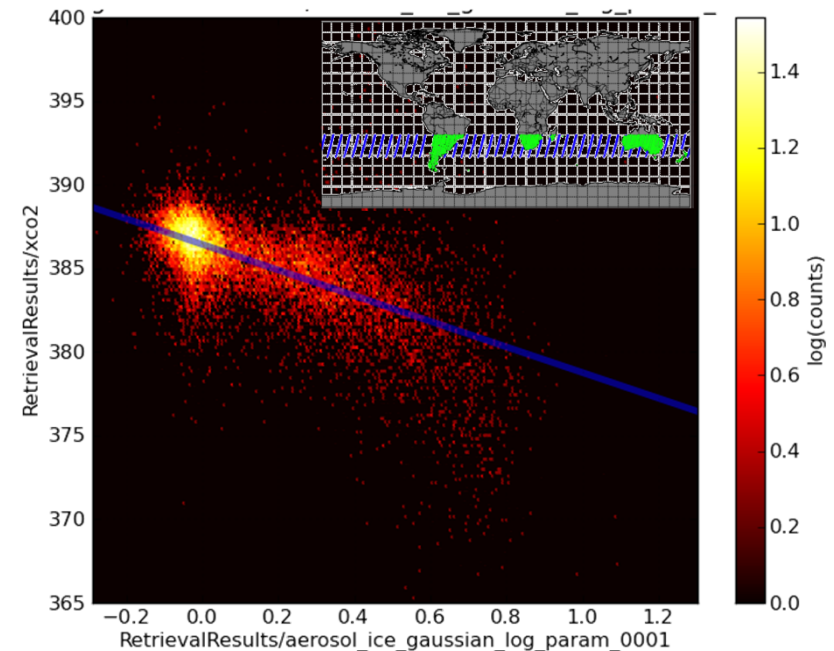
Issue: Retrieval algorithm must reliably generate CO₂ estimates or report failure

Problem: Confounding influences in data and algorithm can generate erroneous CO₂

Approach: Analyze erroneous CO₂ behavior to discover influencing factors

GOSAT soundings in the southern hemisphere, where X_{CO_2} has little variability, are explored to find top factors responsible for

- linear trends in X_{CO_2}
- high scatter in X_{CO_2}
- Used *Recursive Feature Elimination* (RFE) methods that maintain relationships between multiple influencing factors
 - Conventional two-parameter correlation methods often miss multi-parameter relationships
 - RFE catches far more of these relationships



Relationship between retrieved X_{CO_2} and ice cloud distribution in the southern hemisphere. Such 2-d correlation plots are useful, but often miss multi-parameter relationships, such as the influence of ice clouds over bright surfaces on X_{CO_2} retrievals.

Lukas Mandrake



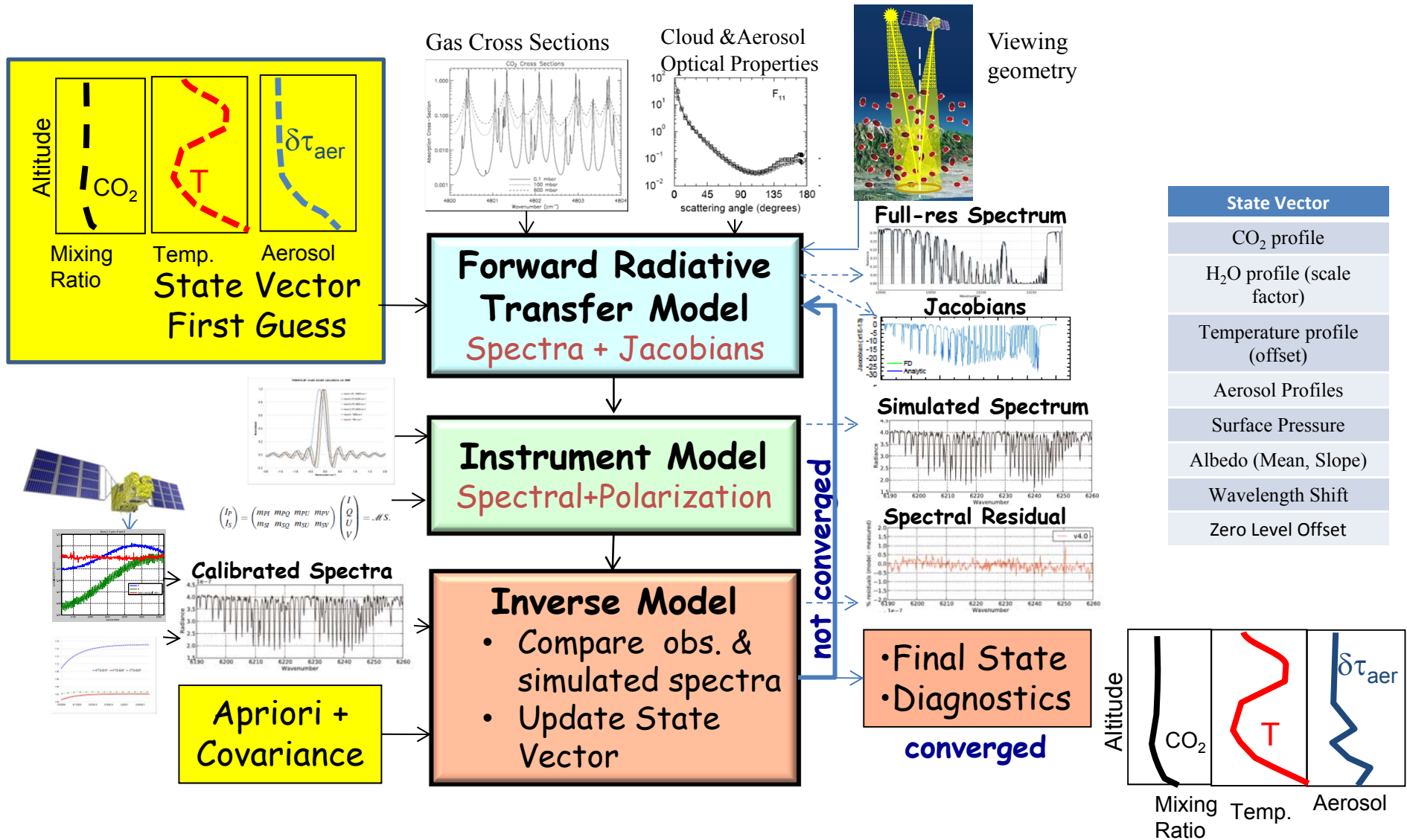
The ACOS X_{CO_2} Retrieval Algorithm

The ACOS Level 2 retrieval algorithm is based on the OCO “Full Physics” algorithm, which incorporates

- A spectrum-resolving (line-by-line) multiple scattering **forward radiative transfer model**, to generate a synthetic spectrum, given an assumed atmospheric state, illumination geometry, and viewing geometry;
- An **instrument model**, to match the spectral resolution, sampling, and polarization of the flight instrument, to produce a simulated spectrum that can be compared to the observed spectrum;
- An **inverse model**, to adjust the properties of the atmospheric state to improve the fit between the observed and simulated spectrum.



The ACOS "Full Physics" X_{CO_2} Retrieval Algorithm





The ACOS/OCO-2 Forward Model

- Given an initial guess for the atmospheric and surface state and the solar illumination and observing geometry for a specific TANSO-FTS sounding, the forward radiative transfer model generates:
 - Synthetic radiance spectra within the $0.76 \mu\text{m}$ O_2 A-band (ABO2) and for the CO_2 bands centered near 1.61 (WCO2) and $2.06 \mu\text{m}$ (SCO2).
 - Radiance Jacobians within each of these bands for use in the inverse model.
- Two types of radiative transfer calculations are performed to generate the Stokes vector at each monochromatic wavelength (c.f. O'Dell et al. 2012):
 - A scalar radiance calculation is performed using the discrete ordinate model, LIDORT 3.0 (Spurr, 2004).
 - A fast, vector 2-orders of scattering model, LRAD (Natraj and Spurr, 2007; Natraj et al. 2008) is used to estimate the degree of polarization for each sounding to correct the scalar results.
- The “Low Streams Interpolation” method (O'Dell 2010) is used to reduce the computational expense of these calculations.



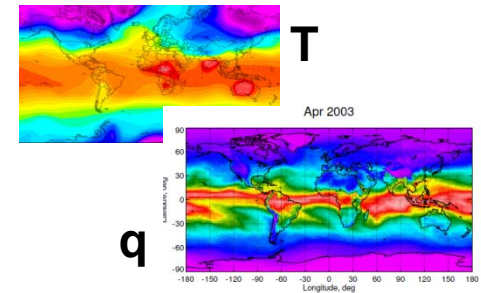
Inputs to the ACOS/OCO-2 Forward Model

- The forward radiative transfer model generates synthetic radiance spectra within the $0.76 \mu\text{m}$ O₂ A-band (ABO2) and for the two CO₂ bands centered near 1.61 (WCO2) and $2.06 \mu\text{m}$ (SCO2), given the following input:
 - Initial guess for the atmospheric and surface state, including surface pressure, surface and atmospheric temperatures, trace gas mixing ratio profiles, and vertical profiles for four aerosol types,
 - Sounding solar illumination and observing geometry,
 - Absorption cross-sections for CO₂, H₂O, and O₂ within these spectral ranges are read from pre-computed tables (Thompson et al. 2012).
 - Tables are currently calculated at 71 pressure levels between 5 and 102,034 Pa.
 - At each level, cross sections are derived for 19 temperatures, spaced at 10 K.
 - The spectral grid is equally-spaced with a resolution of 0.01 cm^{-1} .
 - The wavelength-dependent optical properties of the four airborne particle types are read from pre-computed tables (O'Dell et al., 2011).
 - Top-of-atmosphere solar flux, consisting of a full-disk version of the high resolution solar line list superimposed on a solar continuum from SOLSPEC.
- All of these inputs have received substantial attention through the ACOS effort.



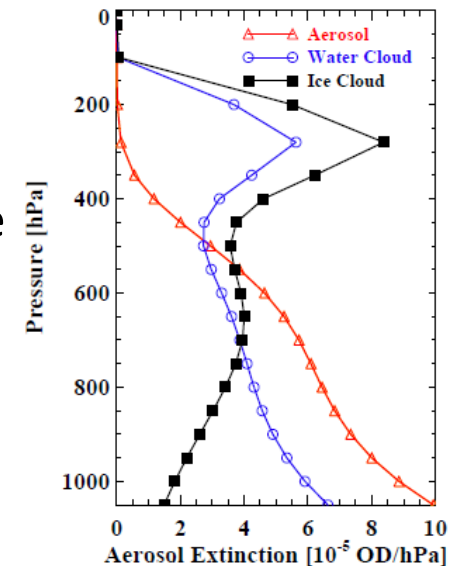
The ACOS/OCO-2 Atmosphere Prior

- Temperature and water vapor profiles - ECMWF forecast profiles are interpolated to the retrieval FOV. For a given retrieval, these profile shapes are fixed and an offset is retrieved with 1-sigma uncertainties of 5K and 0.5, respectively.



- Aerosol profiles - Four aerosol types are used. A Gaussian profile is assigned to each.
 - For a given retrieval, the width, amplitude, and altitude of each distribution is retrieved.

Aerosol Type	Extinction Efficiency			Single Scattering Albedo		
	0.76 μm	1.61 μm	2.06 μm	0.76 μm	1.61 μm	2.06 μm
Kahn Type 2b ¹	0.934	0.842	0.580	0.933	0.980	0.972
Kahn Type 3b ¹	0.773	0.318	0.213	0.881	0.876	0.856
Water Cloud, $R_e = 8 \mu\text{m}^2$	2.131	2.224	2.268	1.000	0.991	0.950
Ice Cloud, $R_e = 70 \mu\text{m}^3$	1.537	1.610	1.678	1.000	0.882	0.794



Vertical Profiles of each aerosol type used in the prior (O'Dell et al., 2012).

Optical properties of cloud and aerosol types in retrieval state vector.

¹ Kahn et al. (2001); ² Gamma distribution (Hansen and Travis, 1974); ³ Non-spherical particles according to Baum et al. (2005a,b)



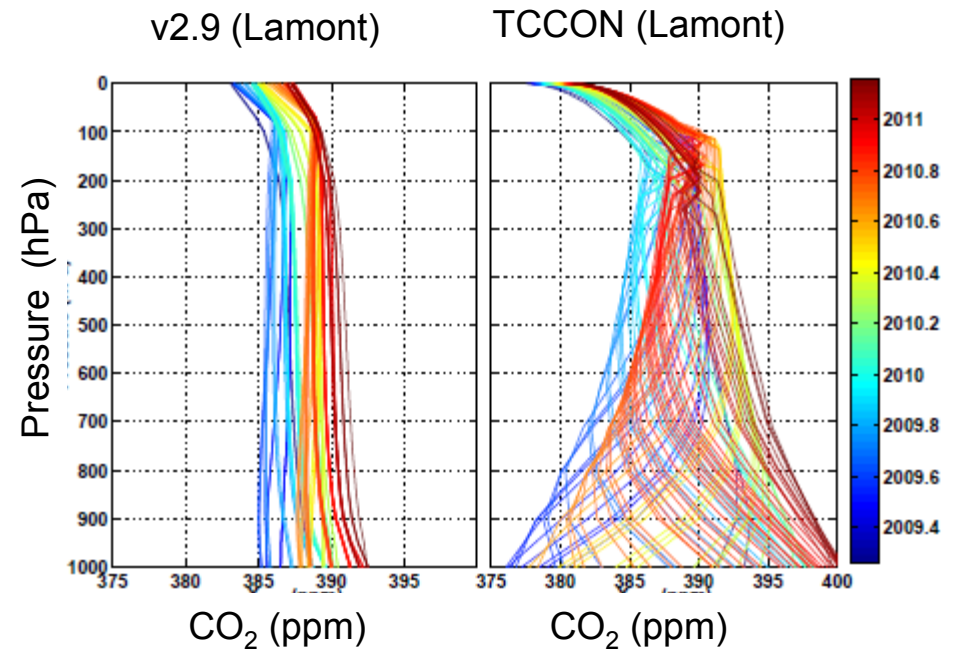
The ACOS/OCO-2 Surface Prior

- Surface pressure - ECMWF forecast values are interpolated to the retrieval FOV and corrected for elevation. For this value, the surface pressure is retrieved with a 1-sigma uncertainty of 4 hPa.
- Surface albedo -
 - Land - Surface albedos are retrieved for each of the three bands by a mean value and slope. The prior means are defined by the continuum radiances in each band and prior slopes assigned to zero. The a priori mean value error is set wide open at 1 and slope error set such that the albedos at band edges vary by 50%.
 - Water - A Cox-Munk distribution is assumed. The prior for its two parameters are defined as follows:
 - The refractive index parameter is taken as constant within each band with a 1-sigma uncertainty of 0.005.
 - The wind speed prior mean is defined by the continuum radiance in the weak CO₂ band through the use of a semi-empirical model with a 1-sigma uncertainty of 3.3 m/s.



The ACOS/GOSAT CO₂ Prior

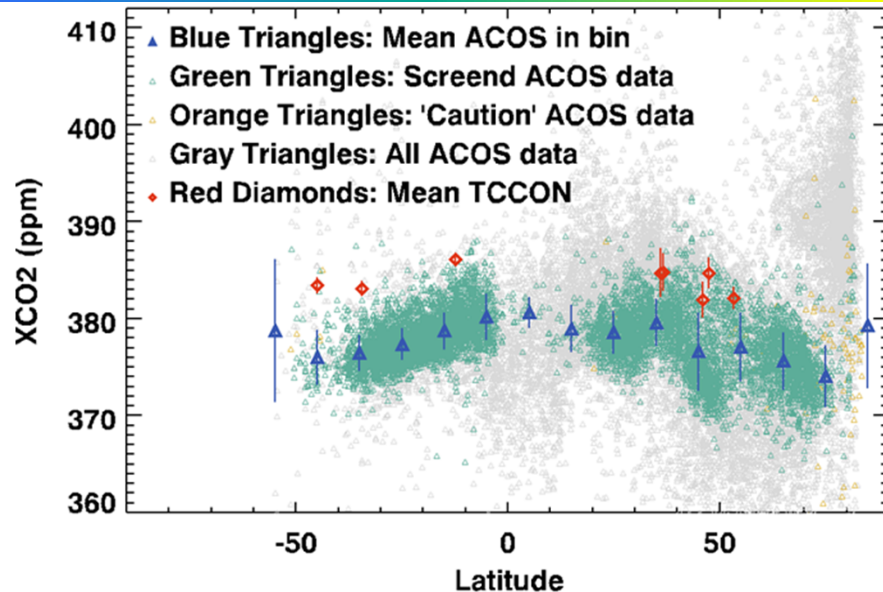
- The ACOS retrieval algorithm started with a relatively narrow CO₂ a priori mixing ratio and covariance in the troposphere, a fixed tropopause height and relatively high CO₂ mixing ratios in the stratosphere.
- Starting with b2.10, the ACOS team adopted the TCCON prior, which accommodates
 - a much larger (less constraining) range of CO₂ mixing ratio in the lower atmosphere,
 - a more realistic, spatially and temporally variable tropopause height
 - More realistic stratospheric CO₂ mixing ratios



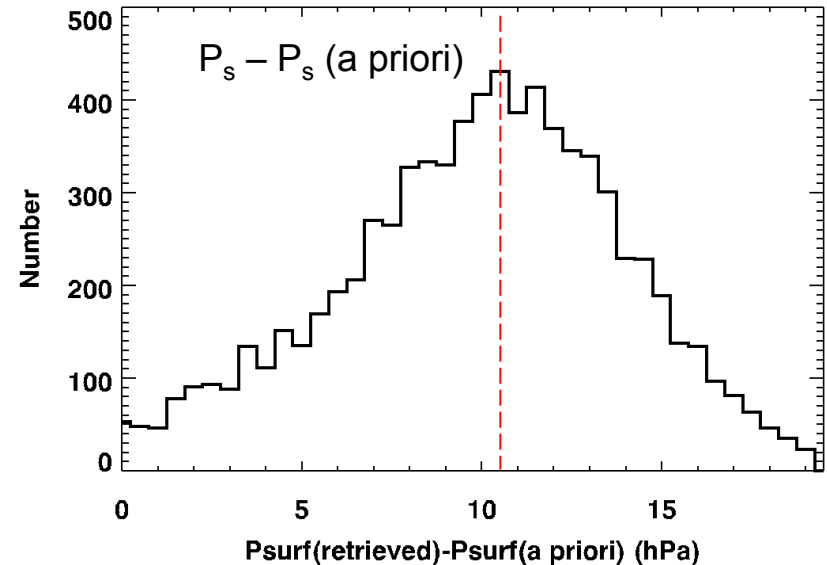
The CO₂ prior used by all ACOS versions before b2.10 (left) is compared to the TCCON CO₂ prior (right). Differences in the priors complicate efforts to interpret differences between X_{CO_2} estimates by these two systems (Wunch et al. 2011).



Biases in Early ACOS X_{CO_2} Products



ACOS GOSAT X_{CO_2} estimates (green and grey triangles) and their zonal averages (blue triangles with 1σ errors) are compared to TCCON X_{CO_2} estimates (red diamonds).



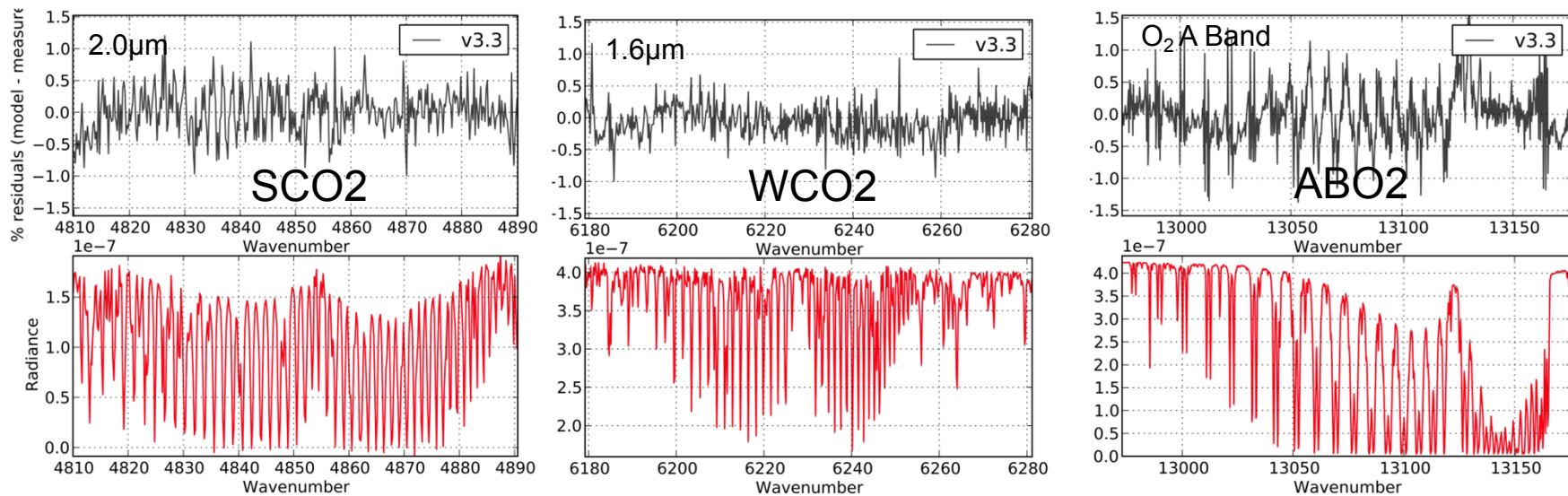
Global histogram of differences between retrieved surface pressures and a priori (ECMWF) surface pressures show a ~ 10 hPa bias.

- Initial comparisons of ACOS GOSAT and TCCON retrievals showed a consistent global bias of $\sim 2\%$ (7 ppm) in X_{CO_2} when compared with TCCON and aircraft measurements.
- About 2/3 of this bias is associated with a ~ 10 hPa (1%) high surface pressure bias, that was traced to limitations in the Oxygen A-band spectroscopy.
- Much of the remaining bias is associated with uncertainties in CO_2 spectroscopy



Evidence of Shortcomings in Gas Absorption Coefficients

- Persistent spectrally-dependent residuals in ensembles of GOSAT and TCCON retrievals provide additional evidence of shortcomings gas absorption cross sections
 - Residuals correlated with spectral features limit the retrieval algorithm's ability to exploit the full information content of the spectra, and converge to a unique, best estimate of X_{CO_2}



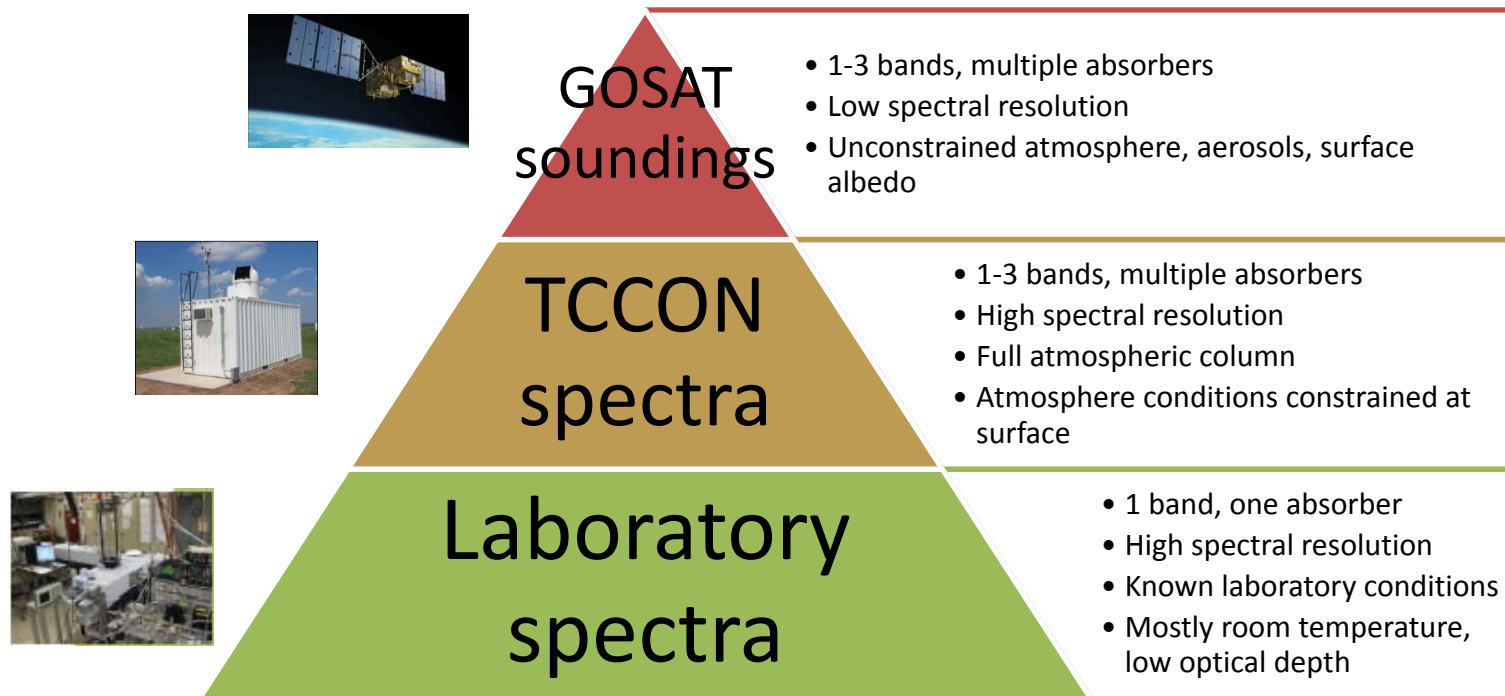
Persistent spectral residuals are seen in all 3 bands used to retrieve X_{CO_2} from GOSAT spectra. Those in the SCO2 and ABO2 are most strongly correlated with the band structure. These issues do not impair TCCON X_{CO_2} retrievals, because TCCON uses the WCO2 and O2 $^1\Delta_g$ band instead of the A-band in these retrievals.



Improved Gas Absorption Cross Sections

The ACOS ABSCO team embarked on a three-element approach to improve our understanding the CO₂ and O₂ absorption bands needed to retrieve X_{CO2}, including:

- New laboratory measurements (Long path FTS, Cavity Ring-down, Photoacoustic)
- Ground-based direct solar observations from TCCON
- GOSAT measurements





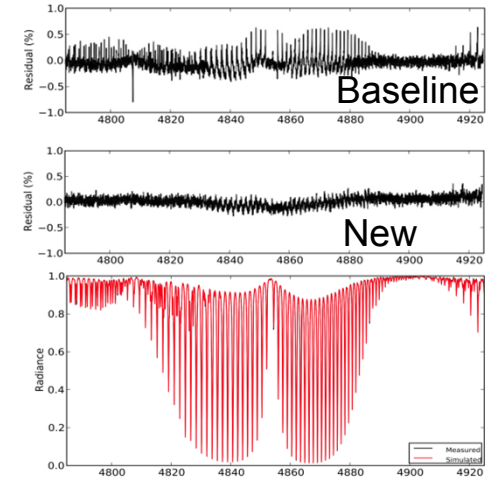
Advances in Laboratory Measurements

- The initial focus was on the CO₂ bands at 1.61 and 2.06 microns
 - Exploiting available measurement capabilities and recent advances in instrumentation and measurement techniques
 - Improved characterization of trace gas composition, temperature, and optical path length in convention, long-path absorption cells
 - New methods, including Frequency Stabilized Cavity Ring-Down (FS-CRDS) and Photoacoustic methods, that provide high signal-to-noise ratios over a wide dynamic range, facilitating measurements of weak absorption
 - Advanced, multi-spectral fitting techniques, that derive spectral line parameters (positions, strengths, widths, pressure shifts) from ensembles of spectra collected for a range of optical paths, pressures, temperatures, and absorbing gas concentrations
 - Self-consistent treatment of line mixing and line shapes that include speed-dependence and collisional narrowing as well as pressure and Doppler broadening effects
 - This investigation has yielded dramatic improvements in our ability to fit laboratory measurements of CO₂

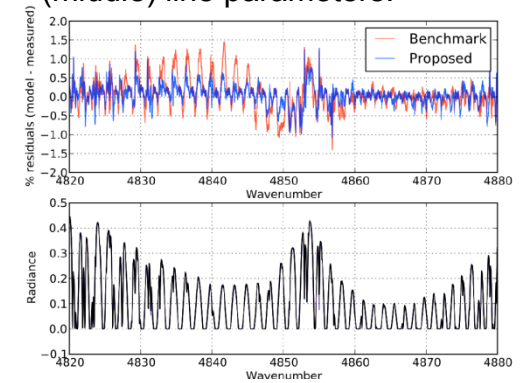


Measurements of Atmospheric CO₂

- The new, self-consistent line parameters yielded substantial improvements in fits to laboratory measurements of CO₂
 - Typical peak-to-peak residuals were reduced from 0.5% to 0.1%
- The use of these new line parameters in X_{CO₂} retrievals from TCCON and GOSAT spectra also yielded reductions in both bias and spectrally-dependent residuals, but these reductions were more modest than those seen in the lab.
- These differences in performance may be associated with the physical conditions (e.g. vertical variations in p, T, or gas amount) or absorbers (e.g. water vapor line and continuum absorption) that were not included in the lab measurements.



Lab measurements of the SCO₂ band (bottom) shown with residuals for baseline (top) and revised (middle) line parameters.



TCCON measurements of the SCO₂ band (bottom) shown with residuals for baseline (red) and revised (blue) line parameters.

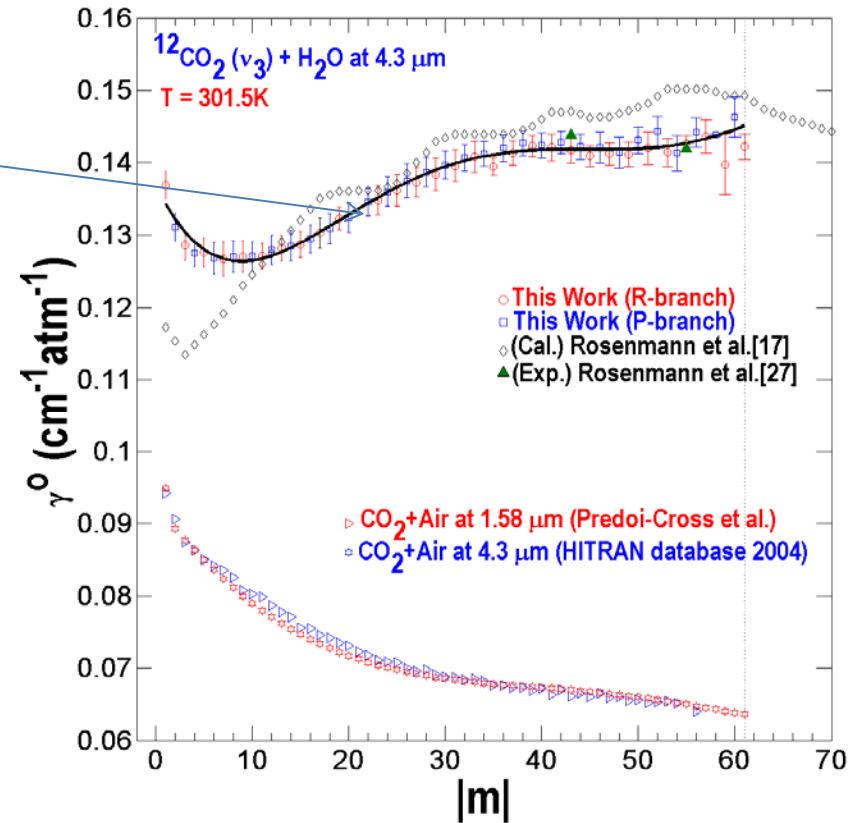


CO₂ lines broadened by H₂O

- Two recent publications suggest that water vapor broadens CO₂ lines much more effectively than air (~1.8x).
- Consistent results now available from 2 different experiments

	Sung et al. (4.3 μm)	Wallace et al. (1.6 μm)
	half widths (cm ⁻¹)	halfwidth (cm ⁻¹)
R14	0.1287 (±1.4 %)	0.136 (±19.8 %)
R16	0.1303 (±1.6 %)	0.134 (±17.9 %)
R18	0.1323 (±1.2 %)	0.133 (±20.3 %)

- Unlike air broadening and self broadening, which decrease with increasing rotational quantum number |m|, water broadening of CO₂ increases with increasing |m|.
- New measurements are being conducted to confirm these results and assess their impact on XCO₂ retrievals from TCCON and GOSAT.



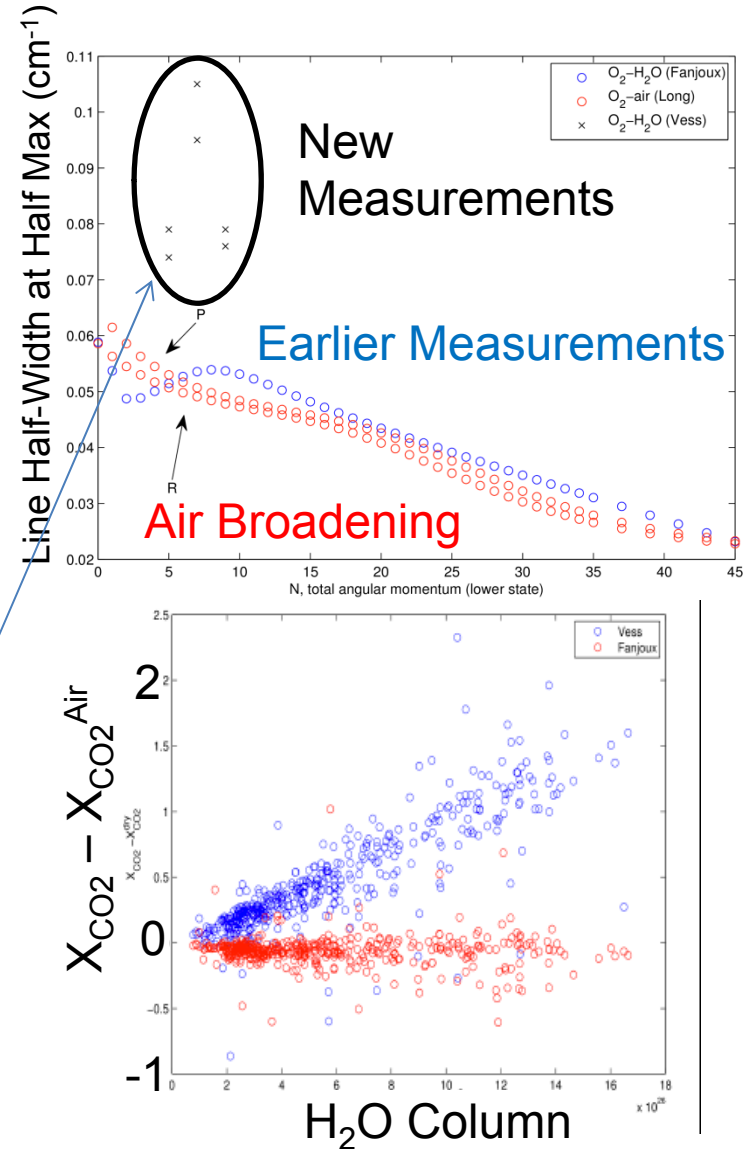
Water broadened half-widths of CO₂ (top) is compared to air broadened half widths (bottom) as function of rotational transition, |m|.

* K. Sung, L. Brown, RA Toth, T. J. Crawford, *Can J. Phys*, **87**, 469-484 (2009)



Causes and Impacts of Column O_2 Biases

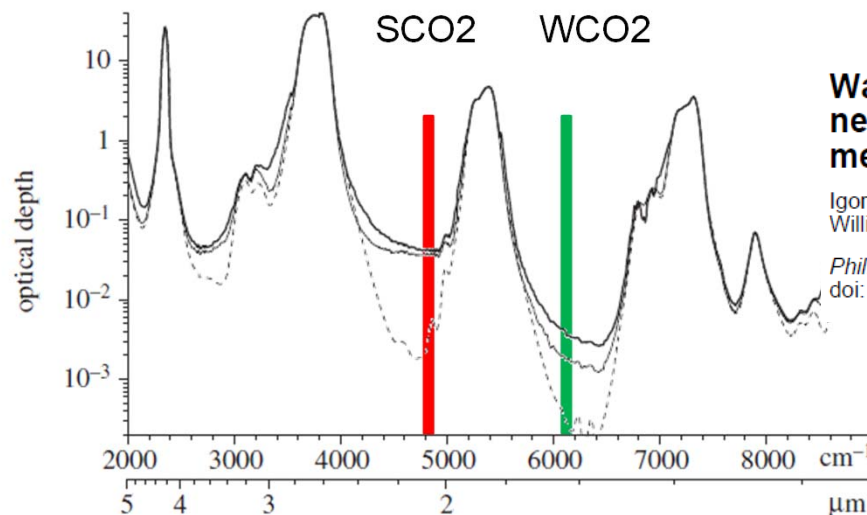
- O_2 A-Band cross sections have been scaled by 1.025 to correct 10 hPa surface pressure bias
 - This is a temporary fix!
- Known errors in the details of O_2 spectroscopy are contributing some of this bias
 - Errors in intensity and pressure shifts
 - Oversimplifications in line shape
 - Uncertainties in Line Mixing
 - Uncertainties in collision-induced absorption
 - O_2 lines broadened by water vapor
 - New measurements indicate a much larger effect than older measurements
 - TCCON observations processed with the air broadened and new water-broadened cross sections show large (2 ppm) X_{CO_2} differences
- New laboratory studies are under way to address these issues.





Other Spectroscopy Issues

- Recent laboratory measurements indicate that the self- and air-broadened water continua absorption in the SCO₂ (and WCO₂) band may be much stronger than previously assumed.
- This continuum absorption could contribute to both the spectrally-dependent residuals, and observed biases between X_{CO_2} retrievals using the SCO₂ and WCO₂ bands



Water vapour foreign-continuum absorption in near-infrared windows from laboratory measurements

Igor V. Ptashnik, Robert A. McPheat, Keith P. Shine, Kevin M. Smith and R. Gary Williams

Phil. Trans. R. Soc. A 2012 **370**, 2557-2577
doi: 10.1098/rsta.2011.0218

Simulated water vapor continuum optical depth in the short wave infrared region for a mid-latitude summer atmosphere by models that use the MTCKD-2.5 continuum (dashed line), which is currently implemented in ACOS algorithm, and for models that use new measurements (Ptashnik et al. 2011) for self- (light grey solid line) and self + foreign (dark solid line) continuum absorption.



Summary of ACOS Gas Absorption Line Lists

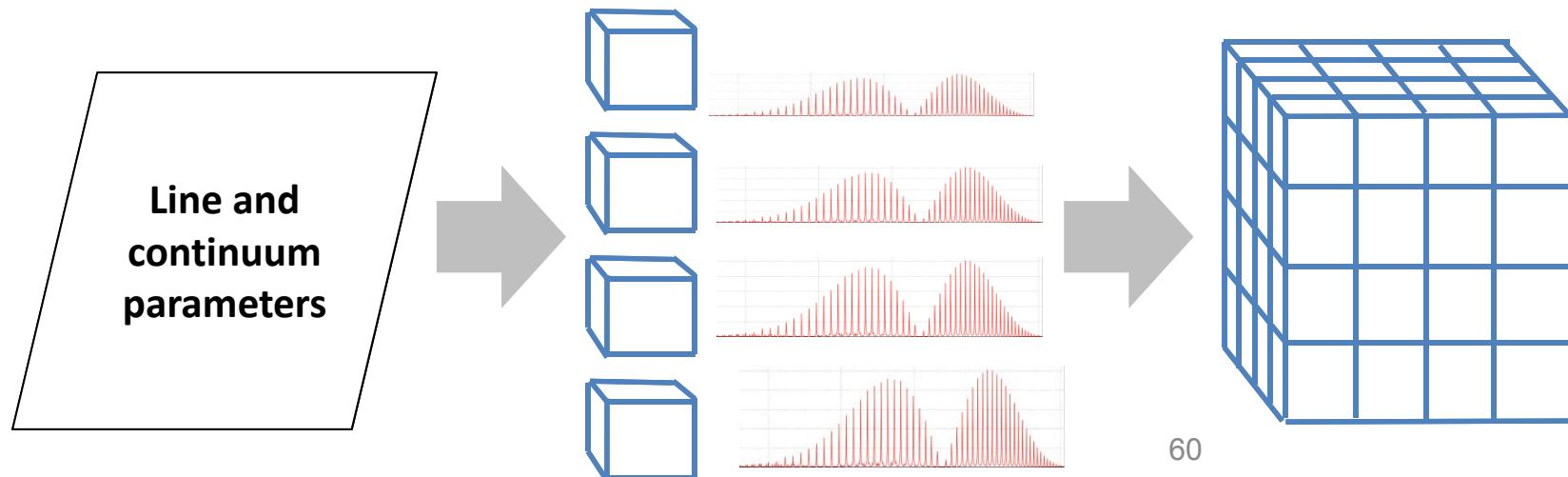
	0.76μm O₂	1.61μm CO₂	2.06μm CO₂	H₂O
Spectral range	12745-13245 cm ⁻¹	4700-6500cm ⁻¹	4700-6500cm ⁻¹	12745-13245 cm⁻¹ 4700-6500cm ⁻¹
Spectral resolution	0.01cm ⁻¹ or 0.002cm ⁻¹	0.01 cm ⁻¹ or 0.002cm ⁻¹	0.01 cm ⁻¹ or 0.002cm ⁻¹	0.01 cm ⁻¹ or 0.002cm ⁻¹
Position	Long (2010), Long (2011)	Devi (2007) ¹	Benner/Devi (2011) ¹	Gordon (2012), Rothman (2010)
Intensities	“	“	“	“
Air-widths	Tran (2008)	Predoi-Cross (2009) ¹	“	“
Air-shifts	Brown (2009) Robichaud (2008a) Predoi-Cross (2008)	Devi (2007b) ¹	“	“
Temp. dep.	Brown (2000) ^{1,2}	Predoi-Cross (2009) ¹	“	“
Line shapes	Voigt / Galatry	Speed-dependent Voigt	Speed-dependent Voigt	Voigt
Isotopologue abundance	Rothman (2009) ¹	Rothman (2009)	Rothman (2009)	Rothman (2009)
H₂O broadening	Vess (2012)	Sung (2009)	Sung (2009)	-
Air-Line mixing	Tran (2008)	Devi (2007)	Benner/Devi (2011)	-
“ Temp. dep.	Tran (2008)	-	-	-
Speed dep.	-	Devi (2007) ¹	Benner/Devi (2011) ¹	-
Continuum	CIA via Tran (2008)	-	*	Mlawer (2012)



Absorption coefficient (ABSCO) Tables

□ Pre-computed ABSCO look-up tables

- **Problem:** Advanced spectroscopic models too slow for online use
- **Solution:** pre-computed lookup table for linear interpolation
- 71 Pressure levels, 17 Temperature
- Recently expanded from 3-dimensions (wavenumber, pressure, temperature) to add a 4th dimension, to accommodate water variable amounts of water vapor broadening





Gas Absorption Line List References (1 of 2)

- Brown, L. R., Plymate, C. Experimental line parameters of the oxygen A band at 760nm. *J Mol Spectrosc* 2000; 199:166–79.
Line list is available in the acos/absco repository at the following location:
acos/level_2/exe/absco/input/line_mixing/o2/lm_o2_inputs_20091026/SDF.dat
- Devi, V. M., D. C. Benner, L. R. Brown, C. E. Miller, and R. A. Toth (2007), Line mixing and speed dependence in CO₂ at 6227.9 cm⁻¹: Constrained multispectrum analysis of intensities and line shapes in the 30013 ← 00001 band, *J. Mol. Spectrosc.* 245, 52-80.
- Anu Dudhia, RFM Software package and user guide available at <http://www.atm.ox.ac.uk/RFM/>.
- I.E. Gordon, L. Lodi, G.C. Toon, J. Tennyson, L.R. Brown, L.S. Rothman. "Evaluation of the experimental and theoretical spectral parameters of water vapor lines in the 2- μ m region using Solar-pointing FTS spectra," (2012) in preparation.
- J.-M. Hartmann, H. Tran, and G. C. Toon, *Influence of line mixing on the retrievals of atmospheric CO₂ from spectra in the 1.6 and 2.1 μ m regions*, *Atmos. Chem. Phys. Discuss.*, 9, 1–26, 2009
- J. Lamouroux, H. Tran, A.L. Laraia, R.R. Gamache, L.S. Rothman, I.E. Gordon, and J.-M. Hartmann, J. Updated database plus software for line-mixing in CO₂ infrared spectra and their test using laboratory spectra in the 1.5-2.3 μ m region, *Quant. Spectrosc. and Rad. Transfer* 111, 2321-2331 (2010).
- D.A. Long, D.K. Havey, M. Okumura, C.E. Miller, J.T. Hodges, O₂ A-band line parameters to support atmospheric remote sensing, *Journal of Quantitative Spectroscopy and Radiative Transfer*, Volume 111, Issue 14, September 2010, Pages 2021-2036, ISSN 0022-4073, 10.1016/j.jqsrt.2010.05.011.
- Mlawer, E.J., V.H. Payne, J.-L. Moncet, J.S. Delamere, M.J. Alvarado, D.D. Tobin, Development and recent evaluation of the MT_CKD model of continuum absorption, submitted to *Phil. Trans. Roy. Soc.A*, June 13, 2012 370 1968 2520-2556.
- Niro, F., Boulet, C., and Hartmann, J. M.: Spectra calculations in central and wing regions of CO₂ IR bands between 10 and 20 μ m. I: Model and laboratory measurements, *J. Quant. Spectrosc. Radiat. Transfer* 88, 483–498, 2004.
- F. Niro, T. von Clarmann, K. Jucks, and J.-M. Hartmann (2005), Spectra calculations in central and wing regions of CO₂ IR bands between 10 and 20 μ m. III: atmospheric emission Spectra, *J. Quant. Spectrosc. Radiat. Transfer* 90, 61–76.
- Predoi-Cross, A., C. Holladay, H. Heung, J.-P. Bouanich, G. Ch. Mellau, R. Keller, and D. R. Hurtmans (2008), Nitrogen-broadened lineshapes in the oxygen A-band: Experimental results and theoretical calculations, *J. Mol. Spectrosc.* 251, 159–175.
- Predoi-Cross, A., A. R. W. McKellar, D. Chris Benner, V. Malathy Devi, R. R. Gamache, C. E. Miller, R. A. Toth, and L. R. Brown (2009), Temperature dependences for air-broadened Lorentz half width and pressure-shift coefficients in the 30013←00001 and 30012←00001 bands of CO₂ near 1600 nm, *Can. J. Phys.* (in press).
- Ptashnik et al. *Journal of Geophysical Research*, vol. 116, D16305, doi:10.1029/2011JD015603, 2011.
- Robichaud, D. J., Hodges, J. T., Maslowski, P., Yeung, L.Y., Okumura, M., Miller, C. E., et al. High-accuracy transition frequencies for the O₂ A-band. *J Mol Spectrosc* 2008;251:27–37.



Gas Absorption Line List References (2 of 2)

- Robichaud, D. J., Hodges, J. T., Brown, L. R., Lisak, D., Maslowski, P., Yeung, L. Y., et al. Experimental intensity and line shape parameters of the oxygen A-band using frequency-stabilized cavity ring-down spectroscopy. *J Mol Spectrosc.* 2008; 248:1–13.
- Robichaud D. J., Hodges, J. T., Lisak, D., Miller, C. E., Okumura, M. High-precision pressure shifting measurement technique using frequency-stabilized cavity ring-down spectroscopy. *JQSRT* 2008;109:435–44.
- Rothman, L. S., et al. (2005), The HITRAN molecular spectroscopic database: Edition of 2004, *J. Quant. Spectrosc. Radiat. Transfer*, 96, 139 – 204.
- Rothman, L. S. et al. *The HITRAN 2008 molecular spectroscopic database*. *Journal of Quantitative Spectroscopy and Radiative Transfer*, 110 (2009) 533–572.
- Rothman, L. S., I. E. Gordon, R. J. Barber, H. Dothe, R. R. Gamache, A. Goldman, V. I. Perevalov, S. A. Tashkun, J. Tennyson (2010). HITRAN, the high-temperature molecular spectroscopic database. *Journal of Quantitative Spectroscopy and Radiative Transfer*. 111:15, p. 2139-2150.
- Keeyoon Sung; L. R. Brown, R. A. Toth, T. J. Crawford. Fourier transform infrared spectroscopy measurements of H₂O-broadened half-widths of CO₂ at 4.3 μ m. *Canadian Journal of Physics*; May 2009, Vol. 87 Issue 5, p. 469.
- Thompson, D. R., D. C. Benner, L. R. Brown, D. Crisp, V. Malathy Devi, Y. Jiang, V. Natraj, F. Oyafuso, K. Sung, D. Wunch, R. Castaño a, C. E. Miller Atmospheric validation of high accuracy CO₂ absorption coefficients for the OCO-2 mission. *Journal of Quantitative Spectroscopy and Radiative Transfer* (2012), <http://dx.doi.org/10.1016/j.jqsrt.2012.05.021>.
- Tran, H, Boulet, C, and Hartmann, J.-M. Line mixing and collision-induced absorption by oxygen in the A band: Laboratory measurements, model, and tools for atmospheric spectra computations. *Journal of Geophysical Research*, vol. 111, D15210, doi:10.1029/2005JD006869, 2006.
- Tran, H. and Hartmann, J. M. An improved O₂ A band absorption model and its consequences for retrievals of photon paths and surface pressures, *Journal of Geophysical Research*, vol 113, D18104, 2008.
- Toth, R. A., C. E. Miller, V. M. Devi, D. C. Benner, and L. R. Brown (2007), Air-broadened width and pressure shift coefficients of 12C16O₂: 4700 – 7000 cm⁻¹, *J. Mol. Spectrosc.* 246, 133-157.
- Toth, R. A., Brown, L. R., Miller, C. E., Malathy Devi, V., and Benner, D. C.: Spectroscopic database of CO₂ line parameters: 4300–7000 cm⁻¹, *J. Quant. Spectrosc. Radiat. Transfer* 109, 906–921, 2008.
- Toon, G. Personal Communication.
- E. M. Vess, C. J. Wallace, H. M. Campbell, V. E. Awadalla, J. T. Hodges, D. A. Long, and D. K. Havey. Measurement of H₂O Broadening of O₂ A-Band Transitions and Implications for Atmospheric Remote Sensing. *Journal of Physical Chemistry*. 2012 (in press).
- Wunch, D., Toon, G. C., Wennberge, P. O. et al. Calibration of the total carbon column observing network using aircraft profile data. *Atmos Meas. Tech. Discuss.*, 3, 2603-2632, 2010. www.atmos-meas-tech-discuss.net/3/2603/2010/ doi:10.5194/amtd-3-2603-2010



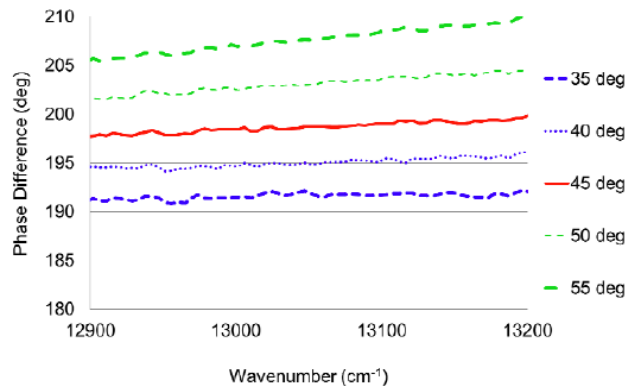
Increasing the Speed and Accuracy of the Forward Model

- The ACOS Level 2 retrieval algorithm team introduced several changes that dramatically improved the speed of the forward model, including:
 - Replacing the Radiant radiative transfer model (Spurr and Christi, 2007) with the more computationally efficient LIDORT model (Spurr et al. 2001, Spurr, 2002);
 - Implementing the Low Streams Interpolator (O'Dell, 2010) to reduce the angular resolution needed to resolve the radiation field;
 - Adopting a non-uniform spectral grid, with higher resolution near line cores and lower resolution in the far wings of spectral lines to reduce the number spectral grid points needed to resolve the spectrum;
 - Replacing the FORTRAN compiler with a more efficient version;
 - Other changes are ongoing to improve efficiency, remove bottlenecks and improve throughput
- These changes, combined with the improvements in pre-screening of soundings are expected to yield the speed needed for routine processing of OCO-2 data.

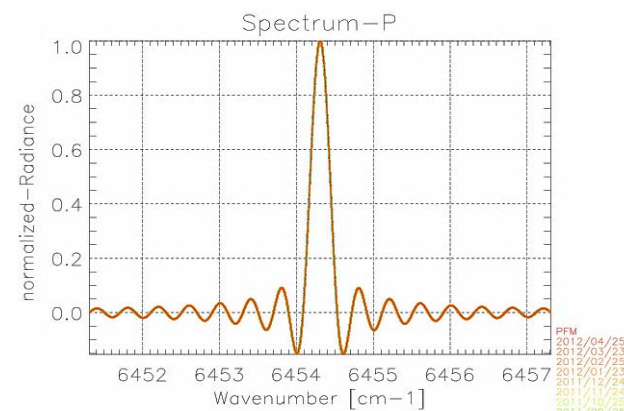


The GOSAT TANSO-FTS Instrument Model

- Given high-resolution, polarization-dependent synthetic spectra in each band, the GOSAT TANSO-FTS Instrument Model is used to:
 - multiply each Stokes parameter by the associated element in the instrument Mueller matrix (Kuze et al., 2009a; O'Brien et al., 2011; Kuze et al. 2012) to correct for the polarization introduced by the instrument and its pointing mechanism, and
 - convolve the resulting spectrum with the instrument line shape (ILS) to simulate the instrument's spectral resolution and dispersion.



The Mueller matrix in each channel was estimated using measurements of witness samples for the pointing mirrors.



The instrument line shape (ILS) was measured prior to launch, and is monitored by an on-board laser diode.

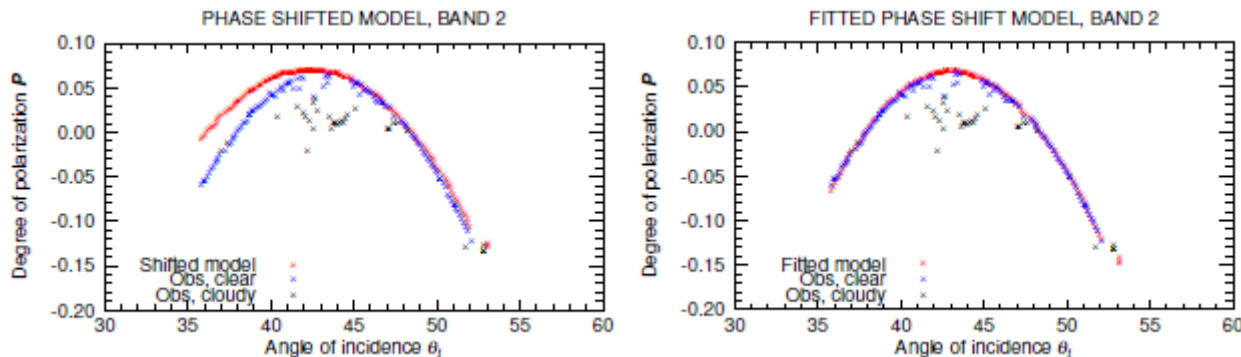


TANSO-FTS-system Mueller Matrix

Mueller matrix elements derived from laboratory measurements of witness samples of the two mirrors in the pointing mechanism.

$$S_{Poutput} = M_{pp} M_{opt} M_r(-2\theta_{CT}) M_p M_m M_r(2\theta_{CT}) S_{input}$$

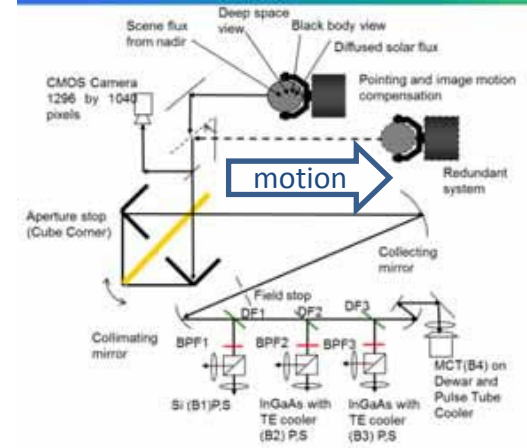
$$S_{Soutput} = M_{ps} M_{opt} M_r(-2\theta_{CT}) M_p M_m M_r(2\theta_{CT}) S_{input}$$



The Mueller matrix used in the ACOS/GOSAT instrument model was validated using observations of ocean glint. Initial tests revealed discrepancies for targets $> 45^\circ$ ahead of the satellite (above left). An empirical adjustment was performed to bring the observations and model into better agreement (above right; see O'Brien et al. 2012).



Laboratory optical bench used to measure the mirror polarization.

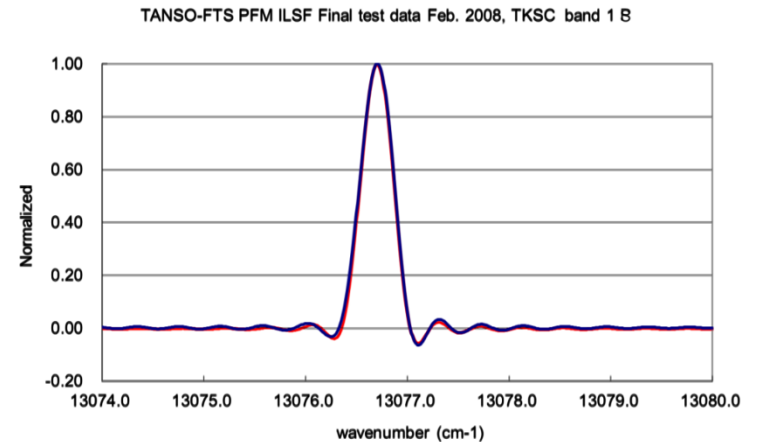


Schematic of the TANSO-FTS and its pointing mirror.



The TANSO-FTS Instrument Line Shape

- The TANSO-FTS Instrument Line Shape (ILS) varies slowly across each band.
- There is also a small difference between ILS for the S and P polarization channels of the A-band
- The JAXA GOSAT team provides tabulated estimates of the ILS intensity as a function of polarization channel and wavenumber at several discrete frequencies across each band.
- To accommodate these variations, the ACOS/OCO-2 Full Physics algorithm Instrument Model interpolates between the discrete ILS values.
- The instrument model also applies a linear stretch to match the instrument dispersion, and corrects for Doppler shifts between the spectrometer, target, and sun



The ILS is shown for the P (blue) and S (red) channels of Band 1 (O_2 A-Band). The TANSO-FTS includes an on-board laser diode to verify the instrument line shape (ILS). There is no evidence of significant changes in the ILS since launch.

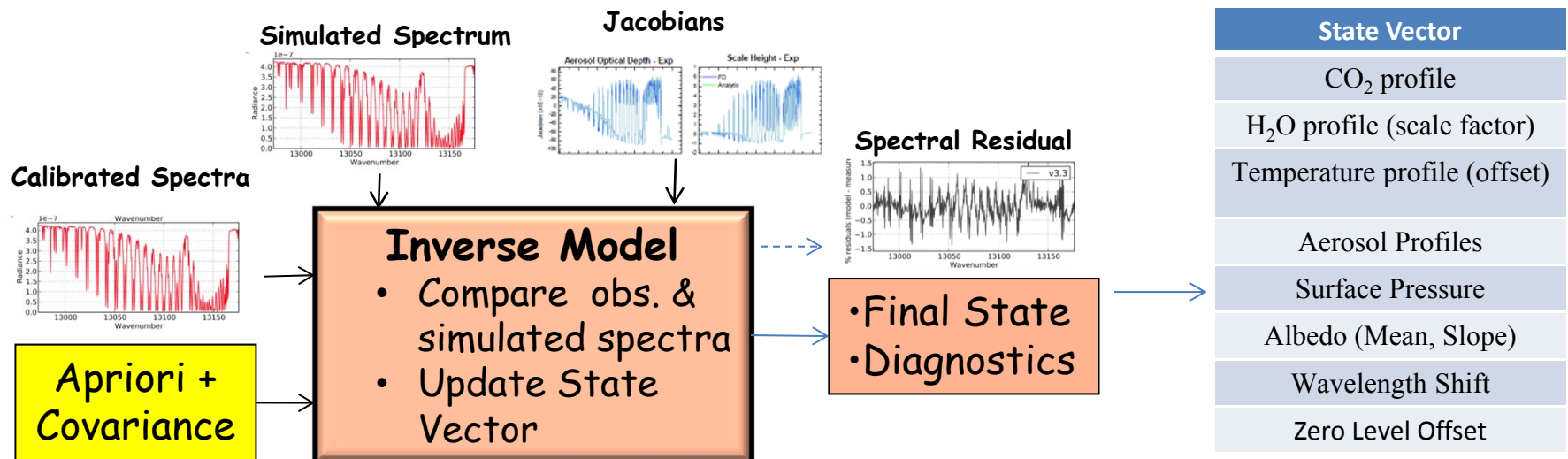


The ACOS/OCO-2 Inverse Model

- The OCO-2 Inverse Model is based on Bayesian optimal estimation
 - Modified Levenberg-Marquardt solver used to minimize the cost function:

$$\chi^2 = (\mathbf{F}(\mathbf{x}) - \mathbf{y})^T \mathbf{S}_\epsilon^{-1} (\mathbf{F}(\mathbf{x}) - \mathbf{y}) + (\mathbf{x} - \mathbf{x}_a)^T \mathbf{S}_a^{-1} (\mathbf{x} - \mathbf{x}_a)$$

- Rodgers 2000; Connor et al. 2008; Boesch et al. 2011; O'Dell et al. 2012
- It finds the differences between the observed and synthetic spectrum in each spectral channel, and uses the Jacobians to modify the state vector to improve the fit.





The Output State Vector

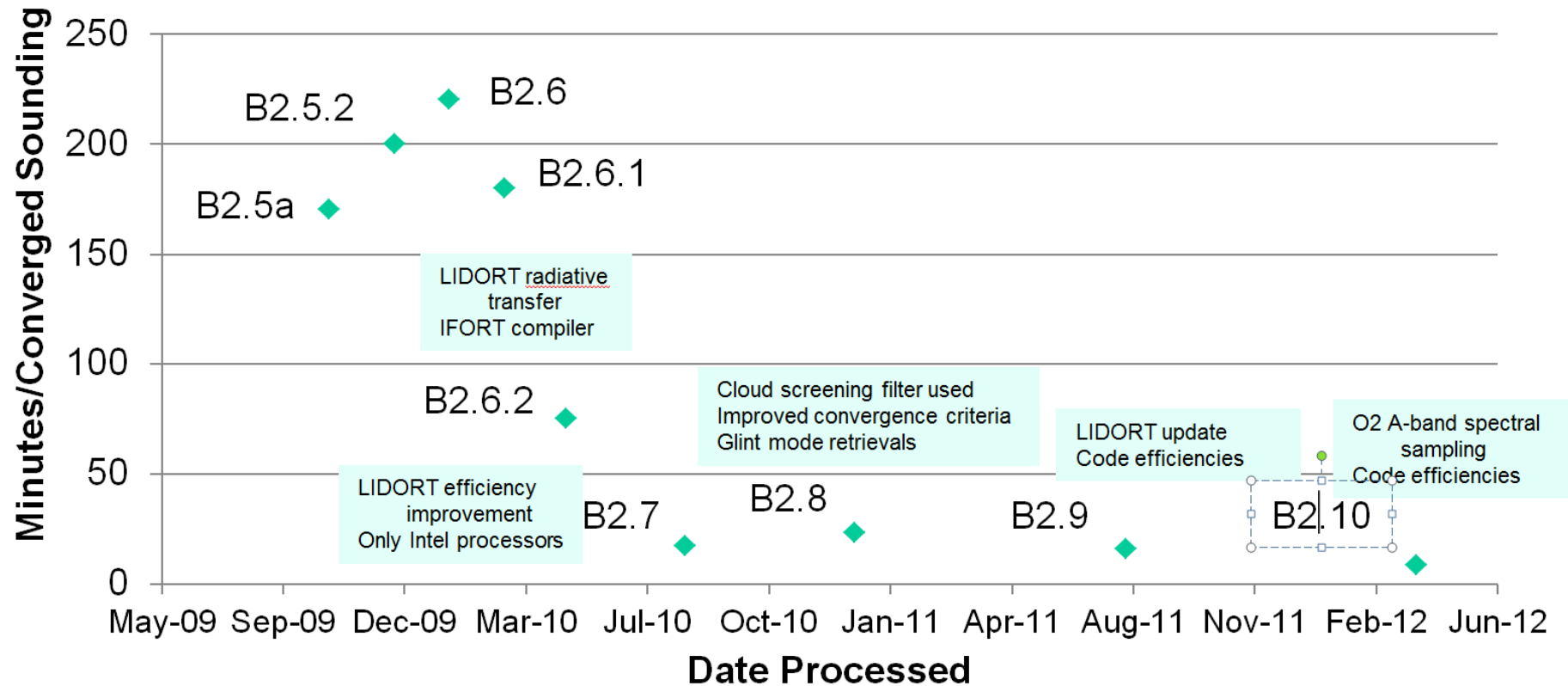
The algorithm performs a simultaneous retrieval on all 3 TANSO-FTS SWIR spectral channels to return estimates for the following state vector properties:

- Atmospheric properties returned at each of the model's 20 pressure levels:
 - CO₂ volume mixing ratio
 - additive offset factor for the input atmospheric temperature profile
 - multiplicative scaling factor for the input water vapor mixing ratio profile
 - extinction coefficients for liquid and ice water clouds, and 2 aerosol types
- Surface properties
 - The atmospheric pressure at the surface.
 - a Lambertian surface albedo over land, and an ocean wind speed and a Lambertian “sea foam albedo” over the ocean
- Instrument Properties
 - Wavelength shift (dispersion, Doppler shift)
 - Zero Level Offset (implemented for B2.9)



Retrieval Processing Time Improvements

Processing Time per Sounding July 24-26, 2009 GOSAT repeat cycle

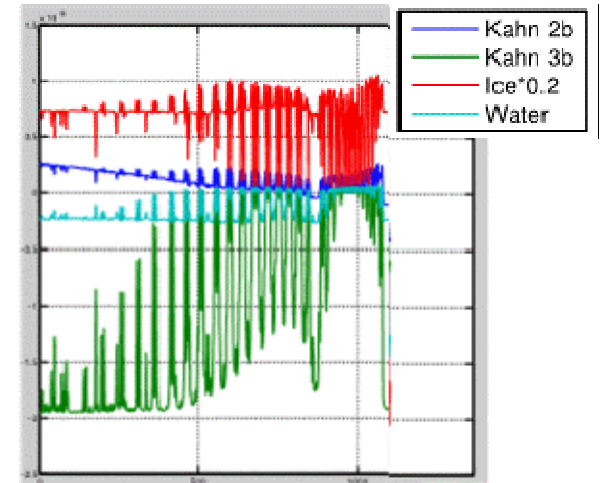


The ACOS task produced dramatic improvements in the speed of the OCO full physics algorithm.

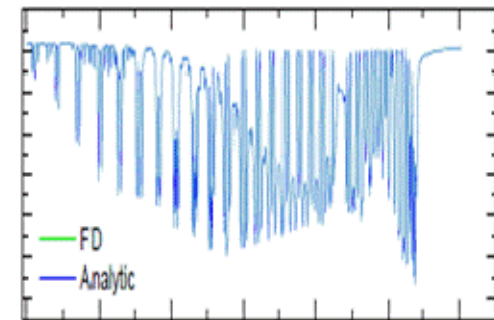


ACOS/OCO-2 Aerosol Challenges

- Retrieves profiles of 4 airborne particle types
 - Ice cloud
 - Water cloud
 - Kahn 2b: 29% sulfate, 13% sea salt, 39% accum dust, 19% coarse dust
 - Kahn 3b: 35% sulfate, 10% sea salt, 47% carbonaceous, 8% black carbon
- The surface pressure retrieval interferes with aerosols retrievals because the surface pressure and aerosol Jacobians are well correlated.
- The quality of the aerosol retrieval is also compromised by systematic errors in the gas absorption coefficients.



O₂ A-band Jacobians for each of the 4 aerosol types.



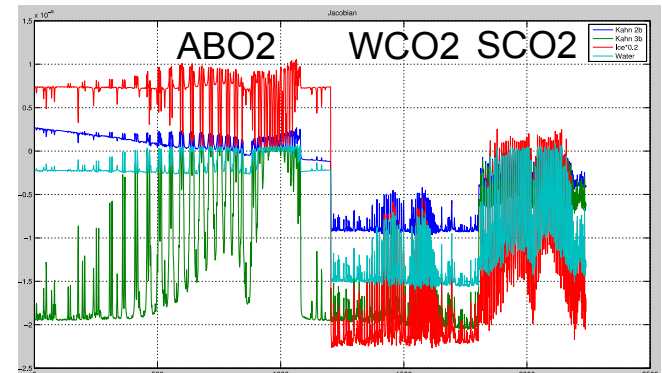
O₂ A-band surface pressure Jacobians.



ACOS Aerosol Retrieval Approach

A significant change in the aerosol prior was implemented between ACOS/OCO-2 Algorithm versions B2.09 and B2.10

- **Old way:** For each of the 4 particle-types, fit 20 layers each independently
→ 80 aerosol state vector elements
 - Typically, the aerosol optical depth (AOD) in each layer is fitted in log-space to prevent negative AOD, from crashing the RT code
- **B2.10 Approach:** For each type, fit a Gaussian shape (similar to Butz et al.) determined by
 1. mean height of the layer
 2. Full width of layer, and
 3. total AOD, still in log-space
- This new approach is currently being tested

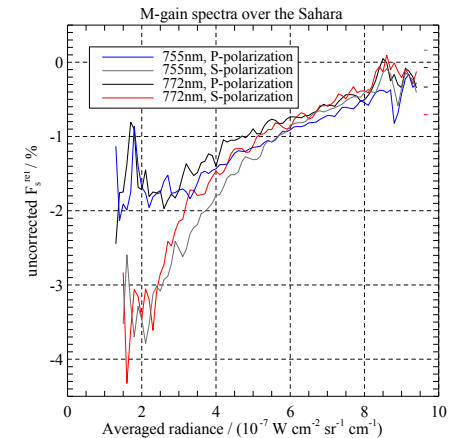


Aerosol Jacobians in the 3 ACOS bands for the 4 aerosol types.

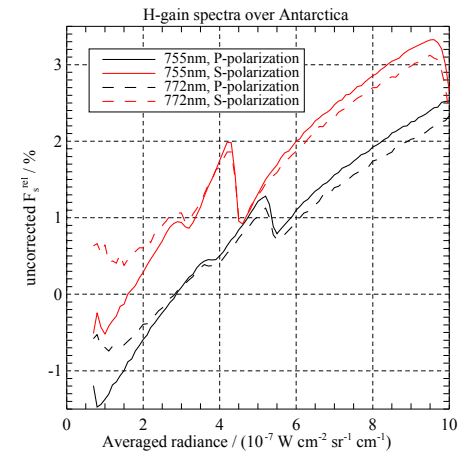


Zero Level Offset

- Added to b2.9 and later
- Motivation: Fluorescence retrievals revealed a zero-level offset in GOSAT O2 A-band spectra, causing biases in O2 fits that depend on signal level.
- Solution: We add a flat (i.e. no special shape assumed) zero-level offset term in the state vector and fit for it.
- Result: Many systematic biases vanish. RMS at TCCON sites reduced. Fitted offset seems to be stable, even for simulator data.
- Differences between M and H-gain seem to increase. Zero-level offset now fits a mix of fluorescence and pure 0-level offset. Need to fit both in the future (or just fluorescence if JAXA can fix the non-linearity problem)



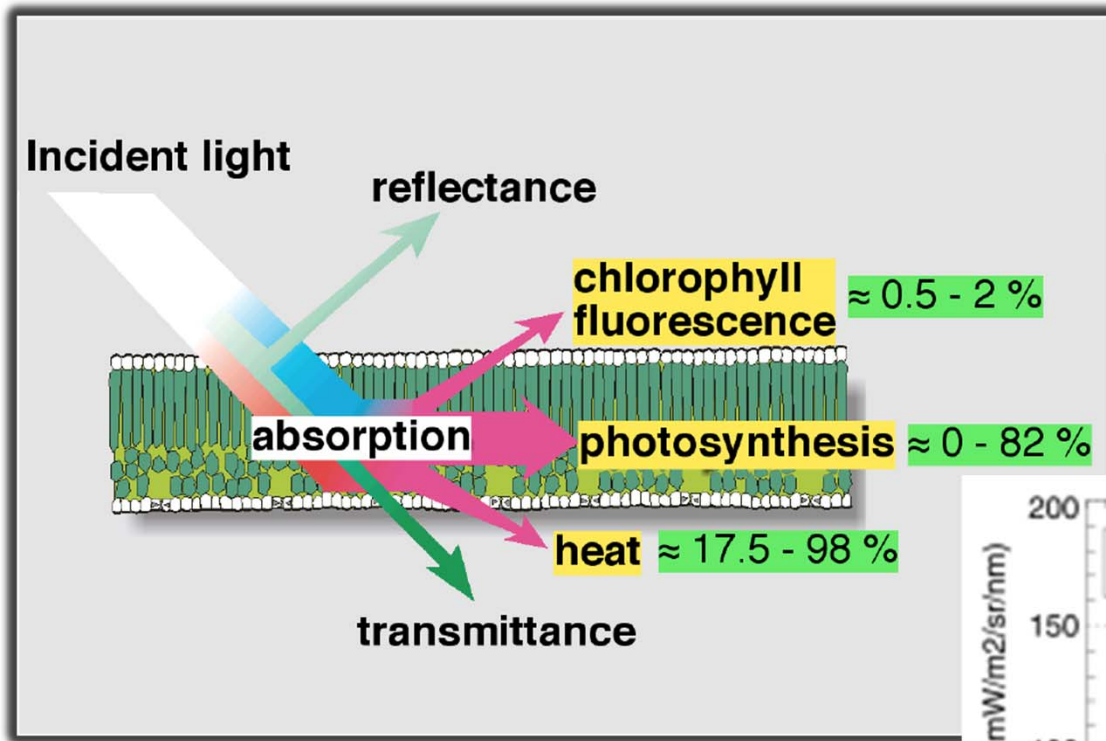
M-gain zero-level offset over Sahara.



H-gain zero-level offset over Antarctica.

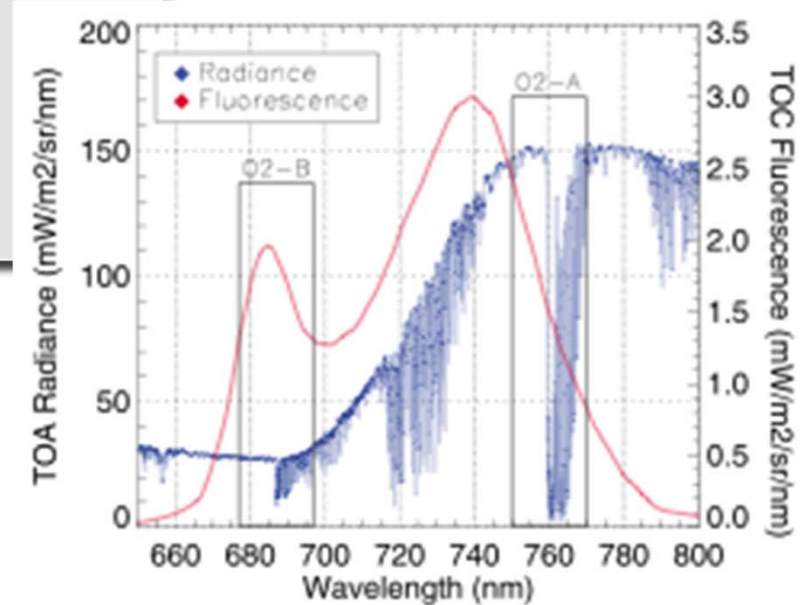


Chlorophyll Fluorescence



Could introduce bias in X_{CO_2} estimates if not included in the retrieval

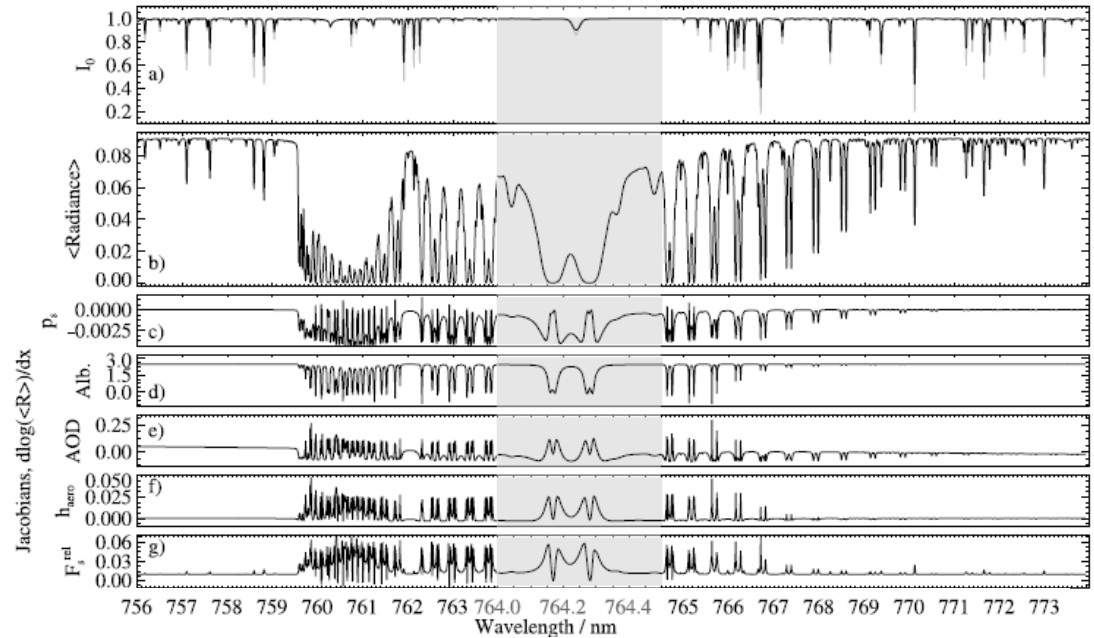
Could yield a useful remote sensing measurement of gross primary production if retrieved.





Impacts of Chlorophyll Fluorescence

- Chlorophyll fluorescence provides a source of illumination that partially fills the cores of strong lines in the O₂ A-band.
- The effects of chlorophyll fluorescence on the A-band spectrum are very similar to that of clouds and aerosols.
- If these effects are neglected, they can introduce a bias in the optical path length retrieval.
- These biases will introduce errors in the XCO₂ retrievals that are spatially correlated with Gross Primary Production (GPP).



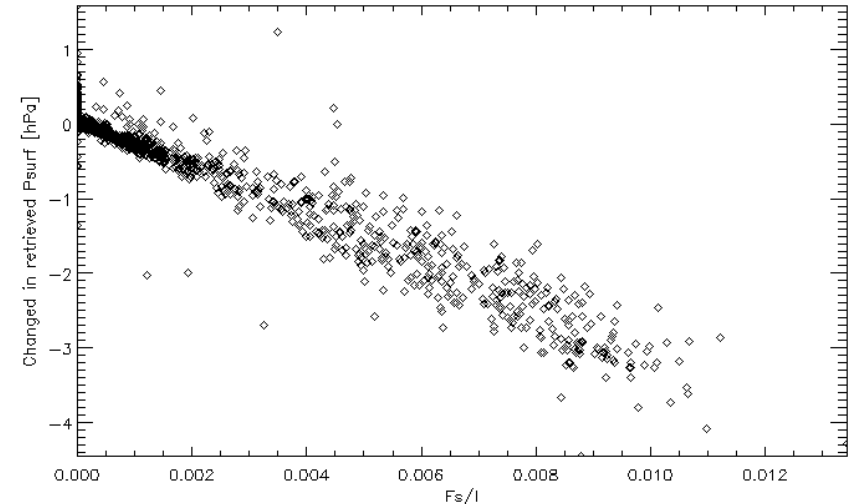
a) Spectrum of incoming Solar radiation, I_0 , b) O₂ A-band spectrum, c)-g) spectral Jacobians for surface pressure (P_s), albedo (Alb), aerosol optical depth (AOD), aerosol layer height (h_{aero}), and chlorophyll fluorescence (F^{rel}). The grey region is a blow-up of a single O₂ doublet, shown at full resolution. The remainder of the spectrum is shown at GOSAT resolution.

Frankenberg, et al. Geophys. Res. Lett., 38, (2011).

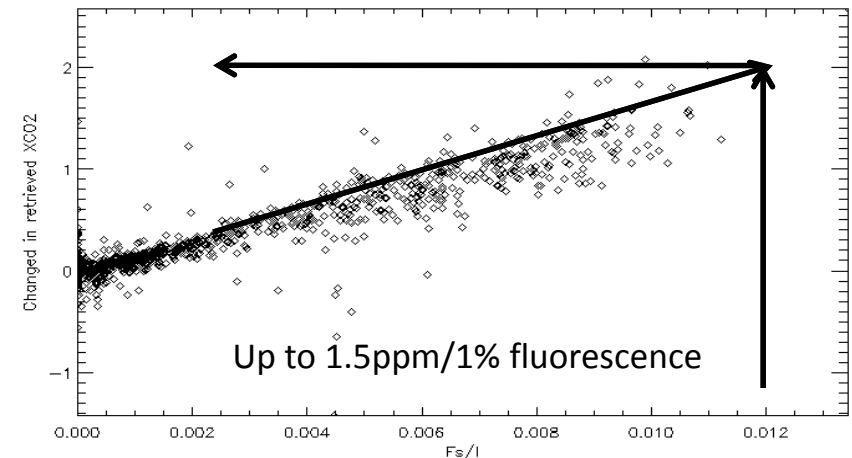


Impact of Neglecting Fluorescence on Surface Pressure Retrievals

- Even modest amounts of chlorophyll fluorescence can introduce significant surface pressure and X_{CO_2} errors, if this process is neglected in the retrieval process.
 - The surface pressure bias is inversely correlated with fluorescence
 - X_{CO_2} biases are correlated with fluorescence intensity
- These biases should be particularly problematic for flux inversion studies, because they are spatially correlated with GPP.
- Fortunately, these biases can be detected and corrected by fitting isolated Fraunhofer lines.



Surface pressure bias vs fluorescence intensity.



X_{CO_2} bias vs fluorescence intensity.



Retrieving Chlorophyll Fluorescence

Chlorophyll fluorescence fits
(isolated Fraunhofer lines)

Vegetation type map
(barren/glint: fix
fluorescence to 0)

Take retrievals (and uncertainty) as
fluorescence prior for the full-physics code

Final fit of fluorescence in the FP-code (or fixing
it to the prior, whatever will be more robust)

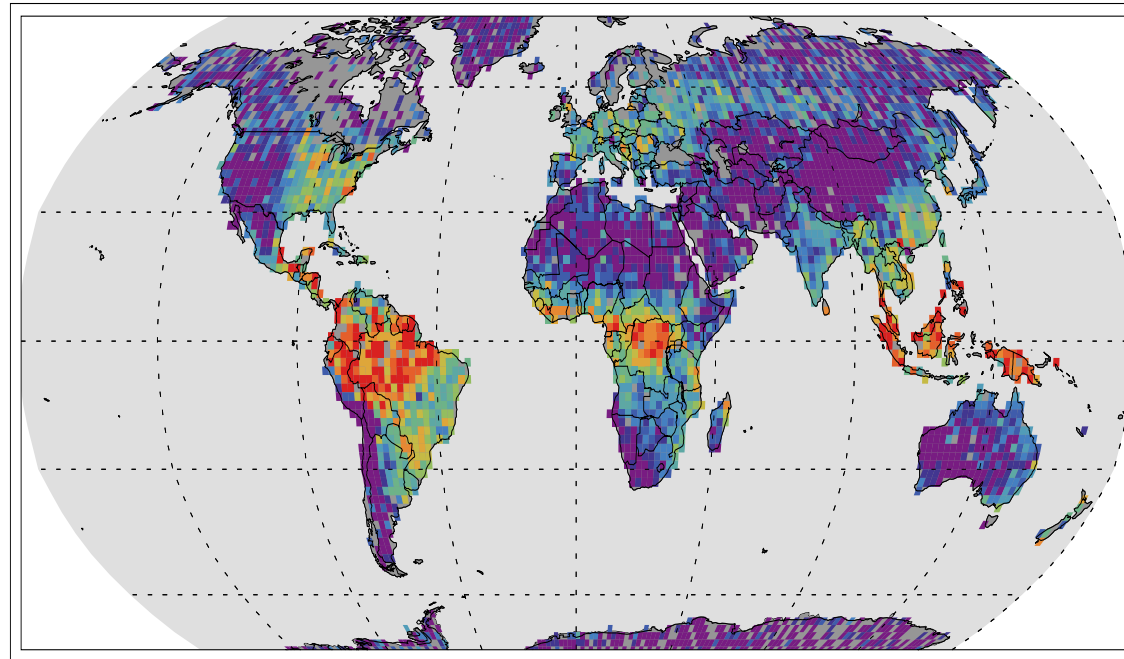
Build 3.3 of the ACOS/GOSAT X_{CO_2} retrieval model has been modified to retrieve chlorophyll fluorescence from GOSAT spectra. This model is currently being tested. A similar approach will be used for OCO-2.



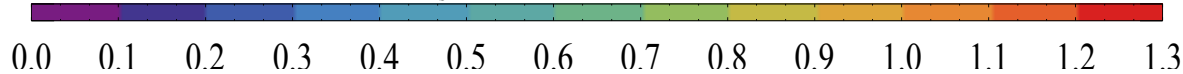
The Potential: A Chlorophyll Product

(Frankenberg et al, GRL, 2011)

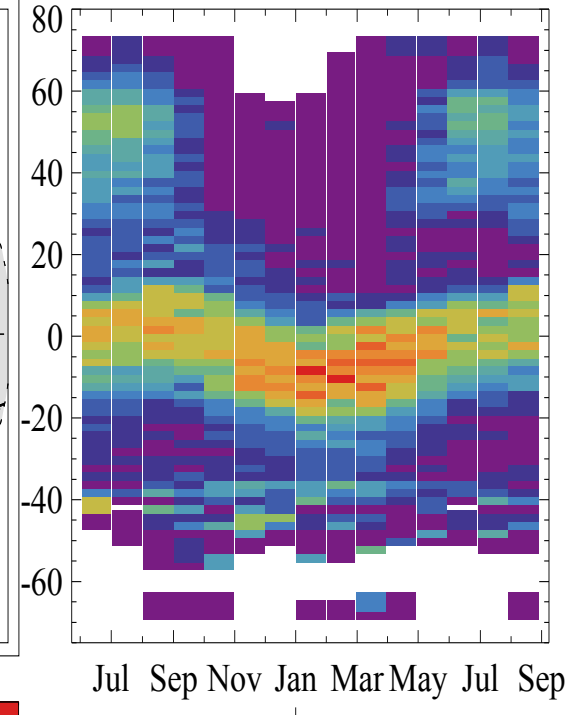
A Chlorophyll a fluorescence at 755 nm, June 2009 through May 2010 average



$F_s / (\text{W m}^{-2} \text{ micron}^{-1} \text{ sr}^{-1})$



B Timeseries



Annual average (June 2009 through May 2010) of retrieved chlorophyll-a fluorescence at 755 nm on a $2^\circ \times 2^\circ$ grid. Only grid-boxes with more than 15 soundings constituting the average are displayed. (b) Latitudinal monthly averages of chlorophyll fluorescence from June 2009 through end of August 2010. (from Frankenberg et al. GRL, 2011).

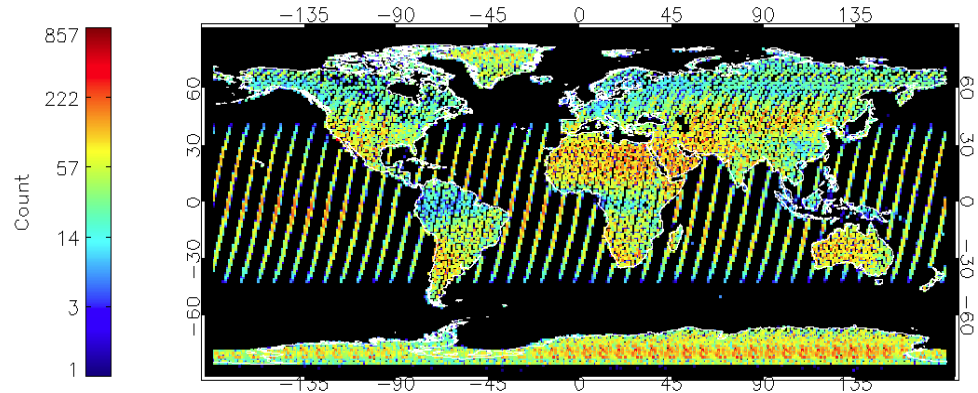


Post-Processing Filters

Post Processing filters use diagnostic information from the retrievals to identify unreliable soundings, so that they can be screened from further use.

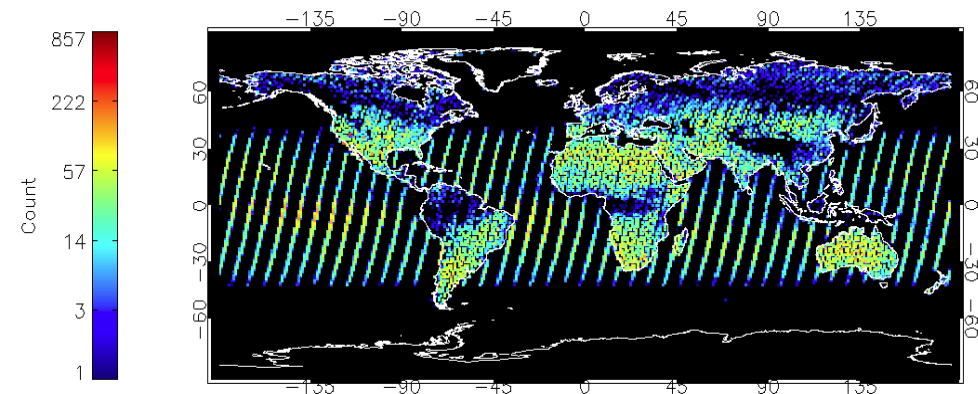
	Converged XCO ₂ Retrievals	Passed Filters	Percent Passed
Glint	185k	79k	43%
Land H	447k	91k	20% (35%*)
Land M	98k	50k	66%

* Over non ice-covered surfaces



Above: All cloud-free soundings processed by the L2 algorithm.

Below: Soundings that passed all Post-Processing filters





ACOS B2.10 Post Processing Filter Summary

Variable	Allowed Range		
	Glint	Land H	Land M
outcome_flag	*	1 or 2	*
AOD Total	< 0.3	< 0.5#	< 0.5#
AOD Water Cloud	*	< 0.15	*
Diverging Steps	*	<= 2	*
altitude_sd [m]	*	< 200	*
CO2_ratio	*	0.985 to 1.005	0.985 to 1.01
H2O_ratio	*	0.96 to 1.10	0.98 to 1.08
$\Delta P_{s,clld}$ [hPa]	*	-8 to 8	-10 to 10
AOD Ice Cloud	*	< 0.02	0.004 to 0.04
Reduced χ^2	< (1.5, 1.8, 2.0)	< (1.25, 1.6, 2.0)	< (1.5, 1.6, 2.0)
X_{CO_2} Error [ppm]	< 1.5	< 2.0	*
Albedo Slope 3	> 1.2e-5	> -1e-4	*
ΔP_s [hPa]	-10 to 10	-10 to 7	-12 to 2
Albedo Slope 1	< 4e-6	< 0	
Albedo Slope 2	-7e-6 to -5e-7		
ΔT offset [K]	> -1		
Band 1 Offset $\cdot 10^7$	< 5.0		
Band 3 Albedo	> 0.01		
Blended Albedo		< 0.8	*
Signal_O2 $\cdot 10^7$		1.5 to 6.5	



Improved Error Analysis Methods

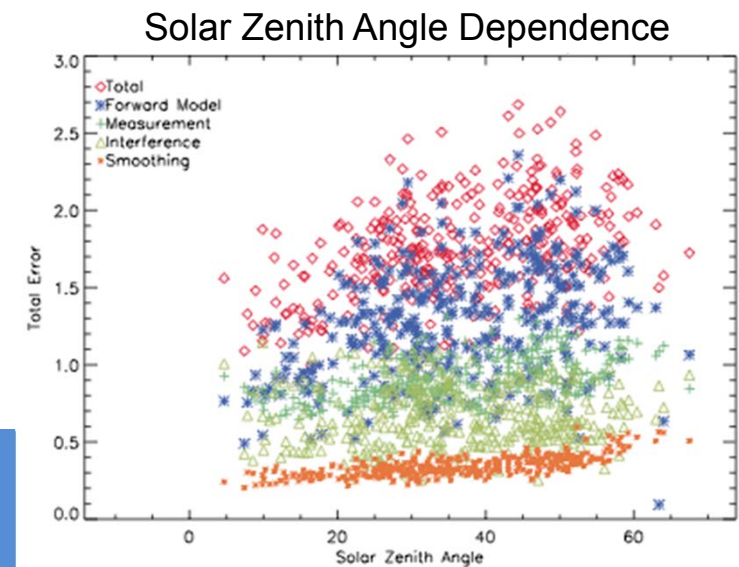
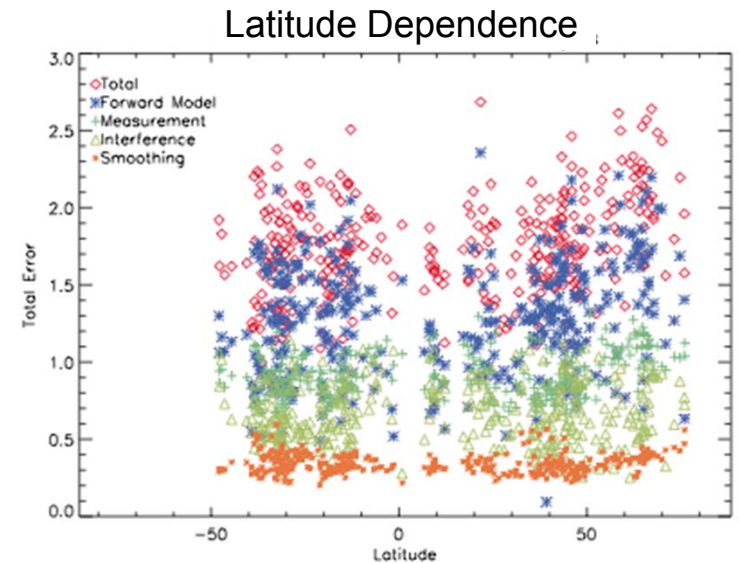
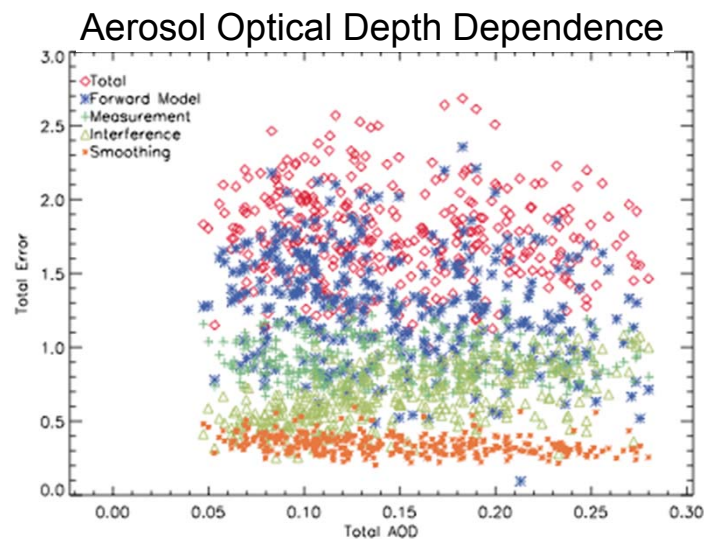
- The goal is to produce comprehensive error estimates that
 - Are referenced to an ensemble of true states
 - Include items not in state vector, such as forward model error
 - Implicitly Include radiative transfer, geophysical and instrumental error

Type	Input
Measurement error	True noise
Smoothing error	CO2 ensemble covariance
Interference error	Ensemble covariance – all state vector components
Forward Model error	Spectroscopy (line parameters, etc.) uncertainty in solar lines or continuum missing species (e.g. CH4) Instrument Line Shape (ILS) uncertainties Calibration Aerosol Types/Properties Etc.



Example of Off-line Error Analysis

- Data: 260-sounding subset of B2.10, that passes latest pre- and post processing screens
- Operational estimates used for measurement, smoothing, and interference errors
- Forward model error simulated by a 1% error in the ILS width



- Errors that produce regional scale biases in XCO₂ are the biggest concern
- ILS error (1% width) dominates the total error in this example.



Spectroscopic Errors

More recently, work has extended to forward model errors due to spectroscopy. For the same soundings, resulting errors are, in ppm:

	CO2-S	CO2-W	O2-A
Band strength ¹	1.0±0.3	1.7±0.4	1.7±0.2
Pressure Width ¹	0.4±0.2	0.3±0.1	1.5±0.2
T-Dep. of Width ²	0.08±0.04	0.10±0.04	0.17±0.05
Band Total	1.1±0.3	1.7±0.4	2.2±0.3
<hr/>			
Total	3.0±0.3		

The true (unknown) error in band strength will introduce an overall bias, affecting all soundings. Line width errors introduce air mass dependent effects that can introduce regional biases. The impact of these biases are being evaluated.

- 1 1% error in parameter
- 2 2% error in parameter



Error Analysis of Retrievals: Nonlinearity of the Forward Model

- Error analysis associated with Optimal Estimation (e.g., Rodgers, 2000) assumes the forward model is linear, to simplify retrieval-error calculations
- Nonlinear forward models are expected, and its effect on error analysis can be assessed using a statistical perturbation approach called the Delta Method
- A multivariate Delta Method was developed for the full state vector (Cressie and Wang, 2012), which depends on both the Jacobian matrix and the Hessian array
- Using an approach based on Statistical Estimating Equations, a weighted Hessian estimate was developed
- When applied to B2.8 ACOS data from central Australia, nonlinearity biases of estimated X_{CO_2} were calculated to be on the order of 1 ppm
- The Delta Method approximates the mean vector and covariance matrix of the retrieval error. From these, an approximate 95% estimation interval for X_{CO_2} was obtained, which addresses directly OCO-2 retrievals' accuracy and precision.



The ACOS GOSAT X_{CO_2} Data Product

- A primary objective of the ACOS L2 development effort was to assess
 - The best methods for retrieving X_{CO_2} from high resolution spectra, like those from GOSAT, and those expected from OCO-2 and GOSAT-2
 - The use these products in source/sink inversion studies
- The ACOS GOSAT product is therefore more an “Exploratory” product than a production science data product
 - It changes frequently as errors are corrected and new capabilities are added to address known problems
 - It includes large amounts of diagnostic information that may or may not be useful for diagnosing errors and performing source/sink inversions
 - Provides as testbed for assessing instrument design & calibration issues
- The ACOS L2 Products are now being distributed on the Goddard Earth Science Data and Information Services Center (GES DISC) Mirador site.



<http://mirador.gsfc.nasa.gov/>



ACOS GOSAT Versions

- July 2010: B2.7 – First major release
- December 2010: B2.8
 - Time dependent calibration coefficients (delivered Aug 2010)
 - Implemented pre-screening (cloud screening, latitude filter)
 - Updated convergence criteria
 - Introduced a sounding quality flag
 - Initial glint retrieval results
- October 2011: B2.9
 - Updated time-varying calibration coefficients (delivered Nov 2010)
 - Added geometric correction factors to L1B geolocation
 - Corrected time-dependent noise (consistent with calibration coefficients)
 - Custom glint flag calculation (fixed omitted glint soundings)
 - Cloud screening applied to glint
 - Added Zero-level offset correction to A-band
 - Updated WCO₂/SCO₂ absorption coefficients, scaled A-band to fix 10 hPa bias
 - Corrected ILS interpolation and other known errors

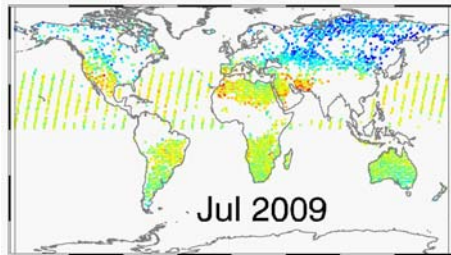


B2.10 – an Experimental ACOS Product

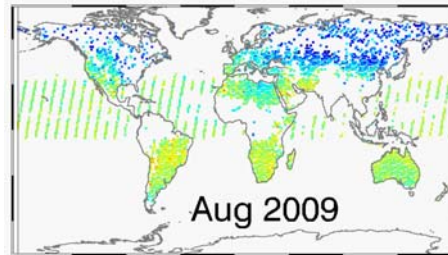
- The last version of the ACOS/OCO-2 retrieval algorithm was B2.10
- This was an “experimental product,” intended to test a number of new capabilities, but not intended for wide distribution
- Version b2.10 includes:
 - Aerosols – profile shape retrievals
 - Non-uniform spectral sampling
 - Sigma level pressure grid
 - Absorption Coefficient (ABSCO) table updates
 - TCCON a priori used for GOSAT retrievals
 - Requested new fields for Data Quality Flag
 - Preliminary sounding selection
 - Cloud screening using an improved ABO2 and IMAP-DOAS in pipeline



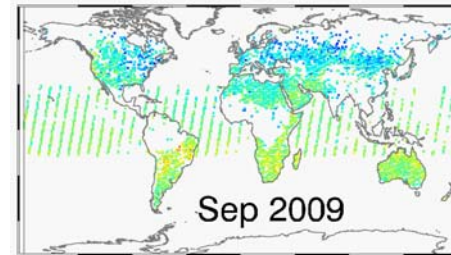
ACOS GOSAT B2.10 X_{CO_2} Retrievals



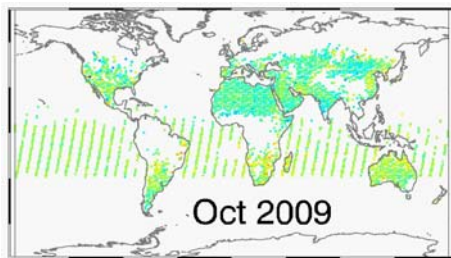
Jul 2009



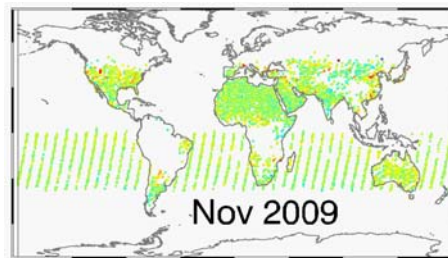
Aug 2009



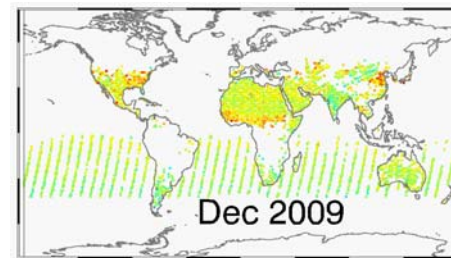
Sep 2009



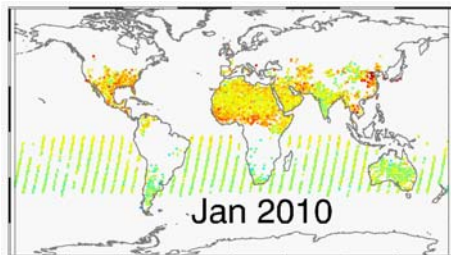
Oct 2009



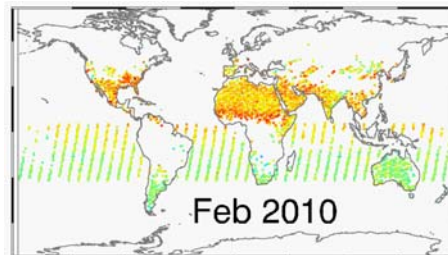
Nov 2009



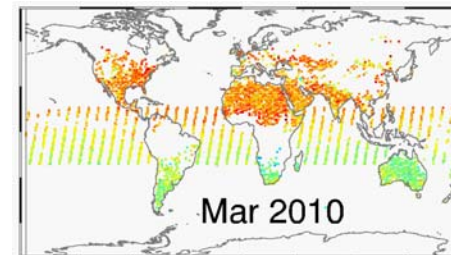
Dec 2009



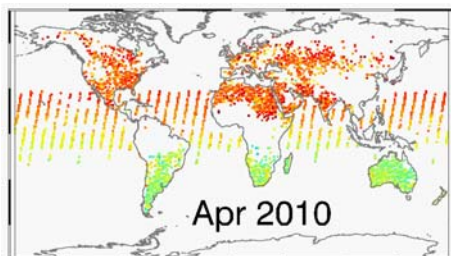
Jan 2010



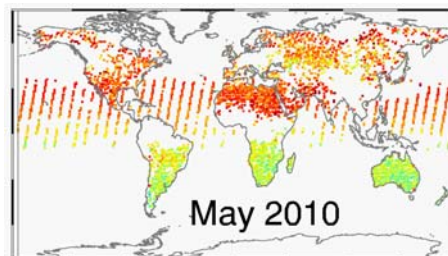
Feb 2010



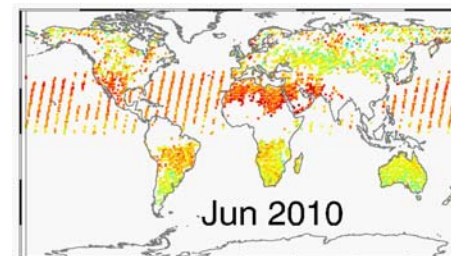
Mar 2010



Apr 2010



May 2010



Jun 2010

395

375





ACOS Retrieval Algorithm Publications (1 of 2)

Boesch, H.; Baker, D., Connor, B., Crisp, D., Miller, C., Global Characterization of CO₂ Column Retrievals from Shortwave-Infrared Satellite Observations of the Orbiting Carbon Observatory-2 Mission.

Remote Sens. 3, 270-304, 2011.

Crisp, D., Bösch, H., Brown, L., Castano, R., Christi, M., Connor, B., Frankenberg, C., McDuffie, J., Miller, C. E., Natraj, V., O'Dell, C., O'Brien, D., Polonsky, I., Oyafuso, F., Thompson, D., Toon, G., and Spurr, R.: OCO (Orbiting Carbon Observatory)-2 Level 2 Full Physics Retrieval Algorithm Theoretical Basis, Tech. Rep. OCO D-65488, NASA Jet Propulsion Laboratory, California Institute of Technology, Pasadena, CA, version 1.0 Rev 4, <http://disc.sci.gsfc.nasa.gov/acdisc/documentation/ACOS.shtml> (last access: December 2011), 2010.

Crisp, D., B. M. Fisher, C. O'Dell, C. Frankenberg, R. Basilio, H. Bösch, L. R. Brown, R. Castano, B. Connor, N. M. Deutscher, A. Eldering, D. Griffith, M. Gunson, A. Kuze, L. Mandrake, J. McDuffie, J. Messerschmidt, C. E. Miller, I. Morino, V. Natraj, J. Notholt, D. M. O'Brien, F. Oyafuso, I. Polonsky, J. Robinson, R. Salawitch, V. Sherlock, M. Smyth, H. Suto, T. E. Taylor, D. R. Thompson, P. O. Wennberg, D. Wunch, and Y. L. Yung: The ACOS CO₂ retrieval algorithm--Part II: Global XCO₂ data characterization, *Atmos. Meas. Tech.*, 5, 687–707, 2012, doi:10.5194/amt-5-687-2012.

Frankenberg, C., Butz, A., and Toon, G. C.: Disentangling chlorophyll fluorescence from atmospheric scattering effects in O₂ A-band spectra of reflected sun-light, *Geophys. Res. Lett.*, 38, L03801, doi:10.1029/2010GL045896, 2011a.



ACOS Retrieval Algorithm Publications (2 of 2)

- Frankenberg, C., Fisher, J. B., Worden, J., Badgley, G., Saatchi, S.S., Lee, J.-E., Toon, G. C., Butz, A., Jung, M., Kuze, A., and Yokota, T.: New global observations of the terrestrial carbon cycle from GOSAT: Patterns of plant fluorescence with gross primary productivity, *Geophys. Res. Lett.*, 38, L17706, doi:10.1029/2011GL048738, 2011b.
- Long, D. A., Bielska, K., Lisak, D., Havey, D. K., Okumura, M., Miller, C. E., and Hodges, J. T.: The air-broadened, near-infrared CO₂ line shape in the spectrally isolated regime: Evidence of simultaneous Dicke narrowing and speed dependence, *J. Chem. Phys.*, 135, 064308, doi:10.1063/1.3624527, 2011.
- O'Dell, C. W., Connor, B., Bösch, H., O'Brien, D., Frankenberg, C., Castano, R., Christi, M., Crisp, D., Eldering, A., Fisher, B., Gunson, M., McDuffie, J., Miller, C. E., Natraj, V., Oyafuso, F., Polonsky, I., Smyth, M., Taylor, T., Toon, G. C., Wennberg, P. O., and Wunch, D.: The ACOS CO₂ retrieval algorithm – Part 1: Description and validation against synthetic observations, *Atmos. Meas. Tech.*, 5, 99–121, 2012.
- O'Brien, D. M., I. Polonsky, C. O'Dell, A. Kuze, N. Kikuchi, Y. Yoshida, and V. Natraj: Testing the Polarization Model for TANSO-FTS on GOSAT against Clear-sky Observations of Sun-glint over the Ocean, *IEEE Trans. Geosci. Remote Sens.*, submitted, 2012.
- Taylor, T. E., O'Dell, C. W., O'Brien, D. M., Kikuchi, N., Yokota, T., Nakajima, T. Y., Ishida, H., Crisp, D., and Nakajima, T.: Comparison of cloud-screening methods applied to GOSAT near-infrared spectra, *IEEE Trans. Geosci. Remote Sens.*, 50, 295-309, doi: 10.1109/TGRS.2011.2160270, 2012.
- Thompson, D. R., D. C. Benner, L. R., Brown, D. Crisp, V. M. Devi, Y. Jiang, V. Natraj, F. Oyafuso, K. Sung, D. Wunch, R. Castano, C. E. Miller, Atmospheric Validation of High Accuracy CO₂ Absorption Coefficients for the OCO-2 Mission, *J. Quant. Spectro. Radiat. Trans.*, In press, 2012.



Validation of ACOS Products

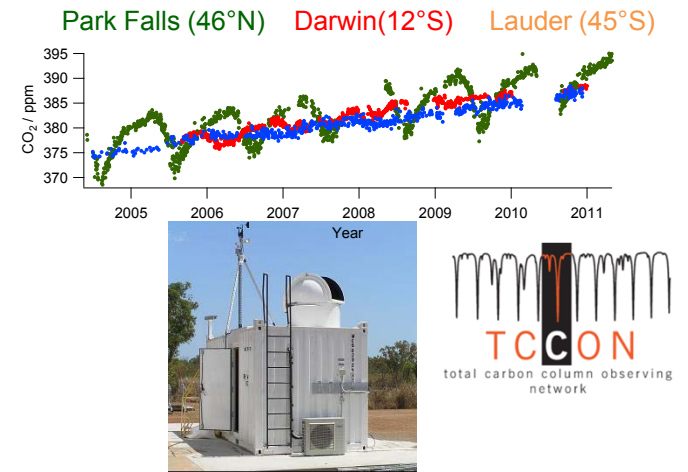




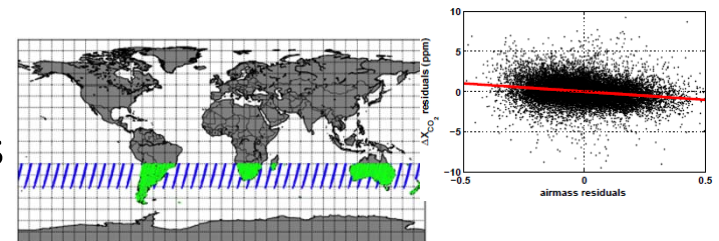
Identifying and Correcting Regional Scale Biases in ACOS/GOSAT X_{CO_2}

- The ACOS task developed three approaches for identifying and correcting regional scale biases

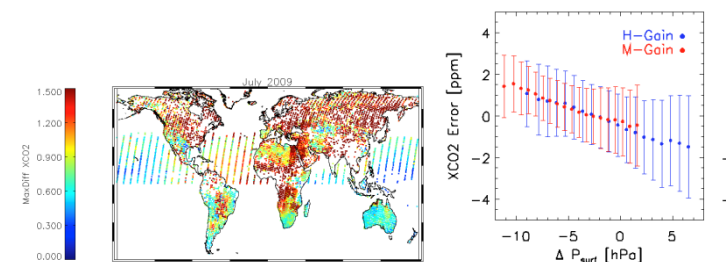
1. TCCON Validation: Uses direct comparisons between nearly coincident ACOS GOSAT and TCCON X_{CO_2} retrievals



2. Southern Hemisphere Approximation: Identifies spurious correlations between X_{CO_2} retrievals and other environment parameters at mid latitudes in the southern hemisphere, where X_{CO_2} variations are known to be small.

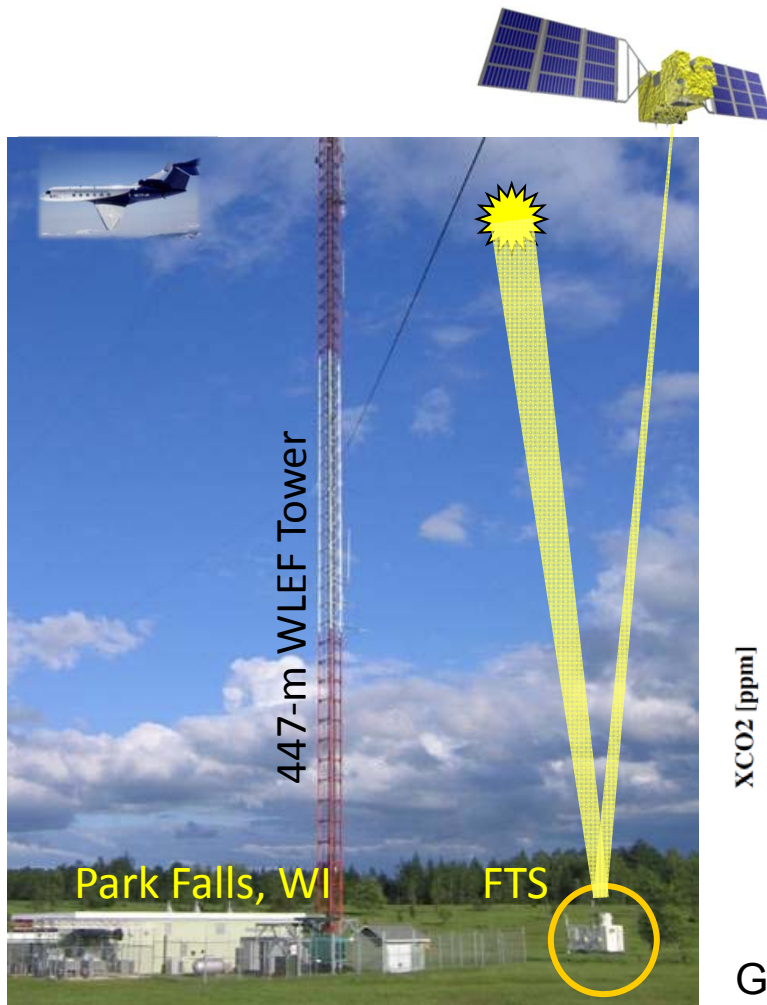


3. Multi-Model Means: Compare ACOS GOSAT X_{CO_2} retrievals to the average X_{CO_2} fields generated by flux inversion models

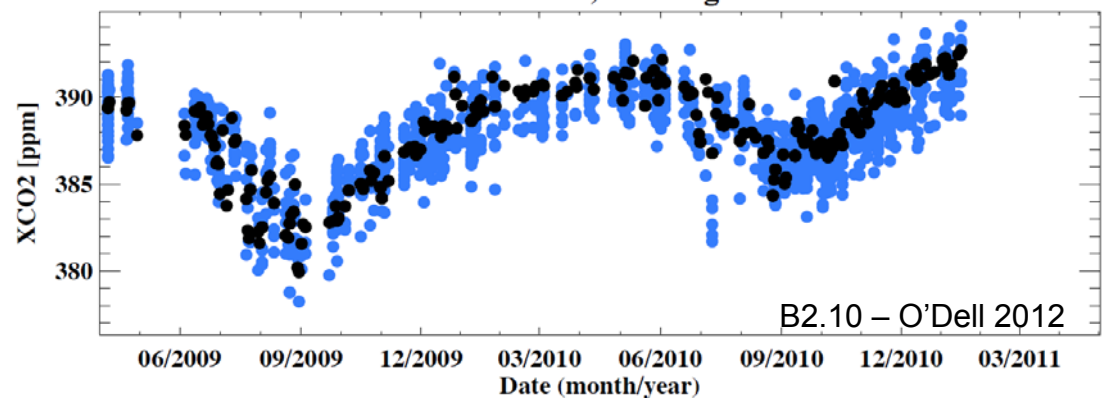
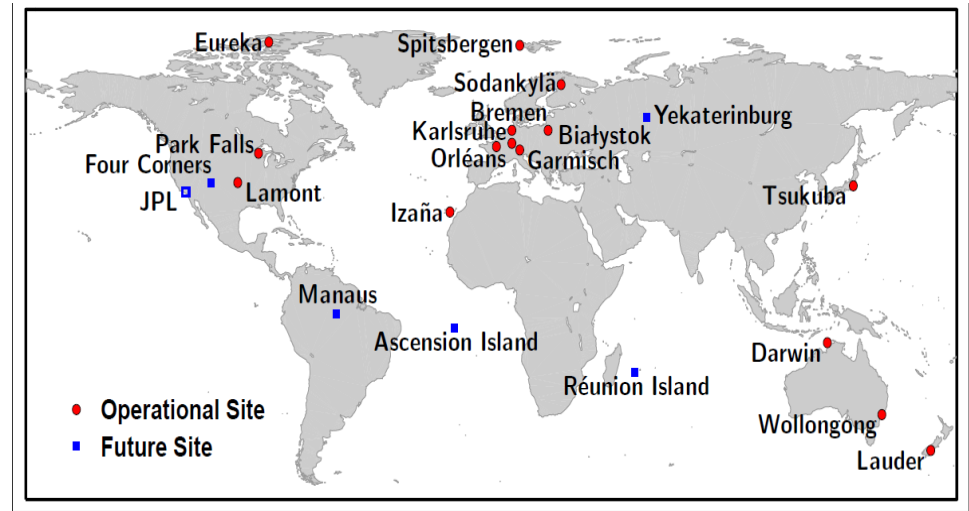




Validation of GOSAT Products against TCCON Reduces Regional Scale Bias



Near-simultaneous observations are acquired over TCCON station.



GOSAT X_{CO_2} retrievals are compared with those from the ground based Total Carbon Column Observing Network (TCCON) to verify their accuracy



Validation of GOSAT Against TCCON



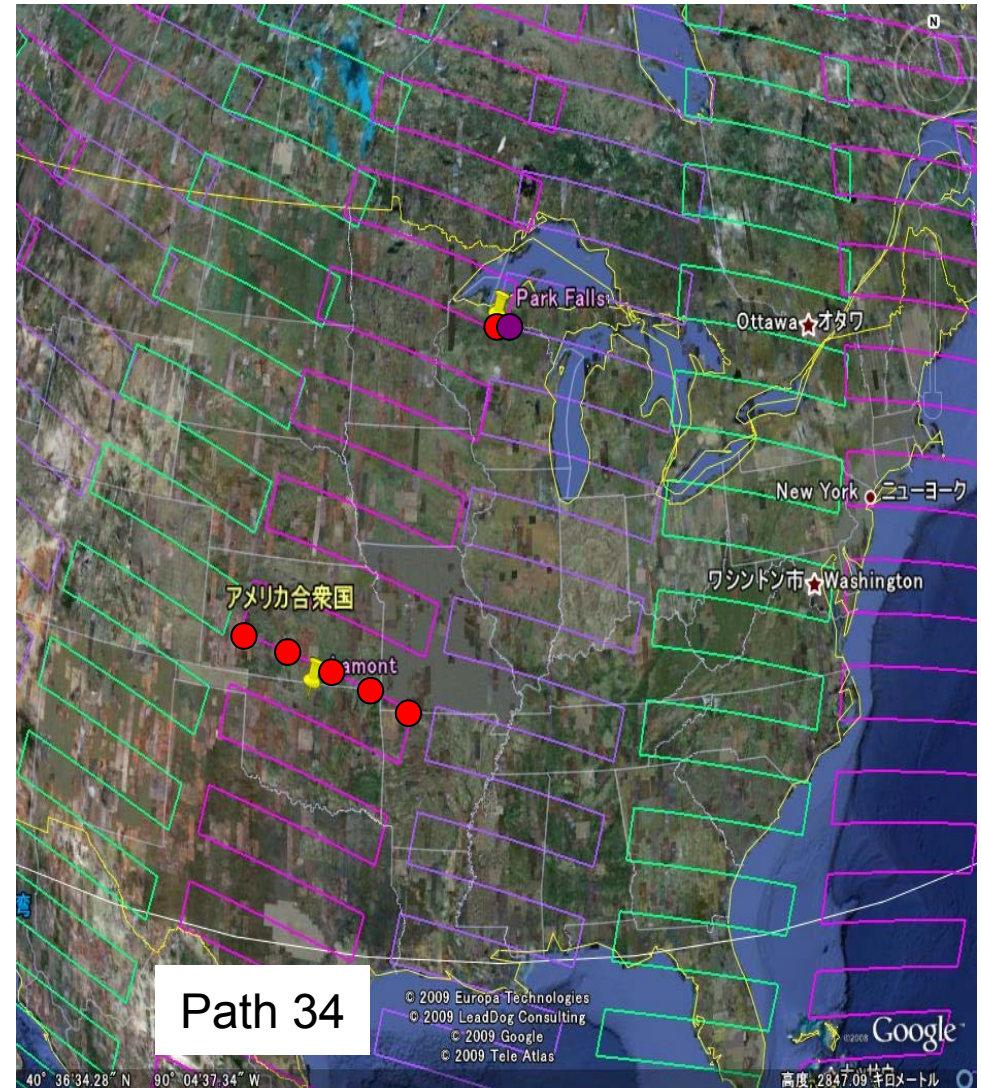
OCO-style, horizon-to-horizon target tracks not possible with GOSAT.

- Typically, only 3 soundings can be soundings over a TCCON site during a single pass
- Limits the S/N of direct comparison with TCCON data.

However, fly-bys are quite frequent

- Fly-by every 3 days (Lamont);
- 2 of every 3 days (Park Falls).
- Similar at other mid-latitude TCCON sites

The ACOS team has explored ways select and use nearby soundings for use in validation.





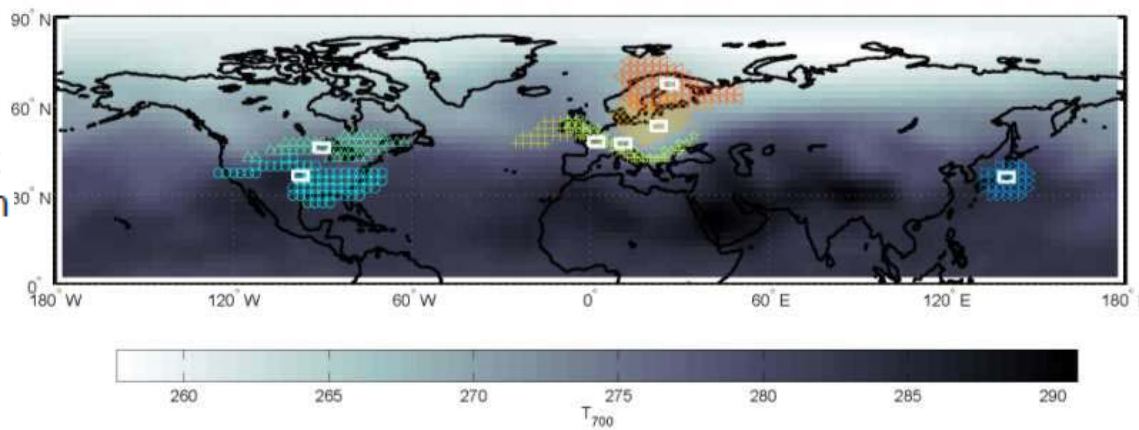
Increasing the Number of Coincident Soundings for Validation



- Strict spatial and temporal coincidence criteria is needed to identify soundings that can be validated against specific TCCON sites.
 - e.g. ± 0.5 degrees of latitude and longitude, ± 1 hour
 - Very few (≤ 3) GOSAT soundings fall within this criteria
- Keppel-Aleks et al. (2011) used TCCON data to show that there is a strong correlation between the potential temperature in the free troposphere (e.g. θ (700 hPa)) and the XCO₂ value
 - A common free-tropospheric potential temperature suggests a common air mass
- Using this approach, the coincidence criteria can be relaxed substantially, yielding far more soundings for comparison

Coincidence Criteria

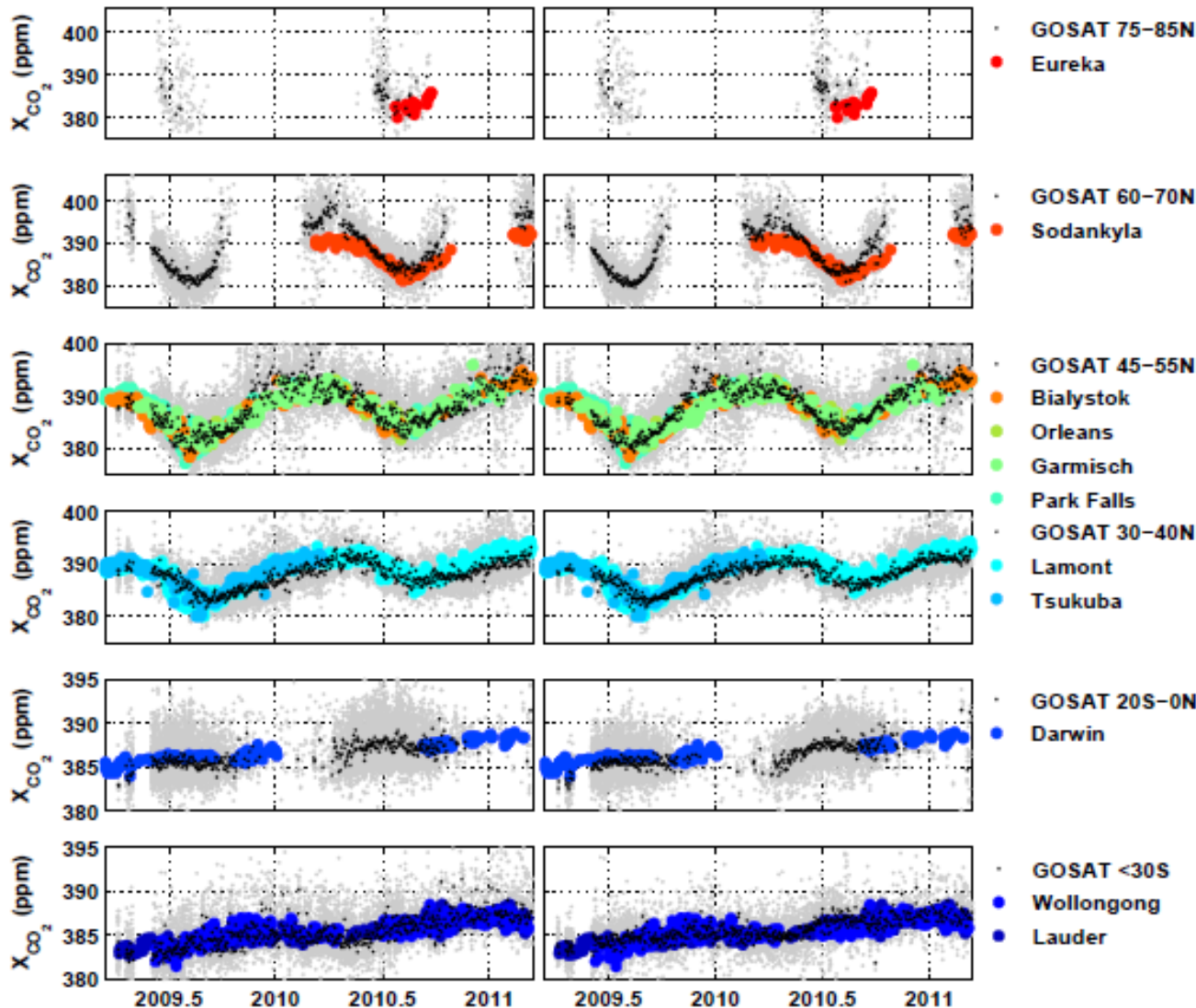
- ± 10 degrees lat
- ± 30 degrees lon
- ± 2 degrees K
- ± 5 days



Map showing areas that meet the coincidence criteria for potential temperature for several TCCON stations (small squares) (c.f. Wunch et al. 2011).



Site-By-Site Comparisons



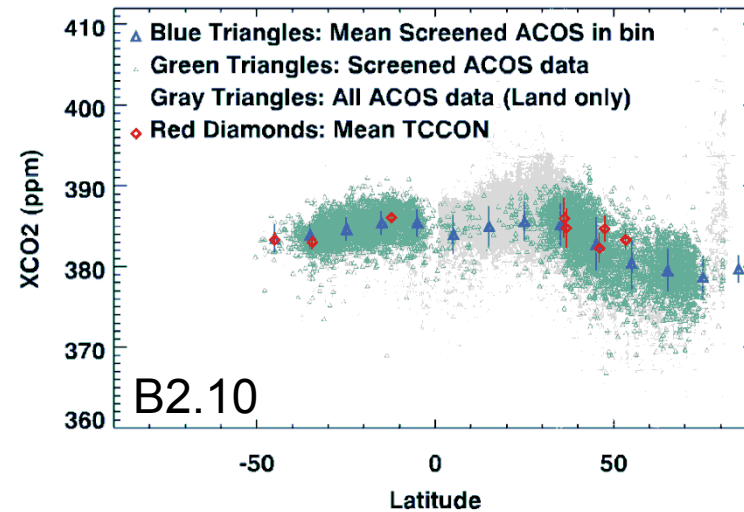
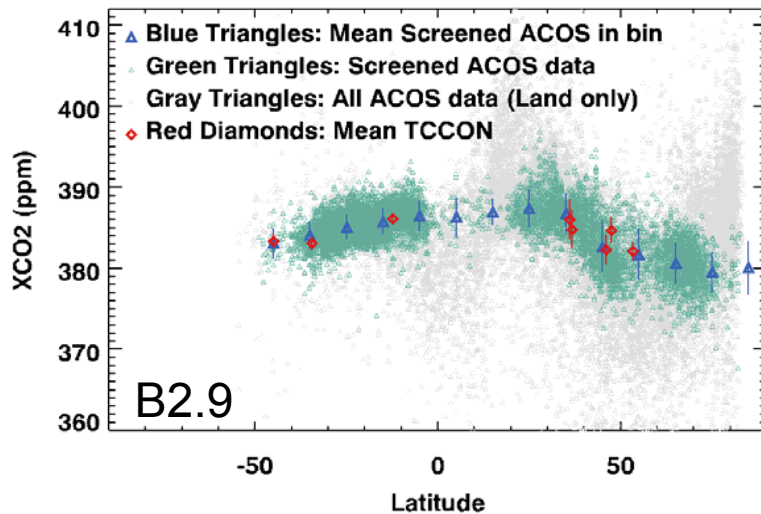
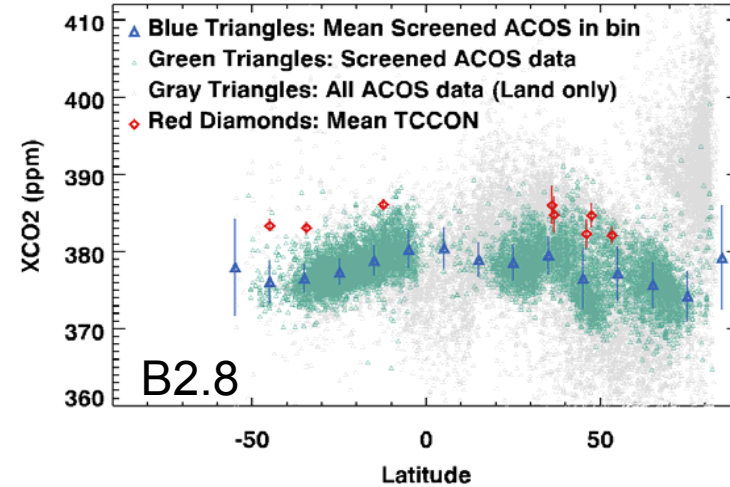
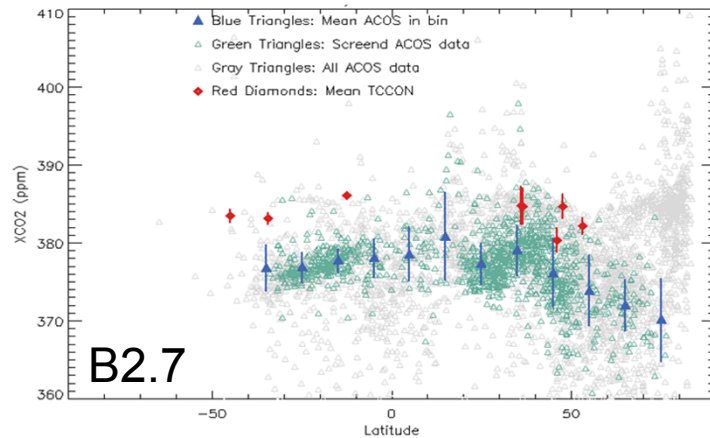
ACOS/OCO-2 estimates of X_{CO_2} from GOSAT TANSO-FTS soundings that meet the potential temperature criteria on the previous page (black dots) are compared to TCCON X_{CO_2} estimates over the seasonal cycle.

These ACOS B2.8 results have been corrected for the most significant biases (see Wunch et al 2011).





TCCON Comparisons Show Improvements in ACOS GOSAT X_{CO_2} Bias and Random Error

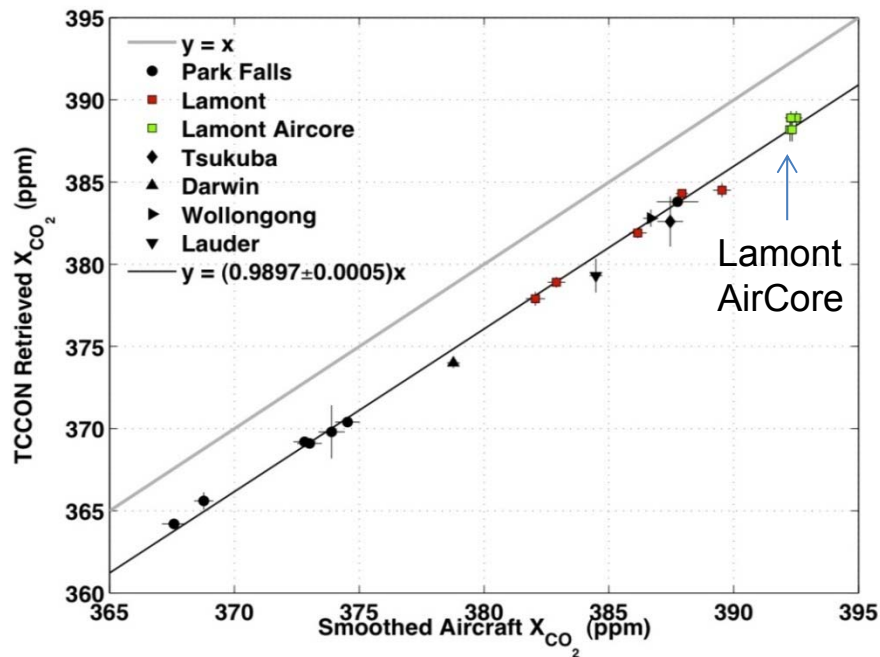


Zonal profiles of ACOS/GOSAT X_{CO_2} estimates (green and grey triangles) are compared to the monthly mean X_{CO_2} estimates from TCCON stations (red diamonds) for July 2009. The precision (scatter), bias, and yield of the ACOS/GOSAT products have improved over time (Crisp et al. 2011).

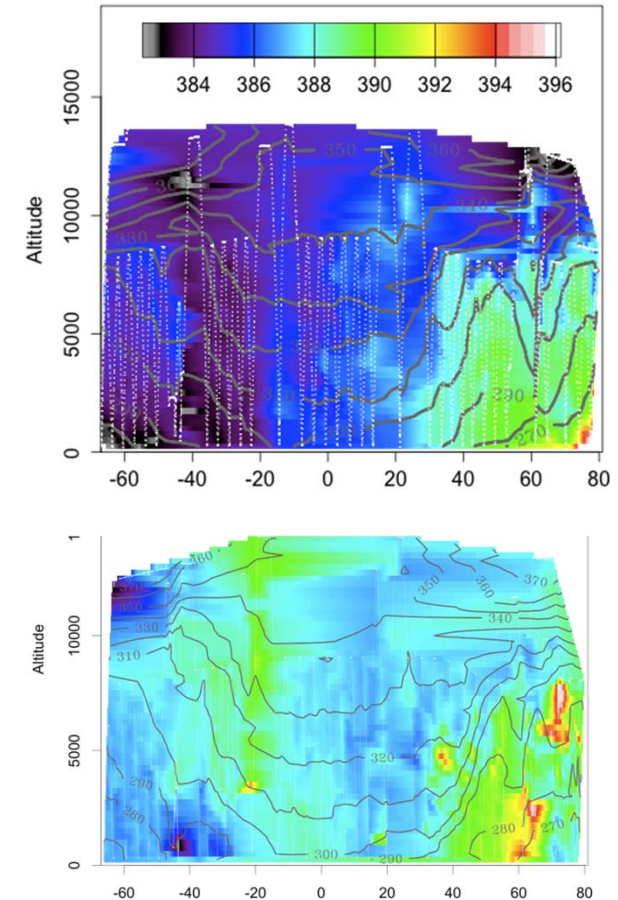


Traceability of the TCCON FTS X_{CO_2} data to the WMO CO_2 Standard

TCCON FTS observations are related to the WMO in situ CO_2 standard by acquiring in situ measurements of CO_2 with high altitude aircraft over TCCON sites.



Comparisons of results from TCCON retrievals and aircraft over flights indicates a TCCON X_{CO_2} uncertainty of ~ 0.8 ppm (2σ); after scaling for a $\sim 1\%$ bias attributed to errors in O_2 and CO_2 spectroscopy. (Wunch, D., et al. *The Total Carbon Column Observing Network (TCCON)*, *Phil. Trans. Roy. Soc. A*, 369, 2087-2112, 2011.)



In situ CO_2 measurements were acquired over TCCON sites in January (top) and November (bottom) 2009 during the HIAPER Pole-to-Pole Observations (HIPPO) campaigns.

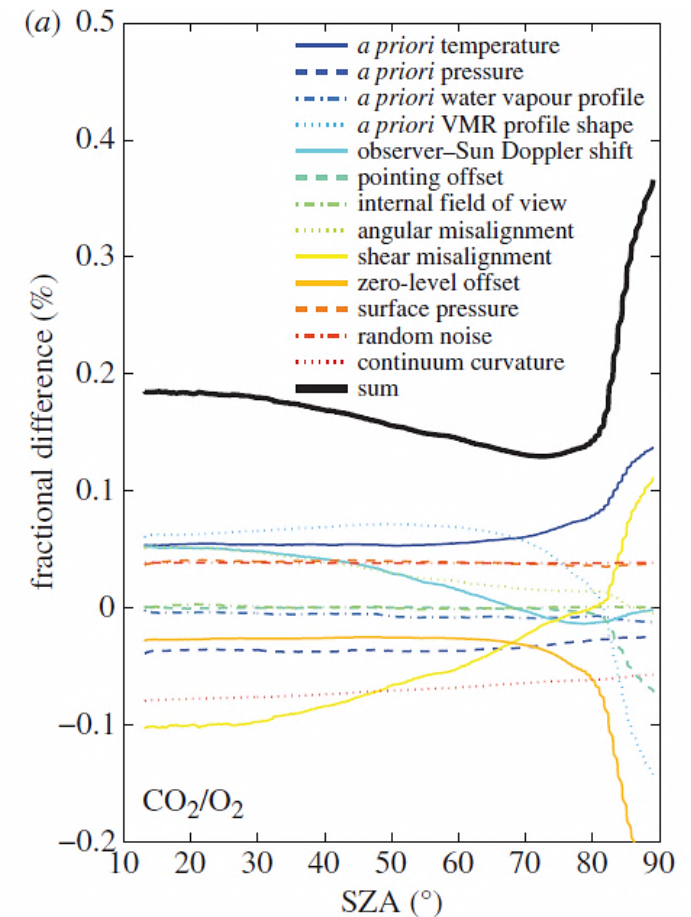


TCCON X_{CO_2} Uncertainty Overview

Effect	relative	Total column
Repeatability (spectrum-spectrum)	0.05%	0.2 ppm (1σ)
Comparability across network	0.1%	0.4 ppm
Uncorrected airmass dependence		0-2 ppm (high sza) <0.5 ppm (GOSAT)
Ghosts	< 0.2%	< 1ppm most sites
ILS	< 0.2%	< 1 ppm
Smoothing error (profile shape)	< 0.1%	< 0.4 ppm

More detail:

Wunch, D., et al. The Total Carbon Column Observing Network (TCCON), Phil. Trans. Roy. Soc. A, 369, 2087-2112, 2011.



Individual contributions to the TCCON error budget.

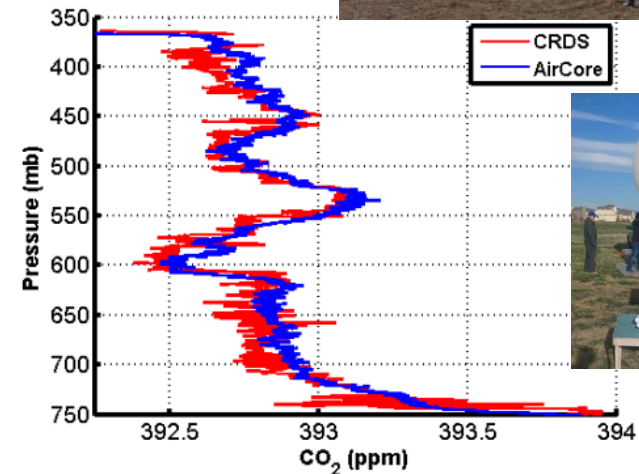


AIRCORE – A New Tool for Tracing TCCON observations to the WMO Standard

- The ACOS activity provided an opportunity to test a new CO₂ profiling system – the AirCore
- An AirCore is a passive CO₂ profiling system, consisting of a 48 – 150 m long, narrow (3-6 mm diameter) tube, with one end open and one end closed, that is coiled into a ring.
- The AirCore is carried aloft by a balloon.
- As the balloon rises, the fill gas in the tube evacuates from the open end.
- The AirCore is then released and falls back to Earth on parachute, capturing a “profile” of the atmospheric gas traversed on descent.
- It is recovered, returned to the lab, and the column of atmospheric gas is pumped out and analyzed using the same instruments used to analyze CO₂ flask samples (WMO reference).
- The AirCore is ideal for acquiring high altitude (24 km) CO₂ profiles over TCCON stations.



Southern Great Plains (SGP)
Field Test
January 14, 2012
January 15, 2012



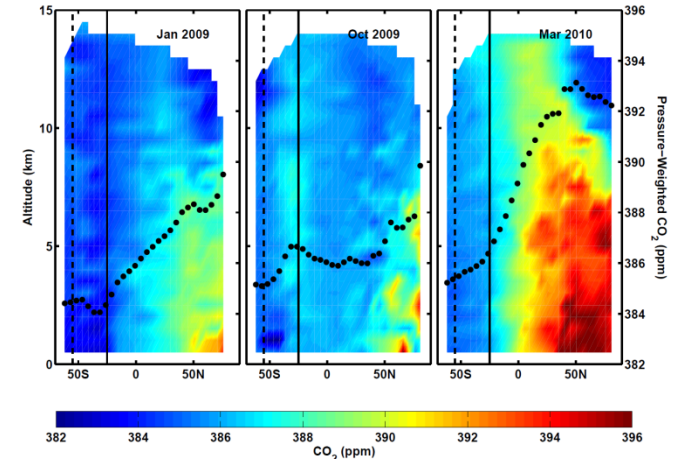
Side-by-side tests with reference instruments verify the accuracy and resolution of the AirCore. High altitude AirCore measurements have been collected over the Lamont TCCON site.

Karion et al., J. Atmos. Ocean Tech., 2010.

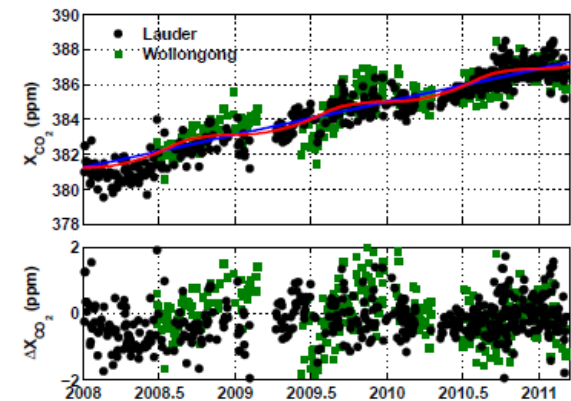


Validation Using the Southern Hemisphere Approximation

- CO₂ observations of mid latitudes in the southern hemisphere (25° to 55° S) indicate little variability (c.f. Wunch et al. 2011).
 - XCO₂ estimates from TCCON stations at Lauder, NZ and Wollongong, AZ, show typical variations of ~ 1 ppm, after correcting for a 1.89 ppm/year trend
- ACOS GOSAT X_{CO₂} retrievals from this region with values that differ substantially from the mean assumed to be spurious
- Differences between X_{CO₂} estimates and the southern hemisphere (SH) mean, ΔX_{CO_2} , have been analyzed with respect to a number observational and environmental factors to diagnose and correct these biases



CO₂ observations collected by the HIPPO campaign show little variability at latitudes between 25° S and 55° S.



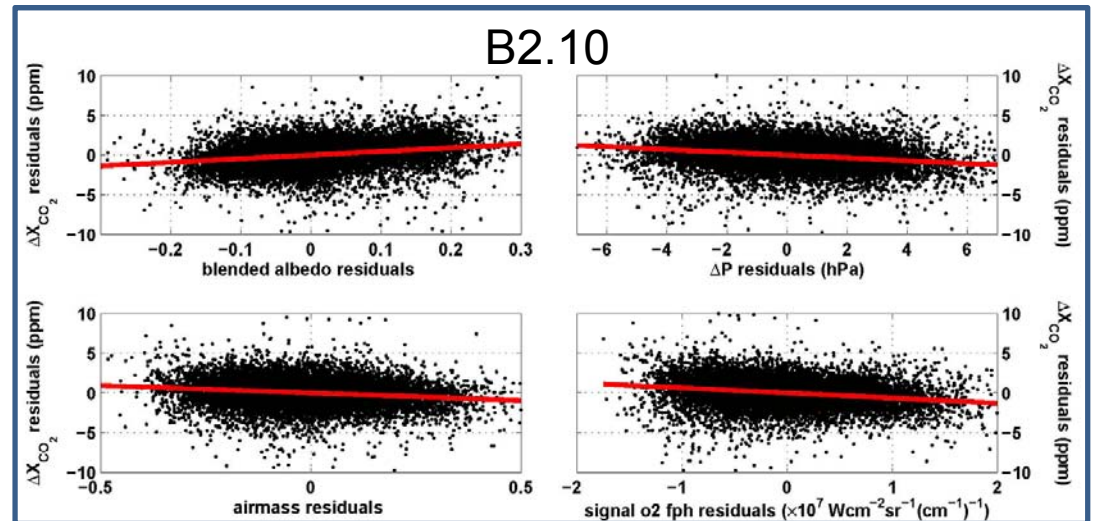
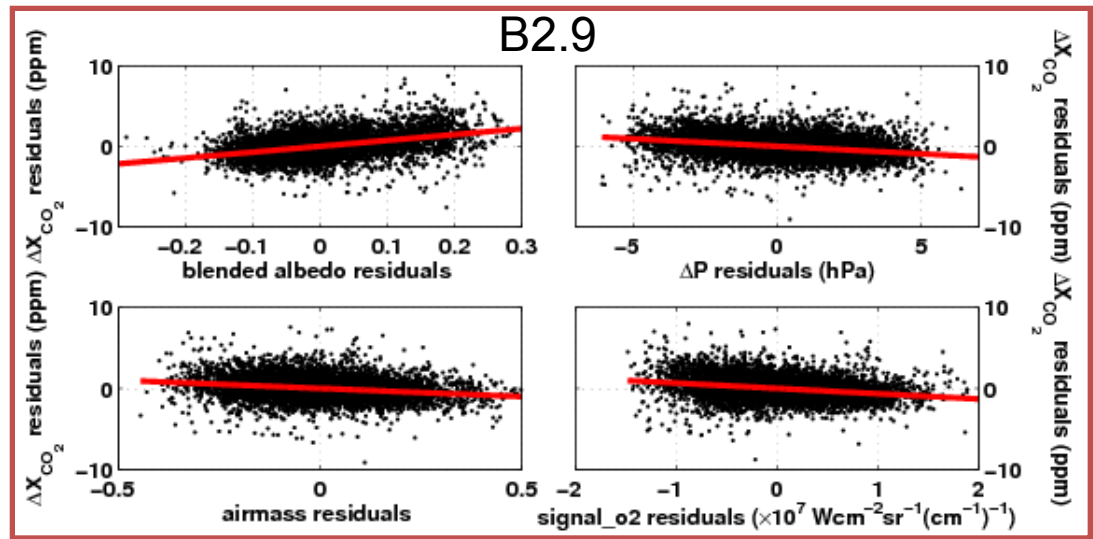
X_{CO₂} retrievals from the Lauder NZ and Wollongong Aus. TCCON stations are used to identify and remove the 1.89 ppm/year CO₂ trend. (D. Wunch et al. 2011.)



Characterizing Biases with the Southern Hemisphere Approximation

The 4 most significant correlations between ΔX_{CO_2} and observing conditions for B2.9 (top) and B2.10 (bottom) are compared.

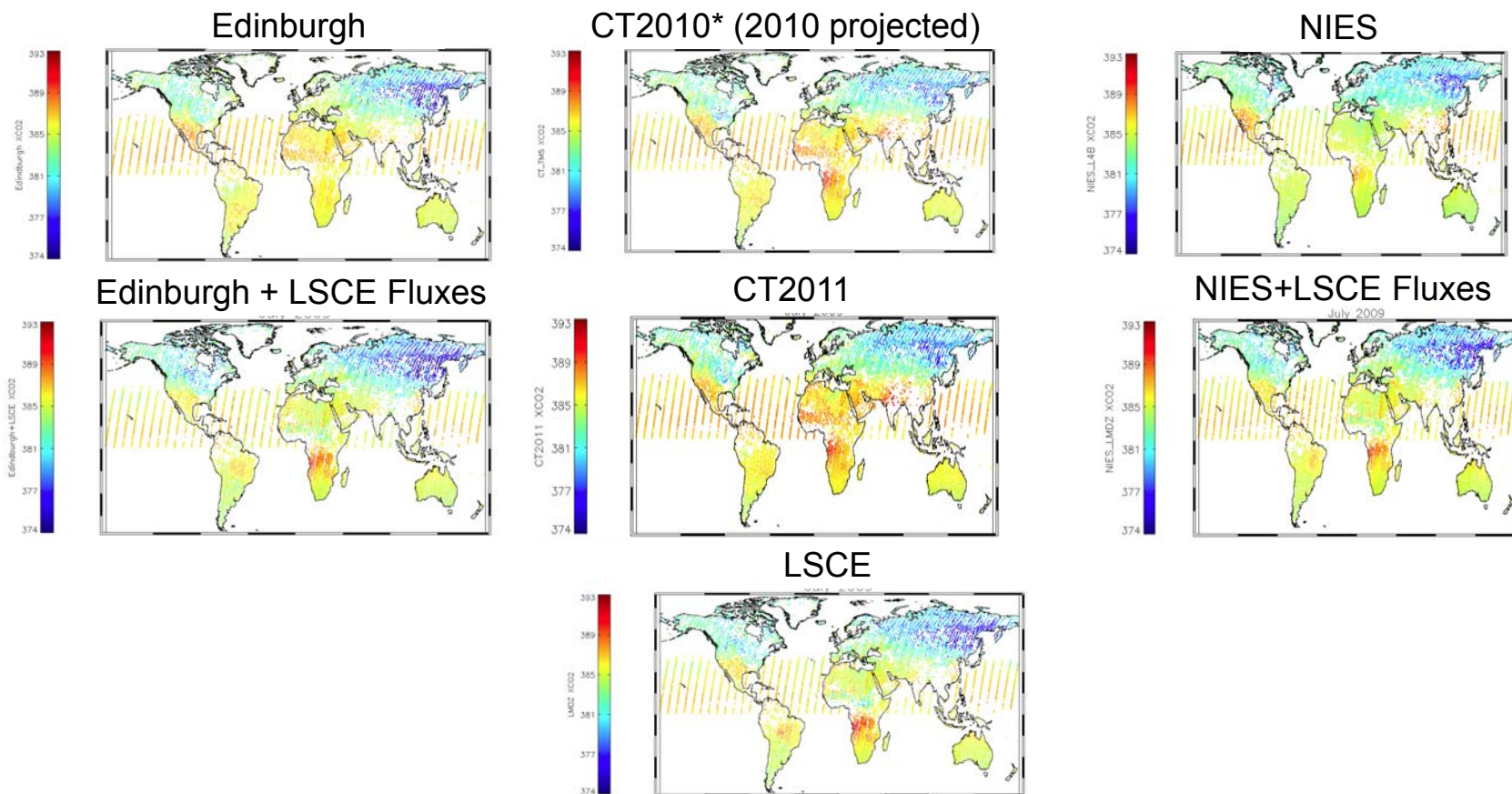
- 13,480 SH points used (matched with filtered points in B2.9)
- blended albedo correlation decreases
- ΔP remains roughly the same
- Other dependencies (signal o2, airmass) increase
- Variability decreased from 1.88 ppm to 1.82 ppm (~3%) (c.f. D. Wunch et al. 2011.)





Validation Using a Multi-Model Mean

- Existing flux inversion models include a number of limitations (transport errors, sensitivity to priors, etc.), but mean results from ensembles of models still provide a tool for identifying and characterizing X_{CO_2} biases.
- So far, 7 models have been used to define a multi-model mean





Error Assessment vs. Models

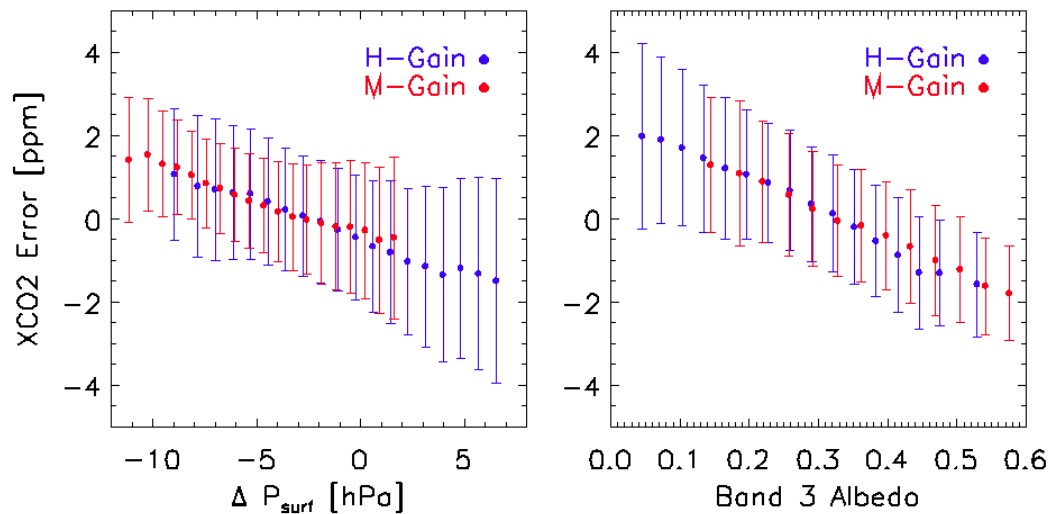
- Multiple Inverse models XCO₂ sampled at GOSAT sounding locations/times
- All models use fluxes optimized against surface observations
- Use **model mean** as truth
- All models run with their own optimized fluxes through 2010, and optionally with those from LSCE.
- Reject soundings that have greater than 1 ppm difference between any model and the multi-model mean for that sounding (~30% of soundings)
- Limitation: Places where all models are wrong in the same way!



Example: Bias-correction (land)

- Perform **multi-linear regression** of XCO₂ error versus different variables.
- In ACOS B2.9, 4 variables explained ~20% of variance (Wunch et al. 2011)
- For B2.10, we use two variables alone and explain ~20% of variance.
- Consistent fit results for **gain M** and **gain H** (disregarding offset)

Multi-Model Mean over land



Bias vs. Models: **-1.25 (-0.2)** ppm
 Bias vs. TCCON: **-0.9** ppm

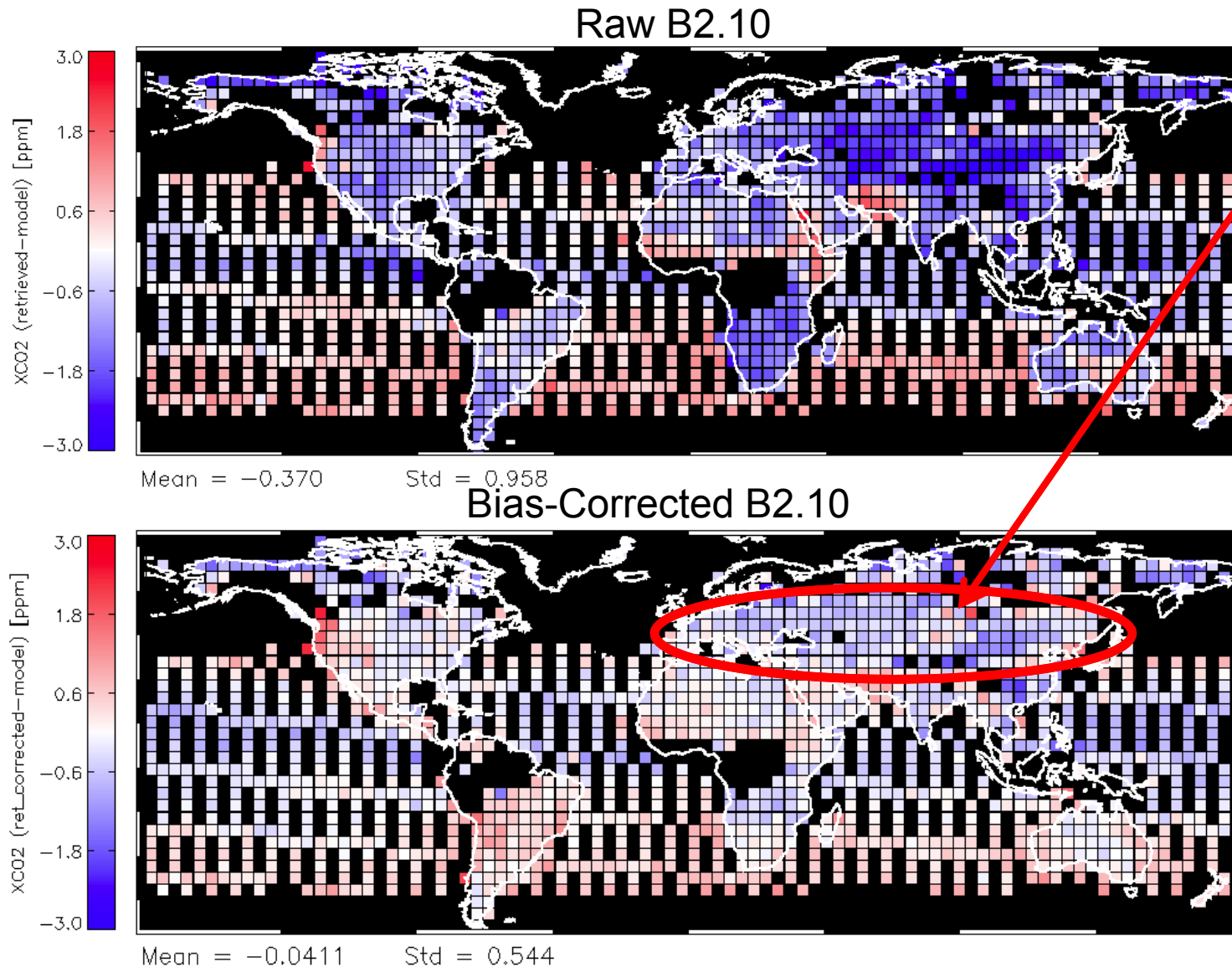
Fit Coefficients:

	ΔP_{surf}		B3 Albedo	
	H	M	H	M
TCCON	-0.23		-7.5	
SH	-0.20		-7.1	
Models	-0.19	-0.17	-7.6	-7.2

~20% of variance explained ($\sigma: 1.7 \rightarrow 1.5$ ppm)



Error Map: Raw & Bias-Corrected



Bias, or indication of stronger drawdown in N.H. summer?

- Land low bias mostly solved
- Residual Ocean bias that has interesting latitude dependence
- Interesting regional differences: real or bias??
- Seasonal bias dependencies show additional interesting features.



Proposed Bias Corrections for B2.10

- Land, Gain H:

$$X'_{CO_2} = X_{CO_2} + 0.19 \cdot (\Delta P_s + 1.0 \text{ hPa}) + 7.0 \cdot (\text{Alb}_3 - 0.20) + 1.2 \text{ [ppm]}$$

- Land, Gain M:

$$X'_{CO_2} = X_{CO_2} + 0.17 \cdot (\Delta P_s + 5.5 \text{ hPa}) + 7.0 \cdot (\text{Alb}_3 - 0.5) \text{ [ppm]}$$

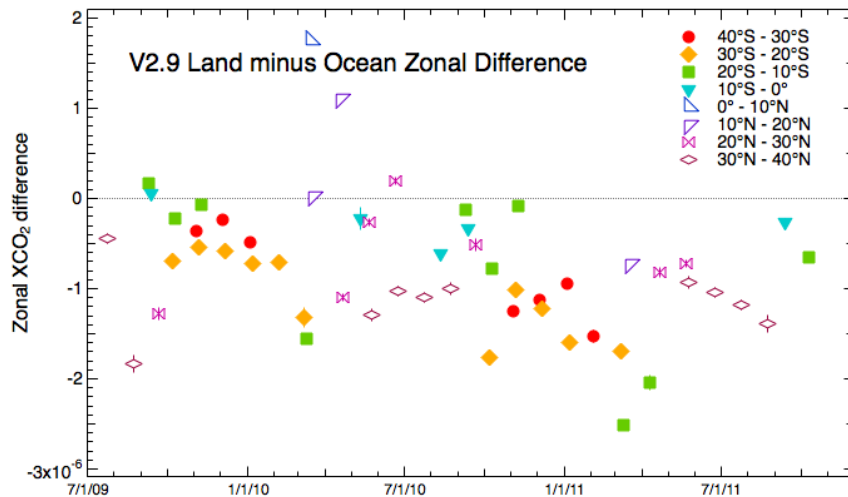
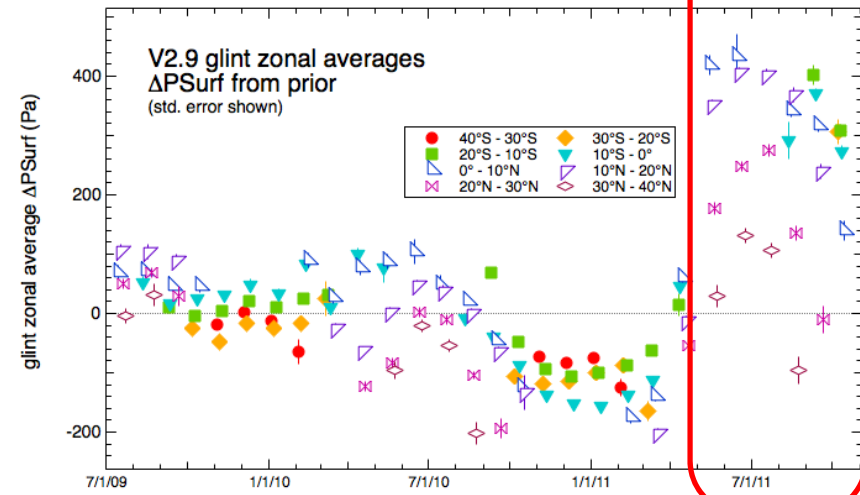
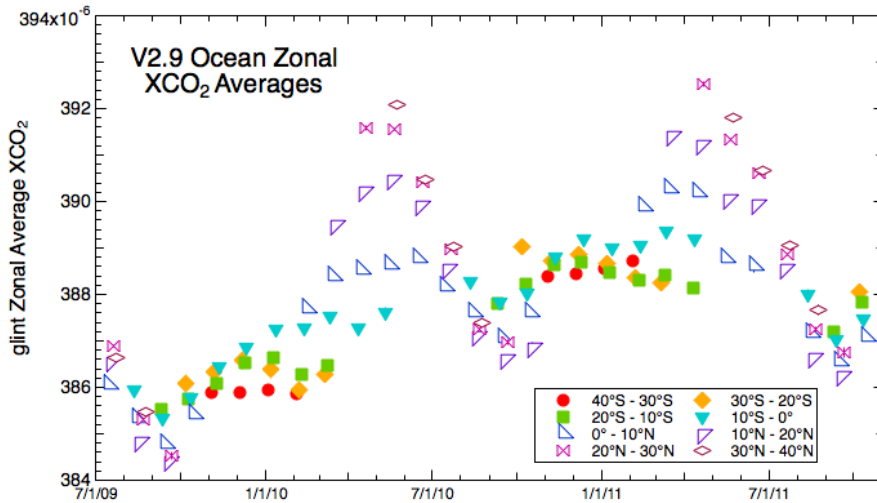
- Ocean Glint:

$$X'_{CO_2} = X_{CO_2} + 0.35 \cdot (\Delta P_s + 1 \text{ hPa}) + 6.8 \cdot (\text{AOD} - 0.2) \\ + 0.45 \cdot \min(\text{Offset}_{\text{Band1}} \cdot 10^7, 2.0) + 0.2 \text{ [ppm]}$$

- Filters and Bias Corrections are ROBUST ACROSS DIFFERENT TRUTH METRICS (TCCON, SH, Models).
- With corrections, surprisingly low RMS errors achieved for B2.10:
 - Ocean: ~ 1ppm
 - Land gain H: ~ 1.5 ppm
 - Land gain M: ~ 1.3 ppm



Other Issues: Glint Biases



Ocean glint soundings show a number of biases over time. Some are associated with known GOSAT L1B calibration errors. Others are currently under investigation.

These errors are due to known issues with GOSAT L1b product V130130.



ACOS Validation Publications (1 of 2)

Butz, A., Guerlet, S., Hasekamp, O., Schepers, D., Galli, A., Aben, I., Frankenberg, C., Hartmann, J.-M., Tran, H., Kuze, A., Keppel-Aleks, G., Toon, G., Wunch, D., Wennberg, P., Deutscher, N., Griffith, D., Macatangay, R., Messerschmidt, J., Notholt, J., and Warneke, T.: Toward accurate CO₂ and CH₄ observations from GOSAT, *Geophys. Res. Lett.*, 38, L14812, doi:10.1029/2011GL047888, 2011.

Wunch, D., Toon, G. C., Wennberg, P. O., Wofsy, S. C., Stephens, B. B., Fischer, M. L., Uchino, O., Abshire, J. B., Bernath, P., Biraud, S. C., Blavier, J.-F. L., Boone, C., Bowman, K. P., Browell, E. V., Campos, T., Connor, B. J., Daube, B. C., Deutscher, N. M., Diao, M., Elkins, J. W., Gerbig, C., Gottlieb, E., Griffith, D. W. T., Hurst, D. F., Jimé'nez, R., Keppel-Aleks, G., Kort, E. A., Macatangay, R., Machida, T., Matsueda, H., Moore, F., Morino, I., Park, S., Robinson, J., Roehl, C. M., Sawa, Y., Sherlock, V., Sweeney, C., Tanaka, T., and Zondlo, M. A.: Calibration of the Total Carbon Column Observing Network using aircraft profile data, *Atmos. Meas. Tech.*, 3, 1351–1362, 2010. doi:10.5194/amt-3-1351-2010, 2010.

Wunch, D., Toon, G. C., Blavier, J.-F. L., Washenfelder, R. A., Notholt, J., Connor, B. J., Griffith, D. W. T., Sherlock, V., and Wennberg, P. O.: The Total Carbon Column Observing Network, *Phil. Trans. R. Soc. A*, 369, 2087–2112, doi:10.1098/rsta.2010.0240, 2011a.



ACOS Validation Publications (2 of 2)

Wunch, D., Wennberg, P. O., Toon, G. C., Connor, B. J., Fisher, B., Osterman, G. B., Frankenberg, C., Mandrake, L., O'Dell, C., Ahonen, P., Biraud, S. C., Castano, R., Cressie, N., Crisp, D., Deutscher, N. M., Eldering, A., Fisher, M. L., Griffith, D. W. T., Gunson, M., Heikkinen, P., Keppel-Aleks, G., Kyrö, E., Lindenmaier, R., Macatangay, R., Mendonca, J., Messerschmidt, J., Miller, C. E., Morino, I., Notholt, J., Oyafuso, F. A., Rettinger, M., Robinson, J., Roehl, C. M., Salawitch, R. J., Sherlock, V., Strong, K., Sussmann, R., Tanaka, T., Thompson, D. R., Uchino, O., Warneke, T., and Wofsy, S. C.: A method for evaluating bias in global measurements of CO₂ total columns from space, *Atmos. Chem. Phys.*, 11, 20899–20946, doi:10.5194/acpd-11-20899-2011, 2011.

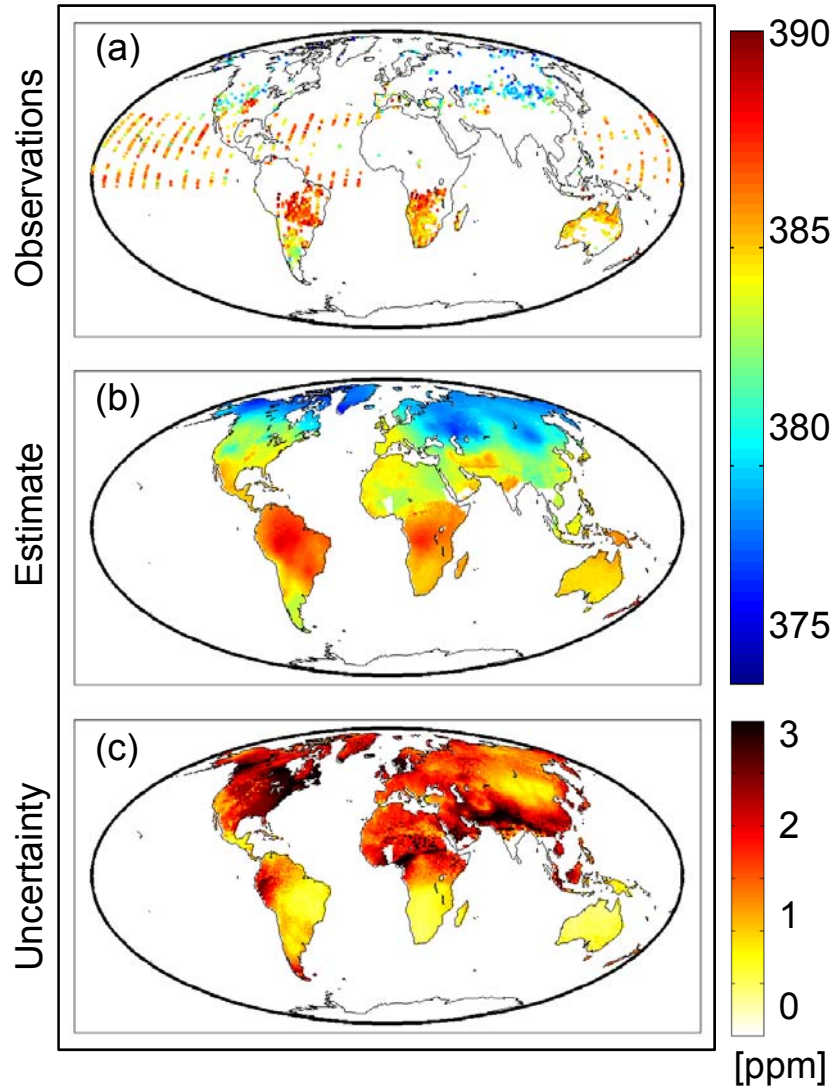


ACOS/GOSAT Higher Level Products





Higher Level Products from GOSAT Data



D. Hammerling et al. GRL, 39, 2012.

- Geostatistical methods are being used to generate gap-filled global X_{CO_2} maps.
- These “Level 3” data products contribute additional insight into the spatial variations in X_{CO_2} by:
 - Providing continuous averages,
 - based on the spatial and temporal statistics of the actual measurements
 - Reduces the contributions of outliers
 - Provides evaluation data for
 - Source and sink estimates
 - Global and regional transport models
 - Retrieval algorithms
 - Also provides spatially resolved estimates of the uncertainties in the X_{CO_2} field

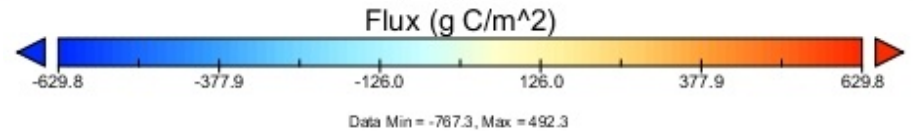
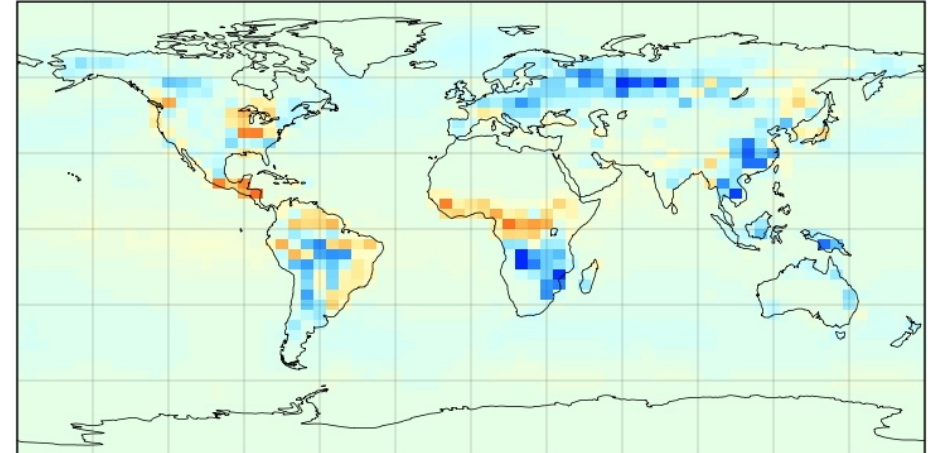
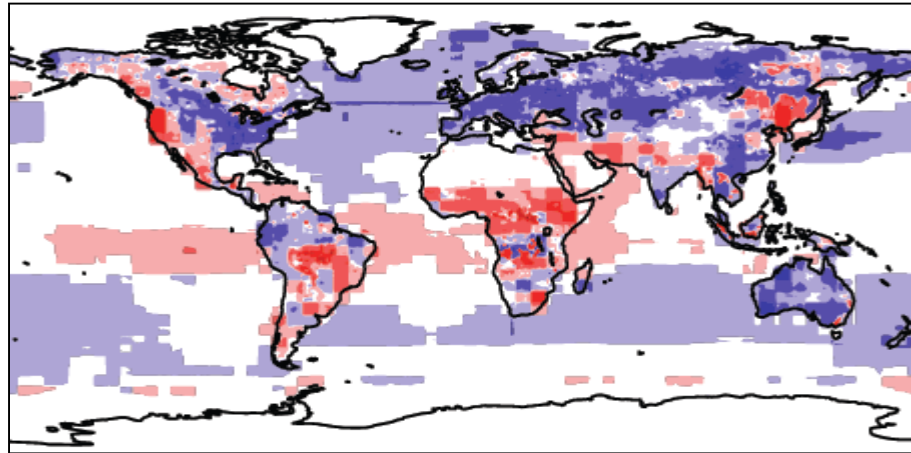


Flux Inversion Studies Using ACOS GOSAT X_{CO_2} Data

- The availability of ACOS GOSAT B2.9 products has motivated a new set of flux inversion studies from several groups, including:
 - David Baker, Colorado State University/CIRA, USA
 - Frederic Chevallier, LSCE/CEA, France
 - Dylan Jones and Feng Deng, University of Toronto, Canada
 - Junjie Liu et al., JPL, U. Md., U.C. Berkeley, USA
 - Paul Palmer and Liang Feng, University of Edinburgh, U.K
- Preliminary results suggest that
 - ACOS B2.9 products generally improve the results over the prior
 - The intensity and distribution of the retrieved fluxes depend on
 - The assumed prior
 - The dynamics used to drive the flux inversion model
 - The details of the GOSAT X_{CO_2} retrievals used
 - Bias corrections applied
 - H-gain only vs H+M Gain data, Ocean glint data, etc.



Examples of GOSAT Flux Inversions for 2010



D. Baker, CIRA

- 4-D VAR assimilation system
- Weekly CO₂ fluxes @ 4½°x6° (lat/lon)
- PCTM off-line transport, GEOS 5 met fields
- Prior fluxes, a CarbonTracker
- ACOS v2.9 with 3-parameter bias correction

Jones & Deng, U. Toronto

- 4-D VAR assimilation system (GEOS-Chem)
- Monthly CO₂ fluxes @ 4° x 5° (lat/lon)
- GEOS-Chem transport, GEOS 5 met fields
- Prior fluxes: Anthropogenic fluxes from several sources, plus annually balanced biosphere fluxes from CASA
- ACOS v2.9, H-Gain only, no bias correction



Assimilation of GOSAT X_{CO_2} from NASA's ACOS v2.10

Frédéric Chevallier
Laboratory for Sciences of Climate
and the Environment (LSCE)

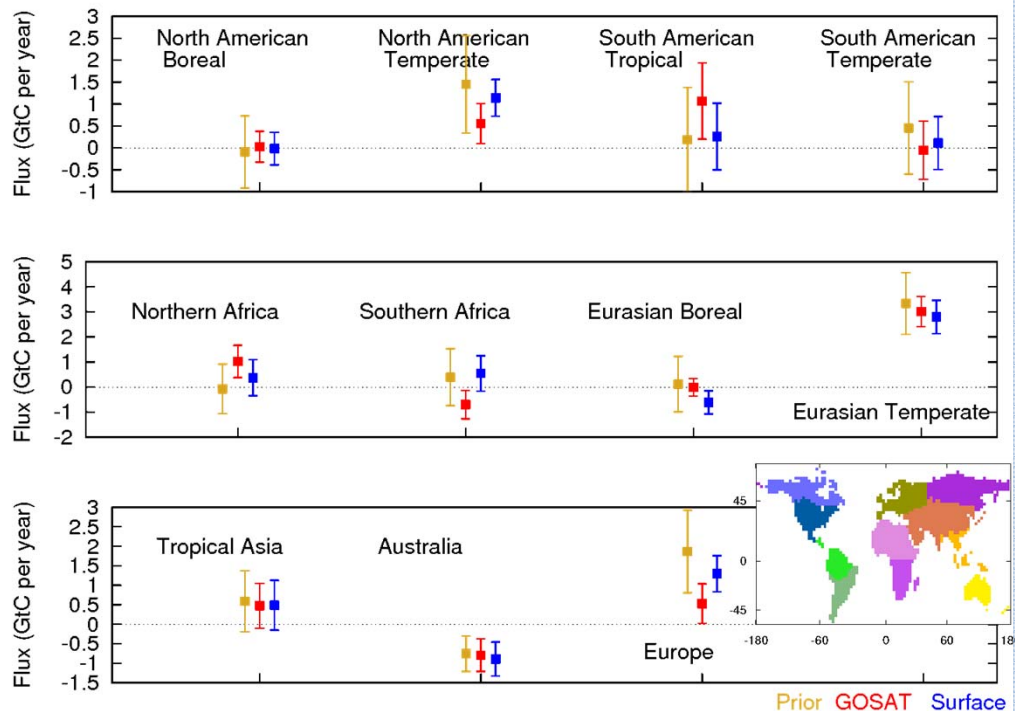
ACOS quality control and bias correction
from C. O'Dell. Ocean glint data included.

GOSAT-based inversion vs.
Air-sample-based inversion for 2010
and vs. prior fluxes.

The inversion works at grid-point weekly
scale (Chevallier et al. 2005) but the
results are presented for subcontinental
annual fluxes.

Total fluxes are shown (including fossil).
Positive values correspond to a source to
the atmosphere.

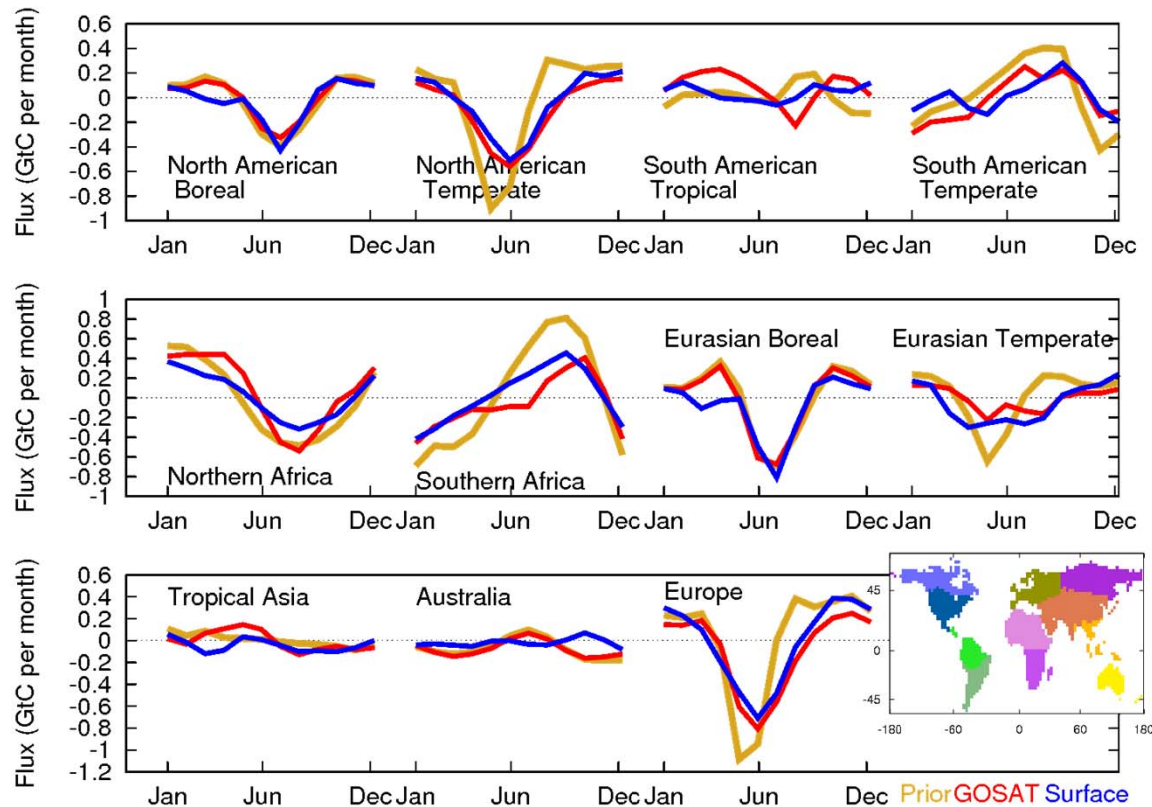
The bars represent the 1- σ Bayesian
uncertainty.



Some regions show unrealistic budgets: Europe and North American Temperate (too much uptake), South American Tropical and Boreal Eurasia (too large source).



Assimilation of GOSAT X_{CO_2} from NASA's ACOS v2.10



Frédéric Chevallier
Laboratory for Sciences of Climate
and the Environment (LSCE)

The inversion works at grid-point weekly scale (Chevallier et al. 2005) but the results are presented for sub-continental **monthly** fluxes.

Natural fluxes are shown (without fossil fuel contributions). Positive values correspond to a source to the atmosphere.

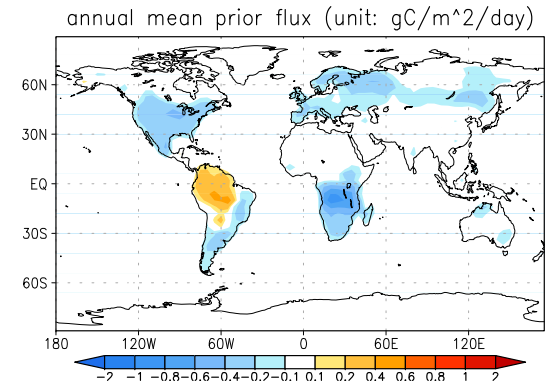
- GOSAT-inferred seasonal cycles agree with the air-sample-inferred cycle fairly well in terms of phase and amplitude (e.g., North American Temperate and Europe).
- However, small differences at the monthly scale lead to unrealistic cumulated budgets at the end of the year in several parts of the globe.



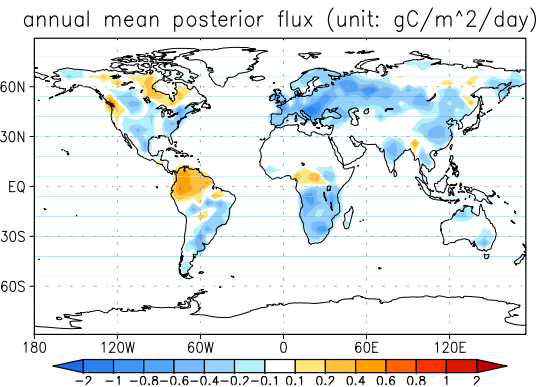
Flux estimates from the NASA CMS Flux Pilot Project

The 4D-Var approach using GEOS-Chem adjoint model (4x5 resolution) was used to estimate the 2010 monthly terrestrial biosphere flux with ACOS v2.9 X_{CO_2} observations

1. The prior biosphere flux (i.e., annual sink is 5.1GtC for 2010) is constructed in a way that the simulated mean CO_2 trend agrees with the observed mean CO_2 trend;
2. The error statistics for observations and prior flux are diagonal.
3. Bias correction method follows Wunch et al. (2011) but with different coefficients;
4. The optimization process redistribute the prior flux: the sink over Eurasia becomes stronger (bottom right panel); sink over the North America continent becomes weaker; Africa has stronger source, while source over Amazon becomes weaker



Prior biosphere flux:
-5.1GtC/year (sink)



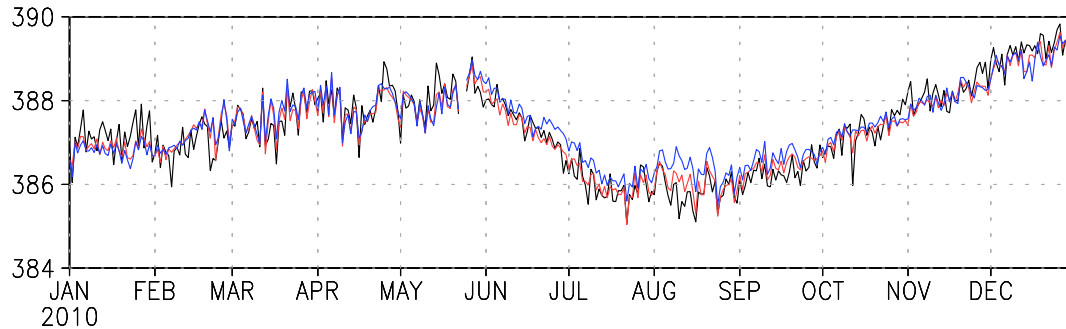
Posterior biosphere flux:
-5.4GtC/year (sink)

J. Liu, K. Bowman, and the NASA Carbon
Monitoring System Flux Pilot Project Team

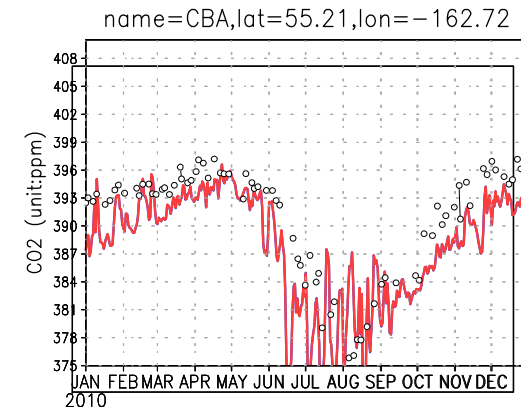
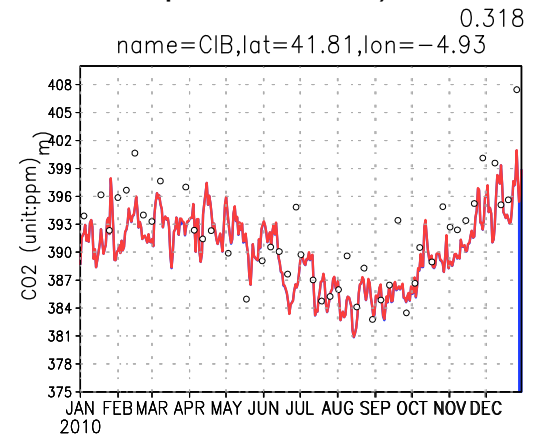


Annual Terrestrial Biosphere Flux Estimates from ACOS v2.9 X_{CO_2} observations

ACOS: black; prior: blue; post: red
obs=386.25, post=386.229, prior=386.345



Compared to independent surface flask CO_2 (open circles, NOAA ESRL); blue: CO_2 forced by prior flux; red: CO_2 forced by posterior flux)



- The posterior CO_2 concentration (red on top panel) agrees well with the ACOS observations (black, global bias is less than 0.03 ppm), and the difference between model simulated X_{CO_2} and the observations become smaller after optimization. The improvement is strongest during boreal summer.
- There is almost no change in CO_2 over the surface flask sites (right panel; red and blue almost on top of each other), which indicates the challenge of using surface flask observations to verify flux estimation from column data.

Junjie Liu, Integrated Carbon Cycle Data Assimilation (ICCDa) 2012



Assessing Biases and Random Errors in ACOS-GOSAT X_{CO_2}

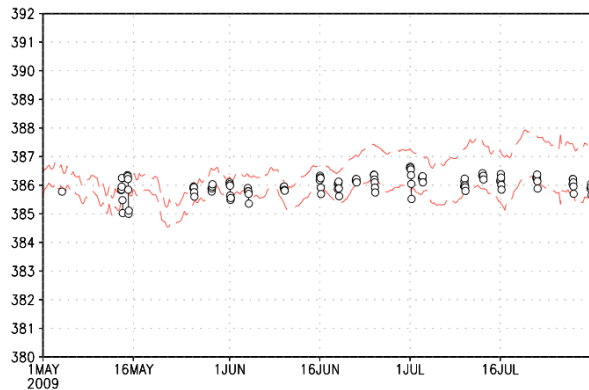
Assessing biases and random errors in ACOS-GOSAT X_{CO_2} with ensemble CO_2 analyses from the Integrated Carbon Cycle Data Assimilation (ICCDa) system

ICCDa: NCAR Carbon-Climate model coupled with ensemble Kalman filter assimilating meteorology observations and CO_2 observations (i.e., surface flask, TCCON, and AIRS CO_2) simultaneously; It estimates the mean CO_2 and the uncertainty of the mean state; The uncertainty includes the impact of uncertainty in meteorology on CO_2 analysis;

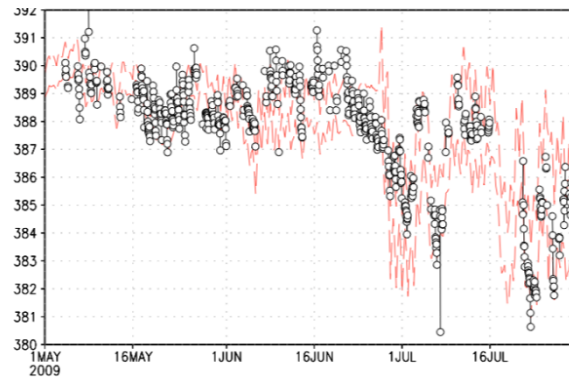
Objective: assess the biases of ACOS-GOSAT X_{CO_2} with ensemble CO_2 analysis generated by assimilating CO_2 from multiple **observation platforms** using Ensemble Kalman filter;

Verification of the accuracy of analysis mean state and analysis uncertainty

Darwin (12.4°S, 130.9°E)



Lamont (36.6°S, 97.5°W)



**Red: 6 hourly mean analysis
± estimated uncertainty;
black: hourly observations**

NASA Carbon Monitoring
System Flux Pilot project

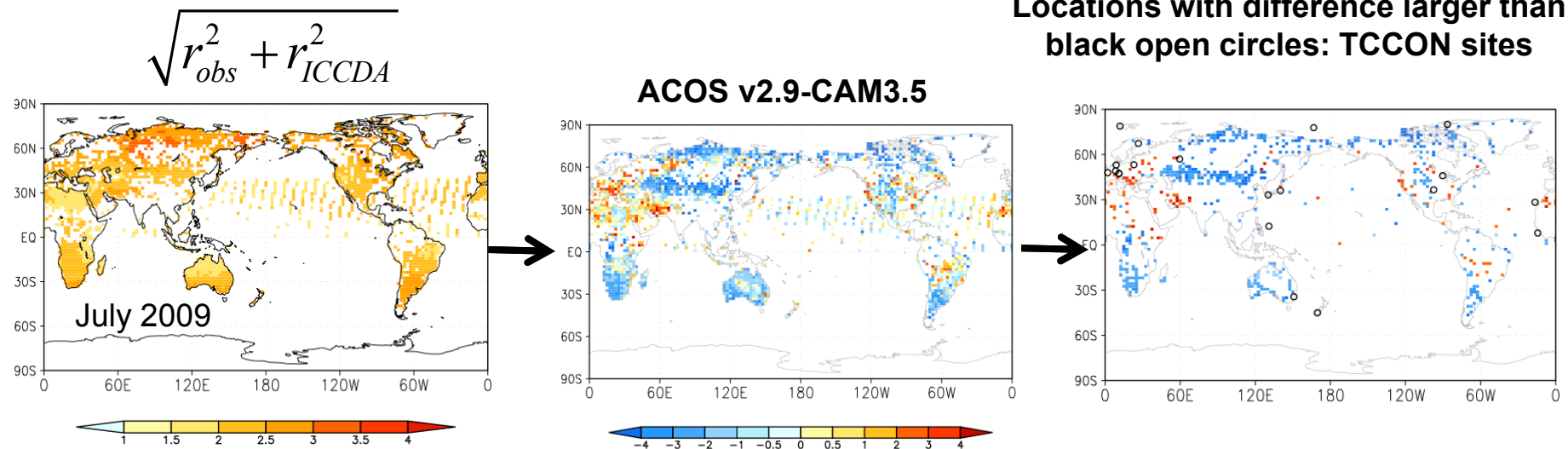
The ensemble CO_2 analyses (red, mean state \pm the uncertainty of the mean state) from the ICCDA encompass the TCCON observations (black) over most of the cases, which indicate the uncertainty estimation from the ICCDA is reasonable



Assessing Biases and Random Errors in ACOS-GOSAT X_{CO_2}

Methodology: the squared difference between the ACOS CO₂ observations (C_{acos}) and the mean CO₂ analysis from the ICCDA ($C_{ICCD A}$) is equal to the sum of the observation error variance (r_{obs})² and the analysis error variance ($r_{ICCD A}$)², when we assume there is no correlation between ensemble CO₂ analyses and the observation. This assumption is valid since ACOS observations has not been assimilated. $(C_{acos} - C_{ICCD A})^2 = r_{obs}^2 + r_{ICCD A}^2$

Using this relationship, we can examine the accuracy of the estimated random errors of ACOS observations over the whole globe.



- The combined uncertainty is less than 3ppm over most of the region;
- The difference is **NOT** significant at TCCON sites;
- The regions with significant difference may indicate that the estimated ACOS errors are too low, and is worth further investigation;

NASA Carbon Monitoring System Flux Pilot project



Summary of Preliminary Source/Sink Inversion results

- Preliminary results clearly demonstrate the utility of total column CO₂ measurements for constraining fluxes, even at substantial distances from the measurements.
- While the X_{CO2} quality control and bias corrections have improved with every new version of the ACOS data product, flux inversion results are still dominated by X_{CO2} variations with amplitudes comparable to the bias corrections
- Large data gaps in the quality-controlled GOSAT data, linked to clouds or weak sunlight, preclude accurate flux inversions over many regions, even on seasonal time scales
- Transport model errors remain an issue



Summary of ACOS GOSAT X_{CO_2} Results

- The ACOS/OCO-2 “Full Physics” retrieval algorithm is:
 - currently in place and is generating an exploratory GOSAT X_{CO_2} product
 - April 2009 – April 2012 delivered to JAXA and to the GES DISC
 - still evolving, to address known errors and biases
- Validation of GOSAT X_{CO_2} retrievals against TCCON results
 - indicate errors < 2 ppm (0.5%) on regional scales over much of the globe
 - are providing valuable insights into the causes of regional-scale bias
- Additional efforts are needed to improve the spatial coverage and yield
- Ongoing efforts to improve the accuracy of the L1B product, the absorption coefficients of CO_2 , O_2 , and other gases, and the aerosol retrieval approach are expected to yield additional reductions in bias and random error
- Lessons learned from this experience are expected to substantially accelerate the delivery of high quality products from the OCO-2 and GOSAT-2



The ACOS Science Data Operations System (SDOS)





The ACOS Science Data Operations System (SDOS)

To implement the ACOS task, the SDOS system:

- Identified new external interfaces and documented requirements and agreements for product deliveries.
- Modified the OCO data processing architecture to accommodate GOSAT TANSO-FTS products.
- Processed over 3.5 years of GOSAT TANSO FTS data (April 2009 – July 2012)
- Implemented dramatic improvements in the Level 2 Algorithm speed and accuracy.



Access to GOSAT Data

- Mission Operation Interface Specification (MOIS) was negotiated between JPL and JAXA, and implemented early in the ACOS task
- The automated data transfer system, based on the JAXA-specified “Connect Direct” software, was tested in October, 2009
- Routine, automated transfers of TANSO FTS L1B data from JAXA to JPL began 27 October 2009 and is continuing successfully.
- Routine, automated transfers of ACOS Level 2 products to JAXA were initiated in March 2010.



ACOS GOSAT Processing History

	1	2	3	4	5	6	7	8	9	10	11	12	13	14	15	16	17	18	19	20	21	22	23	24	25	26	27	28	29	30	31	
January 09																																
February																																
March																																
April																																
May																																
June																																
July																																
August																																
September																																
October																																
November																																
December																																
January 10																																
February																																
March																																
April																																
May																																
June																																
July																																
August																																
September																																
October																																
November																																
December																																
January 11																																
February																																
March																																
April																																
May																																
June																																
July																																
August																																
September																																
October																																
November																																
December																																
January 12																																
February																																
March																																
April																																
May																																
June																																
July																																
August																																

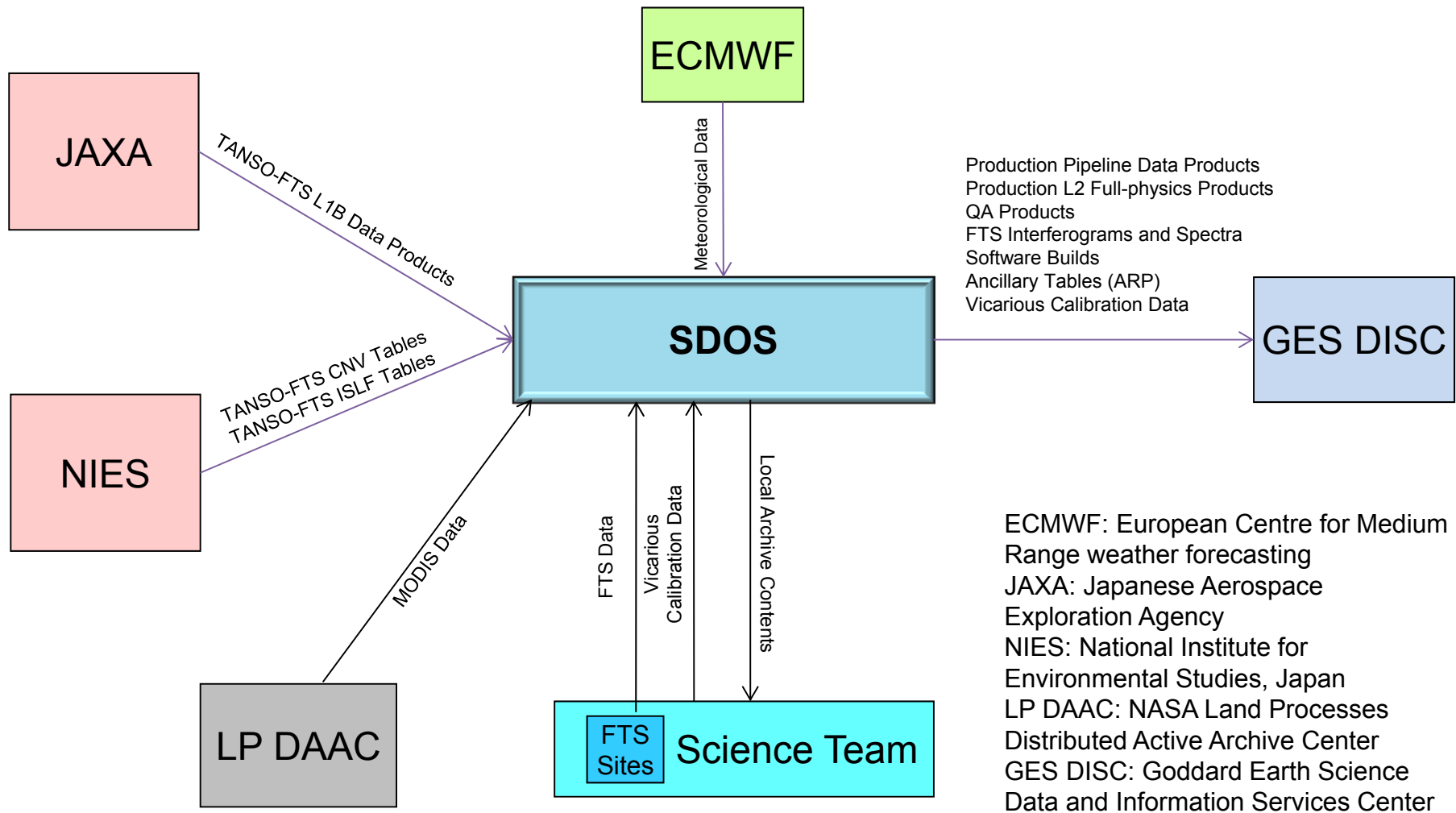
L1B Version

-  GOSAT v050
-  GOSAT v080
-  GOSAT v100
-  GOSAT v110
-  GOSAT v130
-  GOSAT v150
-  GOSAT v151
-  reprocessed V150
-  reprocessed V151

Note: JAXA plans to reprocess all GOSAT data using the v15x algorithm prior to the end of November, 2012.

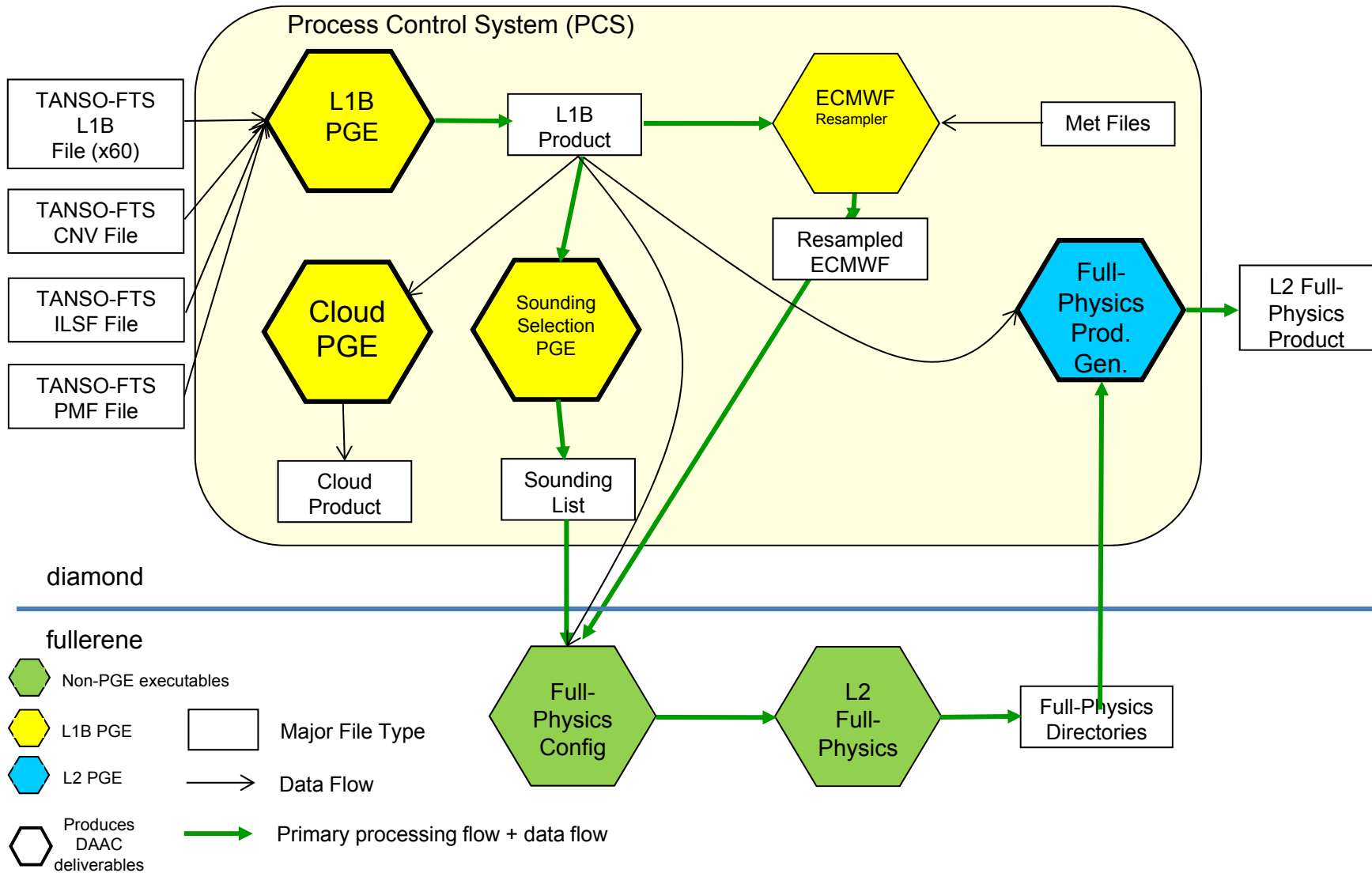


External Interfaces





ACOS GOSAT Data Processing Path





ACOS GOSAT Data Archiving

- The ACOS L2 Standard Products are being archived and distributed through the Goddard Earth Science Data and Information Services Center (GES DISC)

- GES DISC web page:

<http://disc.gsfc.nasa.gov/>

- Data can be accessed through the Mirador search engine:

<http://mirador.gsfc.nasa.gov/>

- Mirador page for ACOS data:

<http://mirador.gsfc.nasa.gov/cgi-bin/mirador/homepageAlt.pl?keyword=ACOS>

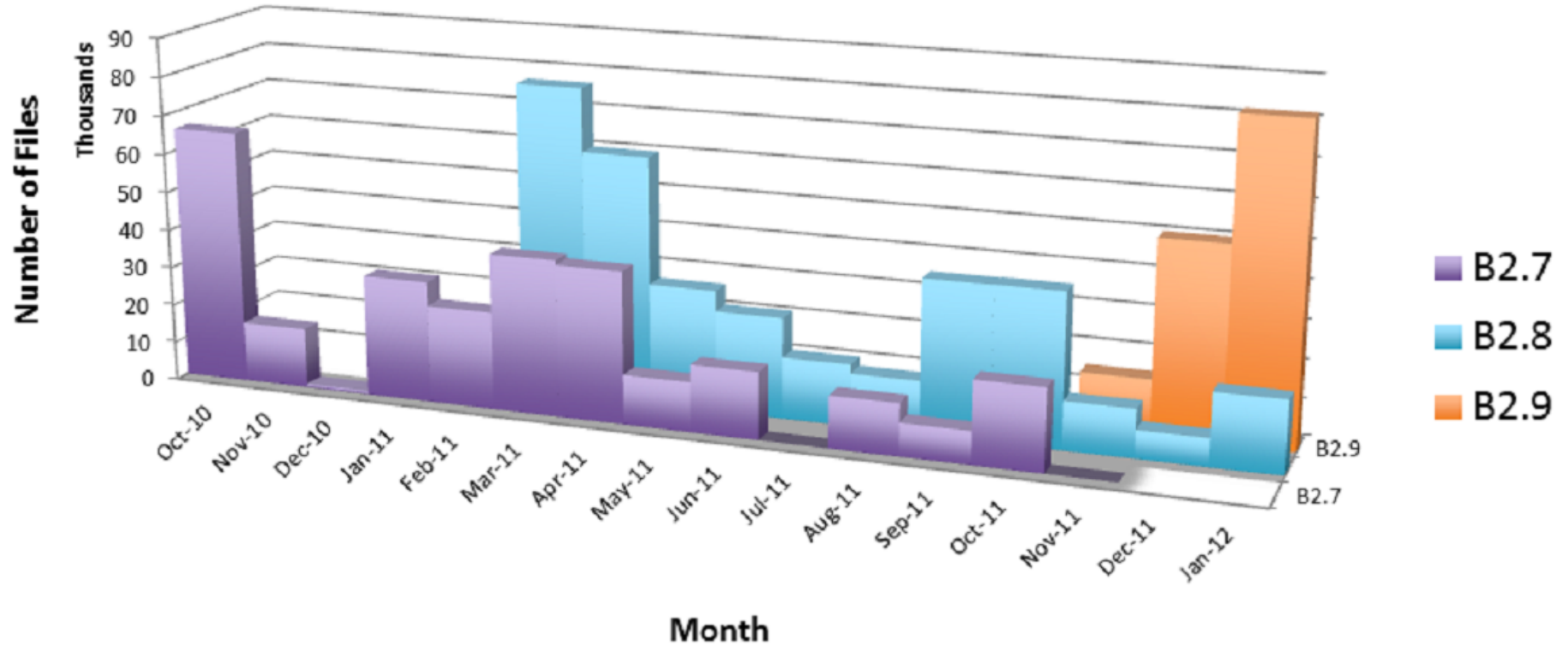
- For direct FTP access:

ftp://aurapar1u.ecs.nasa.gov/data/s4pa/GOSAT_TANSO_Level2/



ACOS Data Downloads

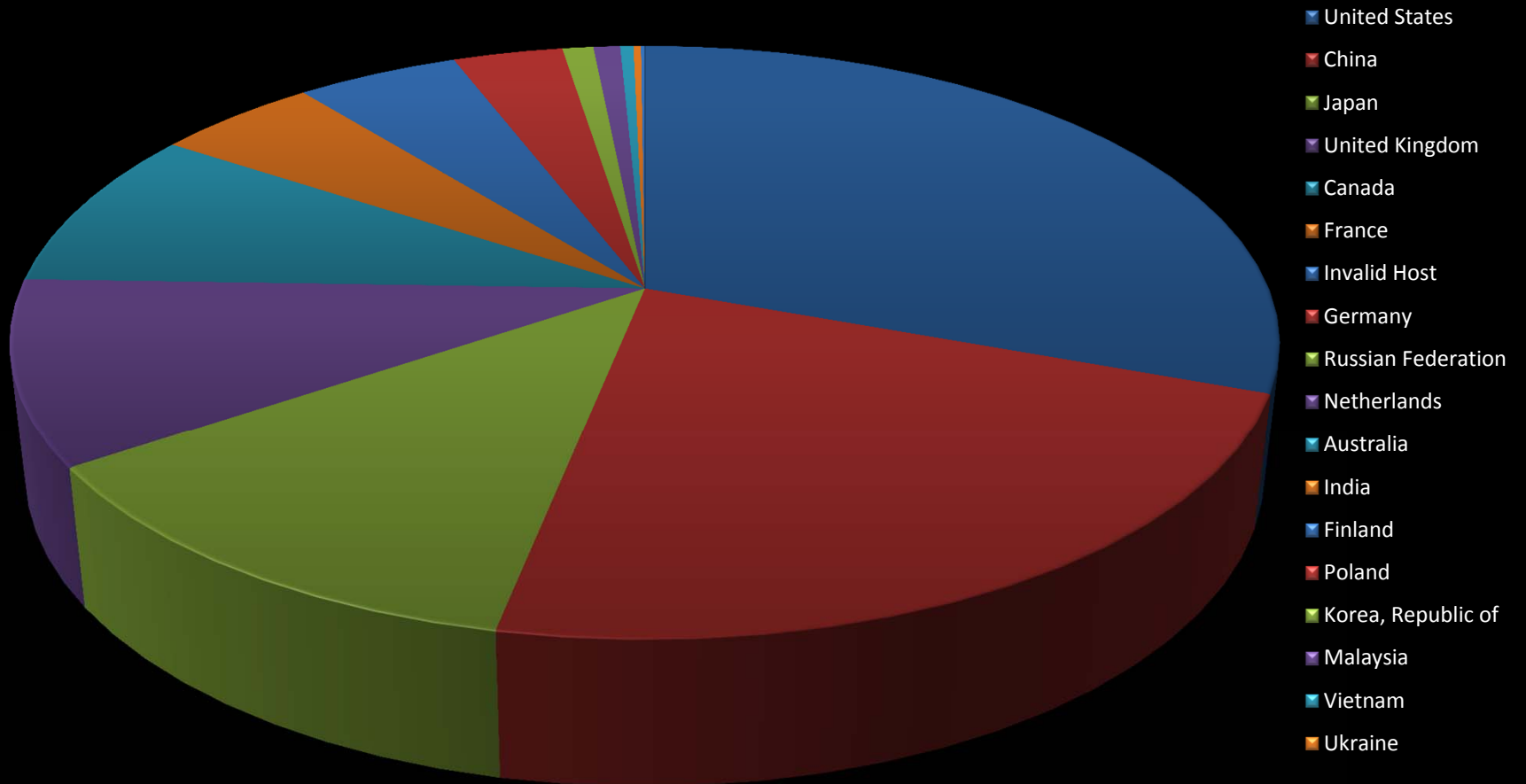
Files Downloaded by Month/Version





ACOS Downloads by Country

1.4M L2S Files Downloaded Since 10/2010





Next Steps in ACOS/GOSAT Processing

- Improvements in the GOSAT L1B data product: v150150
 - v150150 data are being processed using ACOS B2.9, but not being delivered to GES DISC , pending an internal assessment
 - Data collected since 19 April will be released following that assessment
 - B2.10 will also be used to process these v150150 products along with a larger sample for the period covered by v110110 to quantify the differences between the L1B products and L2 processing systems.
- Improvements in the ACOS/OCO-2 Retrieval Algorithm
 - B2.10 is a “research product” that incorporates a few new features (cloud/aerosol shapes, revised CO₂ spectroscopy, updates in the pre- and post-processing screening)
 - B3.3, the next “production” algorithm, will include a number of new improvements (fluorescence retrieval, increased speed, updated A-band spectroscopy, etc.), and will be ready in the fall 2012
 - This version will be used to reprocess all of the v150150 data
 - We begin to deliver that dataset to the GES DISC in Dec 2012.



ACOS/GOSAT Technical Interface Meetings

Technical Interface Meetings (TIM's)

- May 2009 – JAXA, Tokyo, Japan
- Sep 2009 – CSU, Ft. Collins, CO (Polarization)
- Oct 2009 – JPL, Pasadena, CA (Data Transfer)
- Nov 2009 – NIES, Tsukuba, Japan
- Feb 2010 – Kyoto, Japan (at IWGGMS)
- Jun 2010 – JPL, Pasadena, CA (RRV planning)
- Nov 2010 – Tsukuba, Japan
- Dec 2010 – San Francisco, CA (at AGU)
- Mar 2011 – JAXA, Tsukuba, Japan
- May 2011 – U. Edinburgh, Edinburgh, U.K. (at IWGGMS)
- June 2011 – JPL, Pasadena, CA (RRV planning)
- Dec 2011 - San Francisco, CA (at AGU)
- Aug 2012 – JPL, Pasadena, CA (Non-linearity)



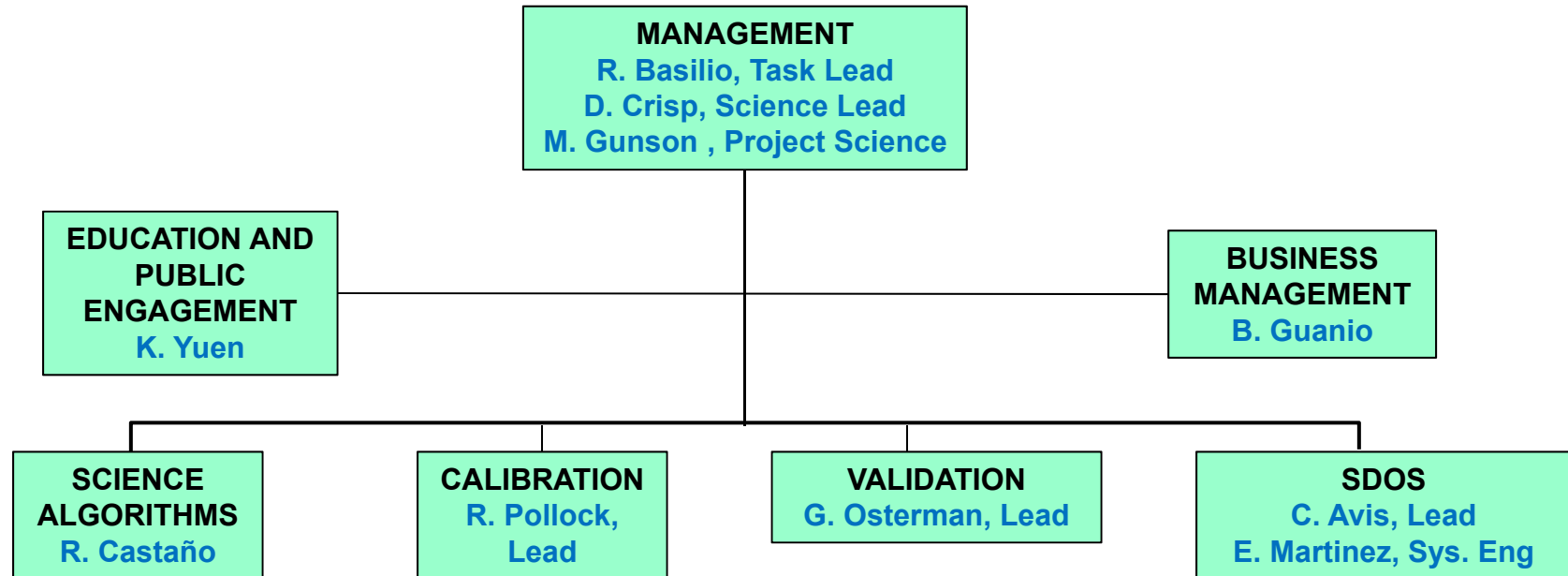


ACOS Programmatic



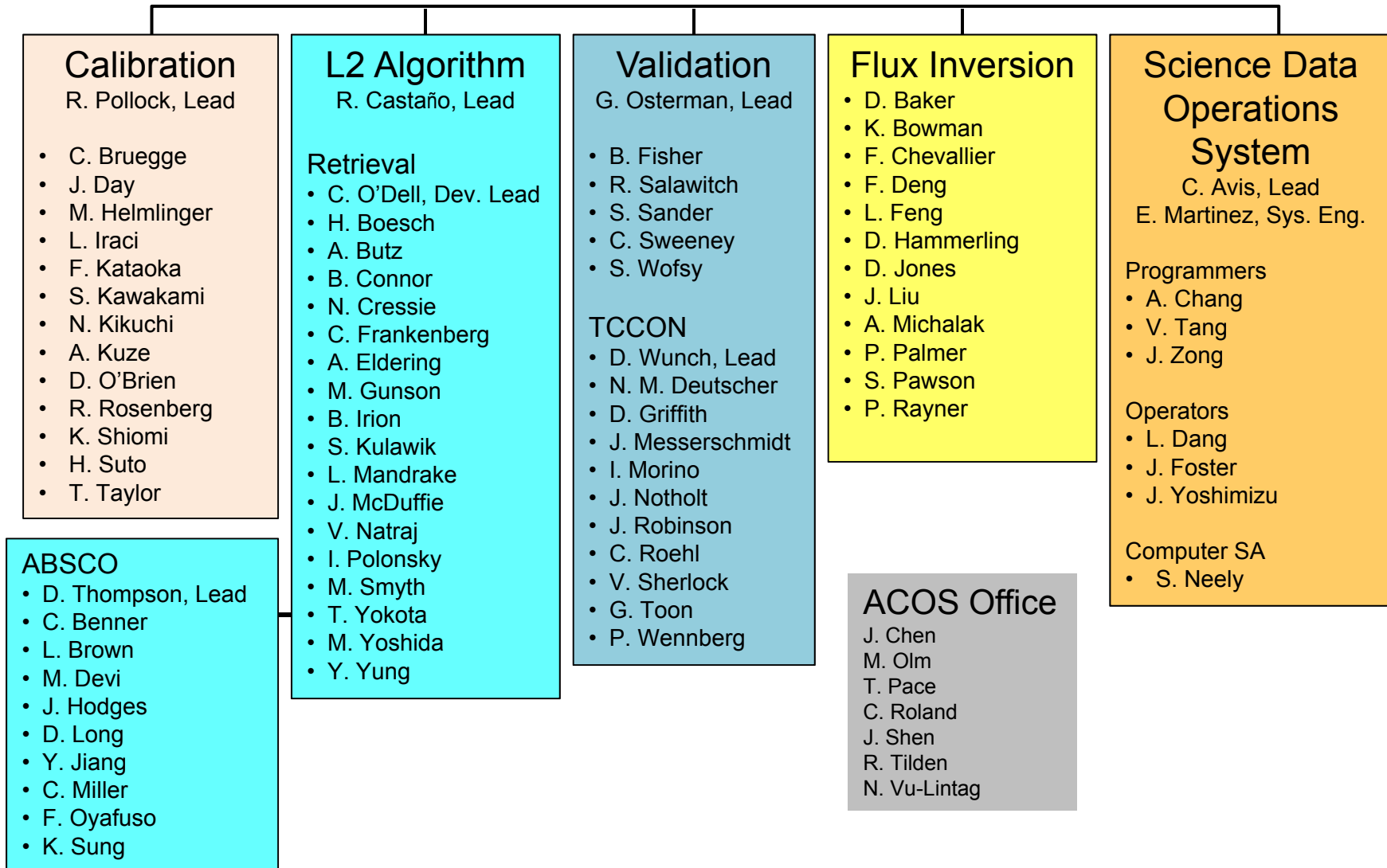


ACOS Management



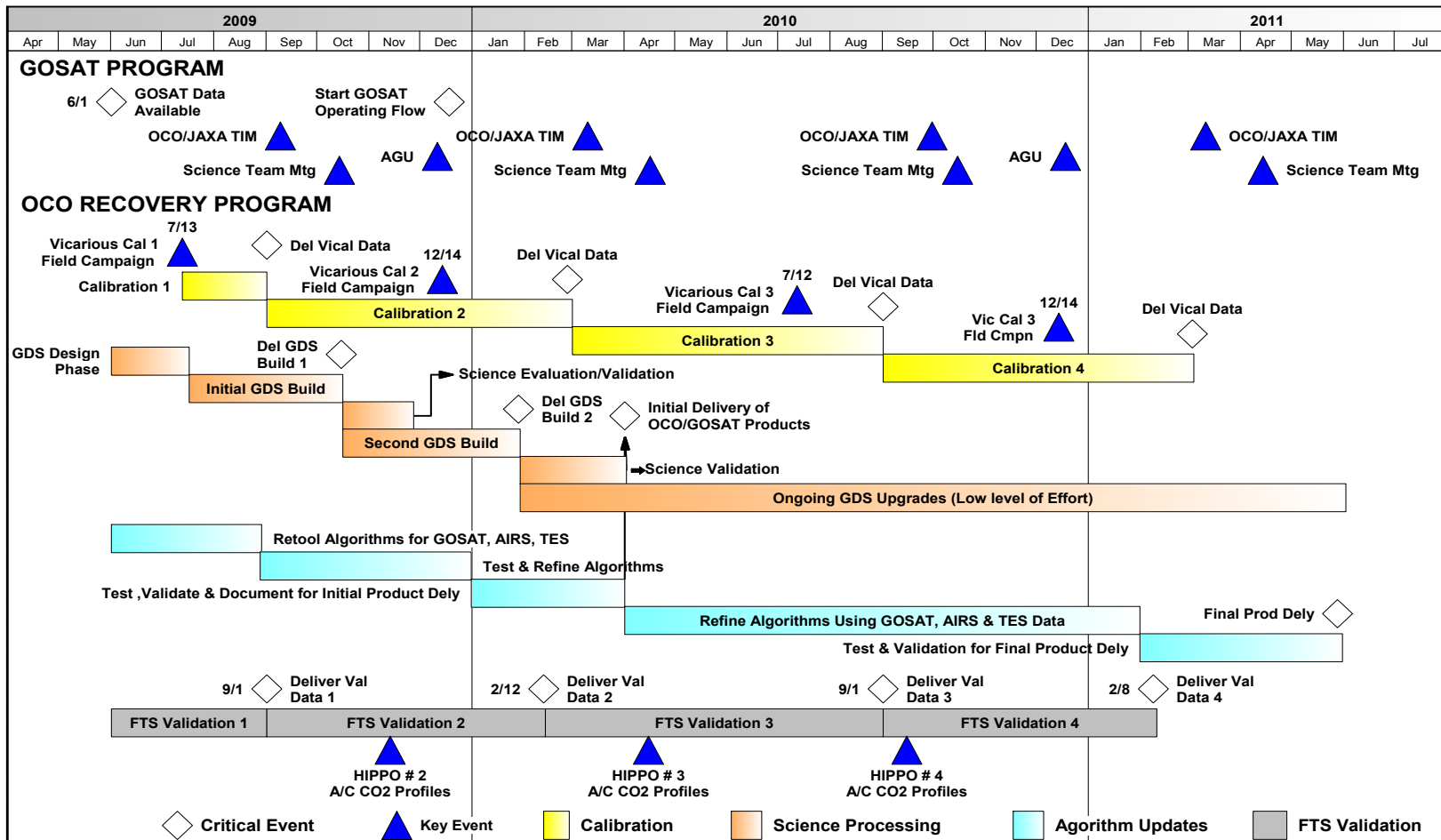


ACOS Implementation Team Organization





Original ACOS Schedule



The ACOS task was originally scheduled from May 2009 through May 2011. The plan was extended through July 2012 to support the 2012 Vicarious Calibration Campaign.



ACOS Assessment

The ACOS task provided a comprehensive, end-to-end test of the OCO/OCO-2

- Vicarious calibration system
 - Retrieval algorithm accuracy and speed
 - Validation approach
 - Science data pipeline processing and data delivery system.
- The ACOS task also
 - Produced a space-based greenhouse gas data product that is widely used by the carbon science community
 - Nurtured a strong collaboration between the NASA and JAXA space-based greenhouse gas remote sensing efforts, that has been extended to the OCO-2 and GOSAT-2 projects
 - This progress is expected to accelerate the delivery of a high quality data product from OCO-2, once it is launched in 2014.